ROLE OF GRAVITY IN PREPARATIVE ELECTROPHORESIS

Prepared for

NATIONAL AERONAUTICS AND SPACE ADMINISTRATION
GEORGE C. MARSHALL SPACE FLIGHT CENTER
MARSHALL SPACE FLIGHT CENTER
Alabama 35812

CONTRACT No. NAS 8-29566

Submitted by

Milan Bier

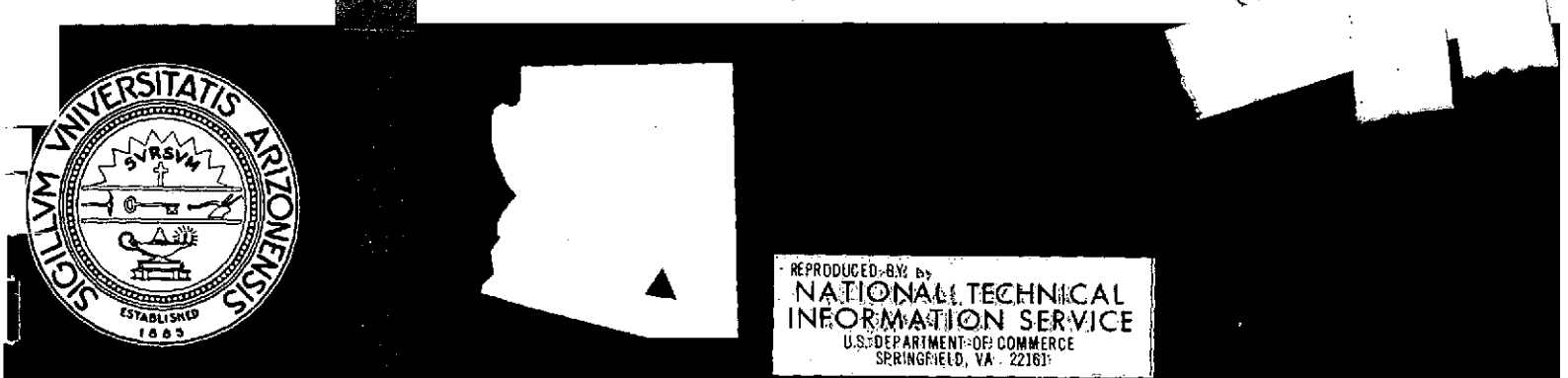

ENGINEERING EXPERIMENT STATION
COLLEGE OF ENGINEERING
THE UNIVERSITY OF ARIZONA
TUCSON, ARIZONA

ROLE OF GRAVITY IN PREPARATIVE ELECTROPHORESIS

Prepared for

NATIONAL AERONAUCTICS AND SPACE ADMINISTRATION
GEORGE C. MARSHALL SPACE FLIGHT CENTER
MARSHALL SPACE FLIGHT CENTER
Alabama 35812

CONTRACT No. NAS 8-29566

Submitted by

Milan Bier

Engineering Experiment Station
College of Engineering
The University of Arizona
Tucson, Arizona 85721

I

INDEX

SECTION A

INTRODUCTION

The interest of the principal investigator (P.I.) in problems of space electrophoresis originated with his participation in the Universities Space Research Association's Committee on Electrophoresis. This Committee had assumed a major responsibility for the planning of the Electrophoresis experiment in the Apollo 16 mission. From the meetings of the Committee, and several other meetings that the P.I. attended, it became obvious that gravity plays a major role in electrophoresis, severely limiting its application to the separation of living cells. These meetings defined the objectives of the NASA program, namely the development of a zero-gravity electrophoresis facility, primarily for the separation of living cells, with a secondary emphasis on proteins. This objective appeared eminently worthwhile on the basis of its potential scientific, medical, social and economic impact.

While the objectives of the program could therefore be clearly specified, the means to attain it were less apparent. Electrophoresis is not a single technique, but has evolved into a family of allied techniques, each utilizing specific apparatus and methodology, and each having equally qualified and vociferous advocates. No consensus could be reached as to the optimum technique, apparatus, etc., for the space program. Part of the reason is that electrophoresis has evolved largely as a result of efforts of biochemists, who may have been skilled gadgeteers and experimentalists, but who paid relatively little attention to fundamentals of theory or optimization of engineering design. It is most significant that electrophoresis has largely escaped the attention of physicists and engineers.

The objective of the contract was to remedy this shortcoming, and bring together a group of physicists, engineers, and experimentalists, who could attempt to obtain a greater insight into the fundamentals of the electrophoretic process. To initiate the research program, a

series of informal seminars were held at the University of Arizona under the joint sponsorship of the Departments of Physics, Aerospace and Mechanical Engineering, and Optical Sciences, in which the general problems of electrophoresis were reviewed in depth. These seminars started before the granting of the contract, and helped to identify those University scientists having an interest in the program. Thus, from its inception, the program had the benefit of the participation of several individuals not mentioned in the report, and not paid by the contract.

As a result, a working group of physical scientists has been brought together which is probably unique in the annals of electrophoresis, comprising theoretical physicists, engineers and experimentalists. The theoretical group, led by Dr. M. O. Scully, Professor, Departments of Physics and Optical Sciences, included Prof. T. W. Nee, and Drs. G. T. Moore, and H.S.T. Shih, as well as other members of his team. The engineering group was initially led by Dr. M. Bottacini, who was replaced because of a sabbatical leave by Prof. M. Coxon of the Department of Aerospace and Mechanical Engineering, with his associate, Mr. M. J. Binder, a graduate student, whose doctoral work will be based on work carried out for this contract. The experimental program is headed by the P.I., whose work in preparative electrophoresis spans more than twenty years. Most important for the success of the work has been the recruitment of Mr. J.O.N. Hinckley, a British biochemist, who has been active in the field of isotachophoresis since 1968, when he participated with Prof. A.J.P. Martin, a Nobel Laureate, in the modern rediscovery of isotachophoresis. He was joined in the experimental work by Mr. A.J.K. Smolka, who has also been active in preparative electrophoresis for several years. Each group has worked relatively independently, with frequent seminar-like meetings, to correlate and organize the overall effort. Prof. J.O. Kessler of the Physics Department has taken an independent active interest in our work, and his contribution was

most valuable.

These seminars played an important role in the development of the research work. Rather than summarizing the topics covered, a reprint is included as Appendix I, giving an up-to-date survey of electrophoresis by the P.I. This reprint has no mention of isotachophoresis, which at the time of writing was still in its infancy. Isotachophoresis, nevertheless, became an important subject of the seminars, and constituted a major part of further work.

The reason for this is that isotachophoresis seems to be particularly attractive as a candidate for the zero gravity facility. This was repeatedly emphasized by the P.I. at the meetings of the Committee on Electrophoresis, and also in several letters and reports to NASA. It has also been discussed in greater detail in a paper presented at the AIAA 12th Aerospace Sciences Meeting (Appendix II). The potential advantages of isotachophoresis became particularly apparent when the results of the Apollo 16 electrophoresis experiment became available. This experiment demonstrated that in zero gravity the major problem of gravity-caused convection is indeed avoided, as was predictable. Separation of latex particles was achieved in a manner not possible in terrestrial electrophoresis. But it also showed that not all problems of electrophoresis were avoided. The boundaries of the migrating particles were diffuse, strongly parabolic due to electroosmosis, and subject to random distortion by as yet undetermined causes. A detailed report on the Apollo experiment is enclosed as Appendix III. It therefore became apparent that a technique with self-sharpening boundaries would be most desirable.

Only two such methods exist: isoelectric focusing and isotachophoresis. Unfortunately, isoelectric focusing appears inapplicable to living cells, as their isoelectric points are not consonant with their survival. This problem is avoided in isotachophoresis. Isotachophoresis has also other advantages. For one, its self-sharpening boundaries are self-restorative and

extremely sharp, largely overcoming the effects of diffusion or minor fluid disturbances. Although isoelectric focusing also has self-restoring boundaries, its boundaries are far less sharp, as the bands are formed at zero electrophoretic mobility, when the electric field has no effect. Moreover, in isotachophoresis, the effective concentration of separated zones is constant throughout the length of the zone, being only the function of so-called leader ion concentration. Thus, the individual steps of a separated mixture will be shorter or longer, depending on the amount of material present. In isoelectric focusing, all material of the same isoelectric point tends to come together in a very narrow boundary of high concentration. This may exceed the solubility of the protein (which is lowest at the isoelectric point) and cause precipitation. These and other advantages of isotachophoresis will be outlined in greater detail in subsequent sections of the report.

Isotachophoresis is in many ways a much more sophisticated technique than the other forms of electrophoresis. As a result, it presented greater challenges for the physicists and engineers participating in the program. Thus, a major part of the work of the physicists, engineers and experimentalists soon focused on the specific problems of isotachophoresis. From an experimental point of view it soon became apparent that gravity plays an even more destructive role in isotachophoresis than in other forms of electrophoresis. The only way to avoid this disruption was by working in gels, which is not compatible with cell separations. Various other methods of circumventing the effects of gravity were attempted, but with only partial success, as will become apparent from the more detailed parts of this report.

Thus, it became of crucial importance for the whole isotachophoresis program when an opportunity presented itself to include an experiment on isotachophoresis in the last Skylab Mission. Two major problems face the earth-bound work:

(1) Will the behavior of soluble proteins in free solution at zero gravity be analogous to

their behavior in earthbound gels?

(2) Will living cells behave in a manner analogous to soluble proteins, once the effects of gravity are eliminated?

There was every indication that the answers to both of these questions would be affirmative, but only a space experiment could provide a definitive answer. Through the efforts of our contracting officer, Dr. Robert S. Snyder, Chief, Bioengineering Section, Astronautics Laboratory, Marshall Space Flight Center, and a number of his associates, the flight experiment came to its realization. It was designed to give an answer to the above two questions, by flying a small test package consisting of two preloaded modules, one with a mixture of two soluble colored proteins, ferritin and hemoglobin, and the other with a suspension of red blood cells. The two colored proteins were selected because of the easy visual or photographic recording of their separation. Moreover, their separation on gels has been thoroughly studied in this laboratory. Erythrocytes were selected because of their longevity. They have a well defined electrophoretic mobility, and are often used for calibration purposes.

Extensive laboratory tests were performed in preparation for the Skylab experiment. Unfortunately, the experiment itself was less than an unqualified success. Most important was the complete failure of the protein experiment. No migration whatever of proteins was observed, and post-flight analysis of the module showed that no current flowed, for reasons impossible to determine. The red cell experiment was marred by leakage of cell contents, which resulted in numerous air bubbles in the observation channel. Though the instructions called for clearance of air bubbles, this was not done in the first run, and the photographs are out of focus. The second run, done on the initiative of the astronauts, showed better photographs. Moreover, the whole experimental package was accidentally left out of the Skylab refrigerator for several weeks, thereby jeopardizing the survival of the red cells.

These difficulties notwithstanding, the experiment has clearly shown the sharp boundaries characteristic of isotachophoresis. Electroosmosis modified the boundary shape, but apparently less so than in zone electrophoresis. Lateral forces seemed to modify the normal parabolic shape, giving it a blunted profile. It is hoped that better results will be obtained in the isotachophoresis experiment planned for the Apollo-Soyuz mission in 1975.

Finally, a few words regarding the organization of this report. Because of the interdisciplinary nature of our effort and the unusual caliber of the participating scientists, it is not possible to submit a straight-forward report, with a single narrative theme brought to its logical conclusion. Instead, each participating team of investigators has prepared its own reports, summarizing their accomplishments, and presenting detailed accounts where available. It should be obvious that not all the tasks have been brought to completion, but that we are only at the beginning of a major undertaking in electrophoresis, involving the collaboration of theoreticians, engineers and experimentalists, which is unprecedented in the field of electrophoresis.

MILAN BIER

SECTION B

REPORT BY THE PHYSICS GROUP

by

M. O. Scully, T. W. Nee, G. T. Moore, and H. S. T. Shih

INTRODUCTION

During the first year (1973) of electrophoresis researches, the theory group has worked the following problems:

I. Isotachophoresis

1. Structure of isotachophoresis front[1]

For a better understanding of the isotachophoresis system which will be in the future Skylab experiment, we have made a fine analysis of the isotachophoresis front structure. The isotachophoresis front is not a simple plane but a region with non-neutral charge distribution. This charge distribution has been calculated in a very simple situation. This is a first improvement of the Kohlrausch theory.[2]

2. Boundary Sharpening Effect in Isotachophoresis[3]

The non-steady state ionic motion of charged fluid is studied by assuming the charge neutrality. The diffusion effect is considered. We found the boundary sharpening effect--the sharpening of an initially diffused boundary region between the leader and terminator ions. This is a characteristic feature of isotachophoresis which is first calculated.

3. Calculation of the characteristic data associated with the November, 1973 Skylab Mission experimental apparatus.[4]

The isotachophoresis apparatus which has been designed to be sent on November, 1973 Skylab Mission was evaluated theoretically. It was found that the time for the front to migrate through the tube is about 11 minutes; the power requirements of the apparatus are less than 0.2 watt; and the temperature rise of the solution is only a few degrees during the course of the planned experiment.

II. Electrophoresis Theory

1. Fundamental Fluid Equation of Motion for Electrophoresis[1]

We have derived the fundamental macroscopic formulas of electrophoresis from the microscopic statistical first principle. This provides a general starting point for any electrophoresis fluid dynamic calculations.

2. The Electrophoretic Mobility[5]

In the electrophoresis experiments, the electrophoretic mobility (E.M.) is a fundamental characteristic parameter to be measured. There have been several theories[6,7] for the calculations of E.M. from special simple models. E.M. is shown to be dependent on the dielectric constant ϵ and viscosity η of the fluid. The major effects that have been considered are those of (1) the Stokes friction and (2) the small electrolyte ion cloud (electric double layer). However, two important effects have been neglected:

(1) Local Field Effect: The true electric force acting on a colloidal particle is not the average Maxwell electric field. The acting field (local field) differs from the Maxwell field by a modification factor which is a function of the dielectric constant of the surrounding medium:

$$\vec{E}_{loc} = M(\epsilon)\vec{E}$$

This effect is very important in any "dense" system such as liquid or solid.[8] In the simplest case of spherical ions,

$$M(\epsilon) = \frac{3\epsilon}{2\epsilon + \epsilon_\infty}$$

where ϵ is the static dielectric constant and ϵ_∞ is the optical dielectric constant of the surrounding medium.

(2) Dielectric Friction Effect: In addition to the Stokes friction there is an additional frictional force on a "charged" colloidal particle in a fluid. This effect has been shown to be very important for a polar liquid.[9] This friction is due to electromagnetic interaction between the charged ion and its surrounding dielectric medium. For spherical moving ions, Zwanzig[10] has calculated this dielectric friction, then the total friction constant is

$$\zeta = \zeta_0 + C \frac{\epsilon - \epsilon_\infty}{\epsilon(2\epsilon+1)}$$

where ζ_0 is the Stokes' frictional constant and C is a constant dependent on the radius of the ion.

By considering both effects, the electrophoretic mobility μ in the simplest case of spherical ions the form

$$\mu = \mu_0 \frac{3\epsilon}{2\epsilon+\epsilon_\infty} \frac{1}{1 + \frac{C}{\zeta_0} \frac{\epsilon-\epsilon_\infty}{\epsilon(2\epsilon+1)}}$$

where

$$\mu_0 = q/\zeta_0$$

is the value without considering these two effects.

3. Internal Ion Friction Effect[11]

We applied the general formula in Reference 1 to calculate the effect of the internal ionic frictional effect in charged fluid. We found there exists spatially charged fluid velocity variation which

can cause the crescent phenomenon for solution with giant ions. This effect is important in a system with charge neutrality, for instance, the isotachophoresis zones. This effect is characteristically different from the electroosmosis effect[12] which might be unimportant in the charge neutrality case.

4. Studies on Possible Instabilities For Electrophoresis[13]

Laminar flows are usually assumed in analytical studies for electrophoretic phenomena. Instabilities could arise however. One example is due to the combined effects of large electric fields and temperature variations in the charged fluids. It is analogous to the Benard instability (for a layer of fluid heated from below) in Hydrodynamics,[14] with the electric field E playing now the role of gravity. In order to gain understanding to the effects of turbulence in electrophoretic problems, we set out, as a first step, to investigate the Benard problem by using techniques developed in the laser theory[15] and in the general theories of non-equilibrium statistical mechanics. As a preliminary step we study the "Benard instability" in very much the same spirit as in the Lamb's semi-classical theory of "laser instability Corresponding to Maxwell equations, hydrodynamic equations are employed. By restricting our attention to the threshold region, the normal-mode method is used and an equation of the form

$$(R - R_c)\, V - \xi V^3 = 0$$

is obtained at steady state. R is the Rayleigh number and the mode amplitude V is the "order parameter". The saturation term ξV^3 is due, in our theory, not to the nonlinear constituent relations like in the laser

case, but to the non-linearities inherent in the hydrodynamic equations themselves. In other words, the convective processes are responsible. A simple application of the result is given to explain the experimentally observed dependence of the Nusselt number on the Rayleigh number.

Langevin-type equations can then be obtained for the coupled modes involving both velocity and temperature variations.

Enclosed is a rough draft of some of the analysis that has been carried out. It will be refined and extended in the next report.

References

1. T. W. Nee, "Theory of Isotachphoresis, (Displacement Electrophoresis, Transphoresis)", submitted to "Journal of Chromatography" (A manuscript is enclosed).
2. H. Haglund, "The Instrument Journal", 17, 2 (1970); and F. Kohlrausch, Ann. Physics, 62, 209 (1897).
3. G. Moore, in preparation and to be published. (A first draft manuscript is enclosed).
4. G. Moore, a draft manuscript is enclosed.
5. T. W. Nee, in preparation and to be published.
6. J. Th. G. Overbeek and J. Lijklema, in "Electrophoresis Vol. I" (M. Bier, ed.), Chapter 1, (Academic Press, New York, 1959).
7. J. Th. G. Overbeek and P. H. Wiersema, in "Electrophoresis Vol. II," (M. Bier, ed.) Chapter 1, (Academic Press, New York, 1967).
8. C. Kittel, "Introduction to Solid State Physics", 3rd ed. Chapter 12, (Wiley, New York, 1967).
9. T. W. Nee and R. Zwanzig, J. Chem. Phys. 52, 6353 (1970).
10. R. Zwanzig, J. Chem. Phys. 38, 1603 (1963), and 52, 3652 (1970).
11. T. W. Nee, "Electrophoretic Crescent Phenomenon", to be published. (A first draft manuscript is enclosed.)
12. Chien Fan, "Convection Phenomena in Electrophoresis Separation," IMSC-HREC TR D306300, Lockheed Missiles and Space Company, Huntsville, Ala.
13. H. S.T. Shih, M. O. Scully and T. W. Nee, a draft manuscript is enclosed.
14. S. Chandrasekhar, "Hydrodynamic and Hydromagnetic Stability", Oxford University Press (1961).
15. V. DeGiorgio and M. O. Scully, Phys. Rev. A2, 1170 (1970).
16. W. E. Lamb, Jr., Phys. Rev. 134, A1429 (1964).

Theory of Isotachophoresis (Displacement Electrophoresis, Transphoresis)*

T. W. Nee

Department of Physics and Optical Science Center

University of Arizona, Tucson, Arizona 85721

Summary

The fundamental formulas of electrophoresis are derived microscopically and applied to the problem of isotachophoresis. A simple physical model of the isotachophoresis front is proposed. The front motion and structure are studied in the simplified case without convection, diffusion and non-electric external forces. This is an essential improvement of Kohlrausch's theory.

*Work supported in part by U. S. National Aeronautics and Space Administration Contact NAS8-29566.

I. Introduction

Electrophoresis[1] is the separation of charged components of a solution in an electric field due to their different electric mobilities. This technique has been extensively used in bio-medical researches. Many different techniques have been developed. A useful one is the isotachophoresis[2] (displacement electrophoresis,[3] transphoresis[4]). Isotachophoresis is the migration in an electric field of different ion species of the same sign, all having a common counter-ion species. In the steady state, these different ion species are saptially separated. The ions of higher mobility are moving ahead of those of lower mobility. The boundaries (fronts) between the different ion species all move with the same velocity. In 1897, Kohlrausch[5] developed a theory for the conditions obtaining in a migrating boundary. He derived a relationship between the two salt concentrations on opposite sides of the boundary and the mobilities of the ions involved. This is the fundamental formula of isotachophoresis experiments.

In this paper, we shall study isotachophoresis from basic microscopic principle. An essential improvement of Kohlrausch's theory will be developed. In the next section we shall review first the microscopic derivation of fluid dynamics. A physical model of ionic solutions will be introduced and the fundamental equations derived. In Section III, we shall present a simple model for the front motion in isotachophoresis. In addition to Kohlrausch's formula, expressions for the electric field and ionic densities in the front region will be derived. Discussion and conclusions are given in the final section.

II. Microscopic Theory of Charged Fluid

A. Classical Theory of Fluid

We consider a fluid system consisting of N identical particles. Each particle has mass m, position $\vec{r}_j(t)$ and momentum $\vec{p}_j(t)$, $(j = 1,2,\cdots N)$ at a given instant of time t. The particle density $n(\vec{r},t)$ and current density $\vec{J}(r, t)$ at position $\vec{r}$ and time t are defined as

$$n(\vec{r}, t) = \left\langle \sum_{j=1}^{N} \delta(\vec{r} - \vec{r}_j(t)) \right\rangle \tag{1}$$

and

$$\vec{J}(\vec{r}, t) = \left\langle \sum_{j=1}^{N} \delta(\vec{r} - \vec{r}_j(t)) \frac{\vec{p}_j(t)}{m} \right\rangle, \tag{2}$$

where $\langle\ \rangle$ is the equilibrium ensemble average. From the classical equation of motion

$$\dot{\vec{r}}_j(t) = \frac{1}{m} \vec{p}_j(t) \tag{3-1}$$

and

$$\dot{\vec{p}}(t) = \vec{F}_j(t), \tag{3-2}$$

we can derive the equation of continuity

$$\frac{\partial}{\partial t} n(r, t) + \nabla \cdot \vec{J}(\vec{r}, t) = 0 \tag{4}$$

and the momentum conservation equation

$$m n \frac{d}{dt} \vec{v}(\vec{r}, t) = \vec{F}^B(\vec{r}, t) + \nabla \cdot \vec{T}(\vec{r}, t) \tag{5}$$

where

$$\frac{d}{dt} = \frac{\partial}{\partial t} + \vec{v} \cdot \nabla \tag{6}$$

$$\vec{v}\,(\vec{r},\,t) = \frac{1}{n\,(\vec{r},\,t)}\;\vec{J}\,(\vec{r},\,t) \tag{7}$$

is the fluid velocity, and

$$\vec{F}^{B}\,(\vec{r},\,t) \;=\; \Big\langle \sum_{j=1}^{N} \delta\,(\vec{r} - \vec{r}_j\,(t)\,)\,\vec{F}_j\,(t)\,\Big\rangle \tag{8}$$

is the bulk force density. $\vec{F}_j\,(t)$ is the force acting on jth particle at time t.

$$\vec{\vec{T}}\,(\vec{r},\,t) \;=\; -\,m\,\Big\langle \sum_{j=1}^{N} \delta\,(\vec{r} - \vec{r}_j\,(t))\Big(\frac{\vec{p}_j\,(t)}{m} - \vec{v}\Big)\Big(\frac{\vec{p}_j\,(t)}{m} - \vec{v}\Big)\Big\rangle \tag{9}$$

is the stress force tensor.

B. Simple Model of Ionic Solution

In order to develop a fundamental theory of ionic motion in solution, we consider a simple model: A system of N ions each with mass m and charge q and moving in a viscous solvent fluid. The force acting on jth ion is

$$\vec{F}_j\,(t) \;=\; q\,\vec{E}\,(\vec{r}_j\,(t),\,t) \;-\; \zeta\,\vec{r}_j\,(t) \;+\; \vec{F}_j^{\,ext}\,(t) \tag{10}$$

where $\vec{E}\,(\,\vec{r}_j\,(t),\,t\,)$ is the electric field at the ionic location, ζ the frictional constant due to the viscous surrounding medium -- the solvent fluid and other ions. $\vec{F}_j^{\,ext}$ is the force due to non-electric external source.

Substituting (10) into (8), we obtain the bulk force density

$$\vec{F}^B(\vec{r}, t) = q\, n(\vec{r}, t)\, \vec{E}(\vec{r}, t) - \zeta\, \vec{J}(\vec{r}, t) + \vec{F}_B^{ext}(\vec{r}, t) \qquad (11)$$

The stress tensor can be written in a standard form[6]

$$\vec{\vec{T}}(\vec{r}\, t) = P_i(\vec{r}\, t)\, \vec{\vec{I}} - \vec{\vec{\sigma}}(\vec{r}\, t) \qquad (12)$$

where P_i is the ionic partial pressure, $\vec{\vec{\sigma}}$ the internal frictional force tensor among the ions[6],

$$-\nabla \cdot \vec{\vec{\sigma}} = \eta \nabla^2 \vec{v} + (\eta + \frac{\nu}{3}) \nabla (\nabla \cdot \vec{v}) \qquad (13)$$

η and ν are the viscosity coefficients. Substituting (11), (12), (13) into (5), we have the formal equation of motion of the ionic fluid:

$$mn \frac{d}{dt} \vec{v} = -\zeta [\vec{J} \mp \mu n \vec{E}] - \nabla P_i + \eta \nabla^2 \vec{v} + (\eta + \frac{\nu}{3}) \nabla (\nabla \cdot \vec{v}) + \vec{F}_B^{ext} \qquad (14)$$

$$\left(\begin{matrix} \text{positive} \\ \text{negative} \end{matrix} q \right)$$

where $\mu = |q|/\zeta$ (15)

is the ionic mobility.

In the electrophoresis experiments, the ions are cells or proteins, they are small macroscopic particles or giant molecules. In this situation, the frictional effect is so great that the inertial effect is not important. In the absence of convection,

$$m\, n \frac{d}{dt} \vec{v} = 0$$

Then from eq. (14) we have the current density

$$\vec{J} = \pm \mu n \vec{E} + \frac{1}{\zeta} \left\{ -\nabla P_i + \eta \nabla^2 \vec{v} + (\eta + \frac{\mu}{3}) \nabla (\nabla . \vec{v}) + \vec{F}_B^{ext} \right\} \tag{16}$$

C. Motion of Ionic Packet in a Uniform Electric Field.

As a practical example, we consider the case of dilute solution where the ions can be considered as a system of dilute gas. The pressure P_i is related to the density by

$$P_i (\vec{r}t) = k_B T n (\vec{r}t)$$

and the ionic internal frictional force tensor $\overleftrightarrow{\sigma}$ is negligibly small. Furthermore, we consider the isothermal case (T = constant) where there is no convection. Equation (16) reduces to

$$\vec{J} (\vec{r}t) = \pm \mu n \vec{E} - D \nabla n \tag{17}$$

where

$$D = k_B T/\zeta \tag{18}$$

is the diffusion constant. If we neglect the electric screening effect, i.e. $\vec{E} \simeq$ constant. We can substitute (17) into (4) and obtain the equation of motion for $n (\vec{r}, t)$:

$$\left[\frac{\partial}{\partial t} - D \nabla^2 \pm \mu \vec{E} . \nabla \right] n (\vec{r}, t) = 0 \tag{19}$$

If we assume initially, t = 0, the ionic packet has the Gaussian form of width $1/\sqrt{\alpha}$

$$n(\vec{r}, 0) = N \left(\frac{\alpha}{\pi}\right)^{3/2} e^{-\alpha r^2} \tag{20}$$

Eq. (19) can be solved and obtain the solution

$$n(\vec{r}, t) = N \left(\frac{\alpha}{\pi}\right)^{3/2} \frac{1}{(1 + 4D\alpha t)^{3/2}} e^{-\alpha(\vec{r} \mp \mu \vec{E} t)^2 / (1+4 D \alpha t)} \tag{21}$$

The ion packet is moving with the drift velocity $\vec{v}_D = \pm \mu \vec{E}$ and being broadened due to diffusion ($D \neq 0$).

III. Simple Model of Isotachophoresis Front

As a simple model of isotachophoresis, we consider two salt solutions $A_1^+ B^-$ and $A_2^+ B^-$ in a long tube of isotachophoresis experiment. According to Kohlrausch's theory[3], the two salts are separated by a plane boundary (front) which is moving with constant velocity v in the steady state. The densities n_1, n_2 of the two ion species A_1^+ and A_2^+ are related by the relation [2, 3]

$$\frac{n_1}{n_2} = \frac{\mu_1}{\mu_1 + \mu_B} \quad \frac{\mu_2 + \mu_B}{\mu_2} \tag{22}$$

where μ_1, μ_2 and μ_B are the mobilities of A_1^+, A_2^+ and B^- ions respectively. The electric field E_1 and E_2 in the two regions are related by

$$\mu_1 E_1 = \mu_2 E_2 = v \tag{23}$$

The physical situations are shown in Fig. 1.

It is shown in Fig. 1 that there is electric field discontinuity across the front plane because of the different mobilities ($\mu_1 < \mu_2$) of the two positive ions, A_1^+ and A_2^+. According to the theory of electromagnetism, there should be surface charges on the front plane. Where these charges come from? What is the mechanism to build up these surface charges? How much are they?

In order to answer these questions, we propose a simple model for the structure of the front as follows. The front is not a "plane" but a "region" of finite thickness " δ." Let n_1, n_2 and n_B be the concentration of the three ions, E the electric field. The fundamental equations are:

$$\frac{\partial}{\partial t} n_i (x, t) + \frac{\partial}{\partial x} J_i (x, t) = 0, \quad (i = 1, 2, B) \tag{24}$$

where

$$J_i (x, t) = \mu_i n_i (x, t) E (x, t) - D_i \frac{\partial}{\partial x} n_i (x, t) \quad (i=1, 2) \tag{25-1}$$

$$J_B (x, t) = - \mu_B n_B (x, t) E (x, t) - D_B \frac{\partial}{\partial x} n_B (x, t), \tag{25-2}$$

and the Poisson's equation

$$\frac{\partial}{\partial x} E (x, t) = 4 \pi \rho_e (x, t) \tag{26}$$

where

$$\rho_e (x, t) = e \left[n_1 (x, t) + n_2 (x, t) - n_B (x, t) \right] \tag{27}$$

is the electric charge density and e is the positive ion charge. We have chosen the x-axis along the isotachophoresis tube axis, and work the simplest one-dimensional case.

It is understood from eqs. (26) and (27) that inside the front region, there is non-vanish negative charge distribution, $e < 0$, which comes from the excess of negative ions n_B over the positive ions $n_1 + n_2$. This non-neutral charge distribution i formed because the two kinds of positive ion packets are moving with different velocities:

$$v_1 = \mu_1 E < \mu_2 E = v_2$$

at where both kinds of positive ions are present during the electrophoretic separation process. This separation mechanism makes the two positive ion clouds become further apart after separation and leave a region with more negative ions.

With this physical picture, despite the mathematical difficulty in solving these non-equlibrium equations (24)→(27), we may study some characteristic and quantative properties in a simplified case: the steady state and non-diffusive case. In the absence of diffusion, from eq. (21), we know the ion packet shape is not changing (D=0). Then we consider the very special situation where the positive ions A_1^+ and A_2^+ have fixed packet with sharp plane boundaries. Therefore, there exist three regions: two neutral regions with $A_1^+B^-$ and $A_2^+B^-$ salt solutions and a front region of finite thickness δ and with ion B^- only. This front region is bounded by the two sharp positive ion boundary planes which are moving with the same velocity v. Inside the front region, there is non-vanishing charge density $\rho_e = -en_B$ which contributed the electric field variation $E_2 - E_1 < 0$ over the front region.

For mathematical simplicity, we chose the moving coordinate axis with origin fixed on the left boundary plane of the front, i.e.

$$n_1(x, t) = \begin{cases} n_1 & x < 0 \\ 0 & x > 0 \end{cases} \tag{28-1}$$

$$n_2(x, t) \quad \begin{cases} 0 & x < \delta \\ n_2 & x > \delta \end{cases} \tag{28-2}$$

and

$$n_B(x, t) = \begin{cases} n_1 & x < 0 \\ n_{Bf}(x) & 0 < x < \delta \\ n_2 & x > \delta \end{cases} \tag{28-3}$$

This physical situation is shown in Fig. 2.

The front velocity v is the same as the velocities of the two positive ion packets, i.e.

$$v = \mu_1 E_1 = \mu_2 E_2 \tag{29}$$

This is the same as eq. (23) of Kohlrausch's theory.

On the moving frame, the velocities of ion packets are

$$v_1' = 0 \tag{30-1}$$

$$v_2' = 0 \tag{30-2}$$

$$v'_{B1} = \mu_B E_1 - v = - (\mu_B + \mu_1) E_1 \quad (x < 0) \tag{30-3}$$

$$v'_{B2} = \mu_B E_2 - v = - (\mu_B + \mu_2) E_2 \quad (x > \delta), \tag{30-4}$$

and the current densities are

$$J'_1 = - e n_1 v'_{B1} = e n_1 (\mu_B + \mu_1) E_1 \quad (x < 0) \tag{31-1}$$

and

$$J'_2 = - e n_2 v'_{B2} = e n_2 (\mu_B + \mu_2) E_2 \quad (x > \delta) \tag{31-2}$$

in the two positive ion regions. In the front region,

$$E = E_f (x) \qquad (0 < x < \delta) \tag{32}$$

and

$$J'_f = e n_{Bf} (x) \left[\mu_B E_f (x) + v \right] \qquad (0 < x < \delta) \tag{33}$$

From equation of continuity, we have

$$J'_1 = J'_f = J'_2 \tag{34}$$

This leads to the Kohlrausch's equation

$$\frac{n_1}{n_2} = \frac{\mu_1}{\mu_1 + \mu_B} \cdot \frac{\mu_2 + \mu_B}{\mu_2} \tag{35}$$

and the negative charged particle density in the front region:

$$n_{Bf}(x) = n_j \frac{E_j + v/\mu_B}{E_f(x) + v/\mu_B} \quad (j = 1, 2) \tag{36}$$

The electric field $E_f(x)$ in front region is related to $n_{Bf}(x)$ by Poisson's equation:

$$E_f'(x) = -4\pi e\, n_{Bf}(x) \tag{37}$$

Substituting (36) into (37) and using the boundary condition

$$E_f(0) = E_1, \tag{38}$$

we obtain

$$E_f(x) = -\frac{v}{\mu_B} + \sqrt{\left(E_1 + \frac{v}{\mu_B}\right)^2 - 8\pi n_1 e \left(E_1 + \frac{v}{\mu_B}\right) x} \tag{39}$$

The thickness δ of the front region can be calculated from another boundary condition

$$E_f(\delta) = E_2 = v/\mu_2 \tag{40}$$

The ion densities, charge density and electric field can be calculated from eqs. (28), (36) and (39). These are shown in Fig. 2.

IV. Discussion and Conclusion

In this paper, we have presented the derivation of the fundamental formulas for electrophoresis from the microscopic statistical theory and some macroscopic fluid aspect. It is applied to the isotachophoresis system. We have proposed a simple model for the "isotachophoresis front," the ions and electric field distributions have been calculated in the simplified situation without convection, diffusion and non-electric external forces. This is an essential improvement of the Kohlrausch's theory.

The fact that the front is a region of charge non-neutrality was also realized by Hall and Hinckley.[7] They call this the "shock region." They discussed some qualitative properties of the shock region, but they did not calculate the charge and electric field distributions.

The general equation of motion (14) is very useful. It provides the basic starting point of any macroscopic fluid dynamic calculations. For a simple demonstration of the existence and structure of isotachophoresis front, we have neglected (i) the diffusion effect, (ii) the ionic shearing stress effect, (iii) the convection effect and (iv) the other possible external forces, for instance, the gravity, magnetic force, etc. In addition, we only consider the steady state case and positive ion packets with sharp boundaries for mathematical simplicity. In other words, we have only presented the "minimum theory" for isotachophoresis. Further calculations compatible with real experimental situations will be interesting for further investigations.

The diffusion has two major effects: (1) the ion packets will be broadened, this has been characteristically shown in Section II-C; (2) there are no sharp boundaries, this was shown by Konstantinov and Oshurkova.[8] It is expected that the positive ions A_1^+ and A_2^+ will diffuse into the front region and further to the regions of other ions.[7] Furthermore, because the diffusive boundary region is very large,[8] it would be meaningless to do any quantitative calculations for real experiment without considering the diffusion. The quantitative solutions can not be obtained without numerically solving the set of exact equations (24)→ (27) in computer. The approximate numerical solutions for steady state has been worked by Coxon and Binder.[9] However, without considering the diffusion, we have clearly seen the qualitative structure of isotachophoresis front from our minimum theoretical calculations.

I wish to thank Drs. M. Bier, M. O. Scully, J. O. N. Hinckly, G. Moore, M. Coxon, J. Kessler, and Mr. M. Binder for helpful discussion.

References

1. M. Bier (Editor), Electrophoresis, Theory, Methods and Applications, Vol. I, II, Academic Press, N. Y., 1959 and 1967.
2. H. Haglund, The Instrument Journal, 17 (1970) 2.
3. A. J. P. Martin and F. M. Everaerts, Proc. Roy. Soc. London, A316 (1970) 493.
4. J. O. N. Hinckley, in E. Reid (Editor), Methodological Developments in Biochemistry, Vol. 2, Longman, London, 1973, P. 207.
5. F. Kohlrausch, Ann. Phys., 62 (1897) 209.
6. L. D. Landau and E. M. Lifshitz, Fluid Mechanics, Addison and Wesley, Reading, Massachusetts, 1959.
7. R. Hall and J. O. N. Hinckley, Written Communication, (1971); J. O. N. Hinckley, Transphoresis (1973), in press. We thank Dr. Hinckley for showing us this written manuscript prior to publication.
8. B. P. Konstantinov and O. V. Oshurkova, Soviet Physics, Tech. Phys., 11 (1966) 693.
9. M. Coxon and M. Binder, Private Communication, to be published.

Figure Captions

Figure 1.

(a) The ions A_1^+ and A_2^+ are migrating in separated zones. The ions A_2^+ in the leading zone have higher mobility than A_1^+ in the terminating zone. B^- are the common counter-ions in the two zones. The zone boundary (front) is moving with constant velocity v in the steady state.

(b) The ion concentrations in the two zones.

(c) The electric fields in the two zones.

Figure 2.

(a) In addition to the leading and terminating zones, there is a front region with counter-ions B^- and moving with constant velocity v in the steady state.

(b) The ion concentrations in the two zones and the front region.

(c) The electric fields in the two zones and the front region.

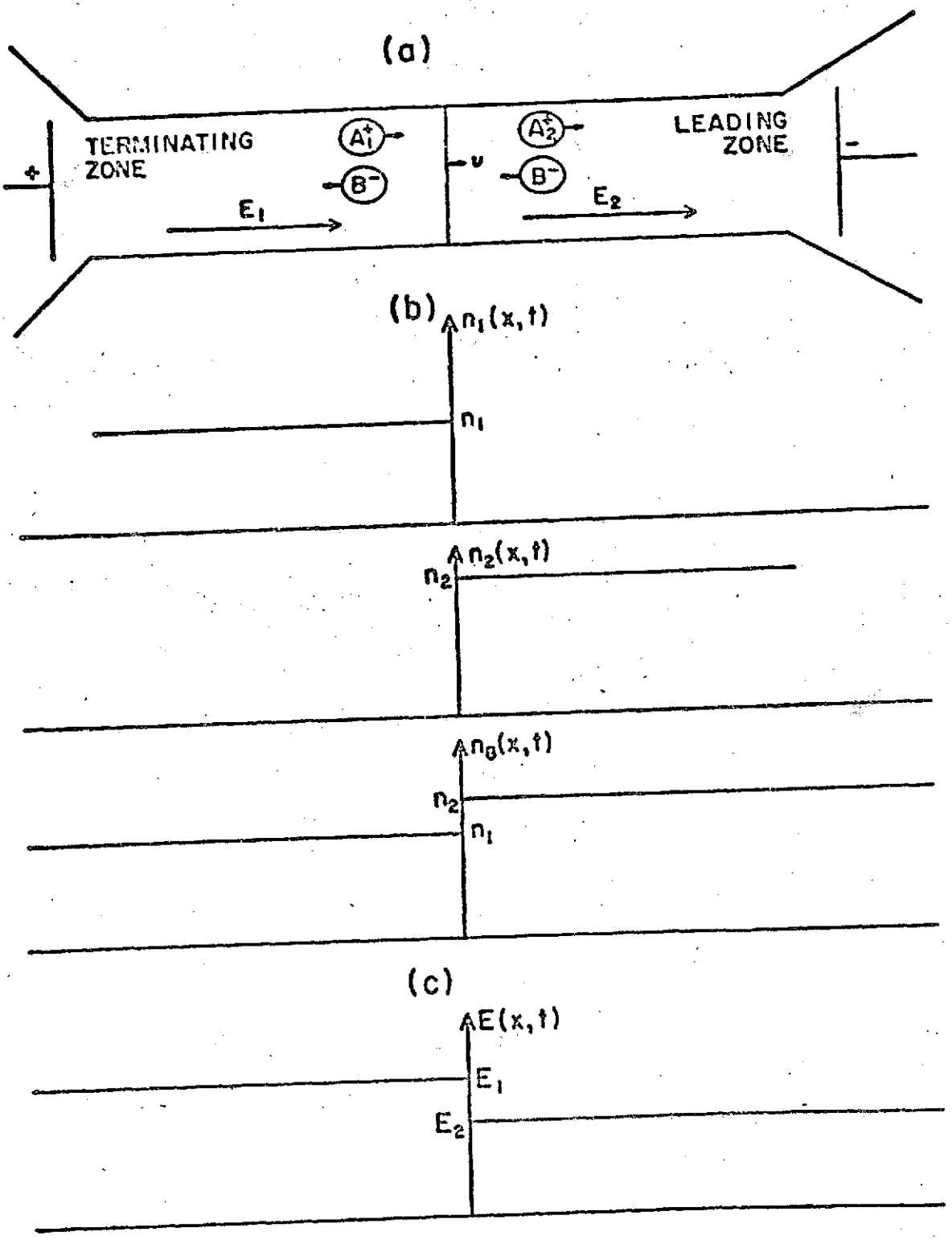
(a)
TERMINATING ZONE
LEADING ZONE
+
-
A_1^+
B^-
A_2^+
B^-
v
E_1
E_2
(b)
$n_1(x,t)$
n_1
$n_2(x,t)$
n_2
$n_3(x,t)$
n_2
n_1
(c)
$E(x,t)$
E_1
E_2

Fig. 1

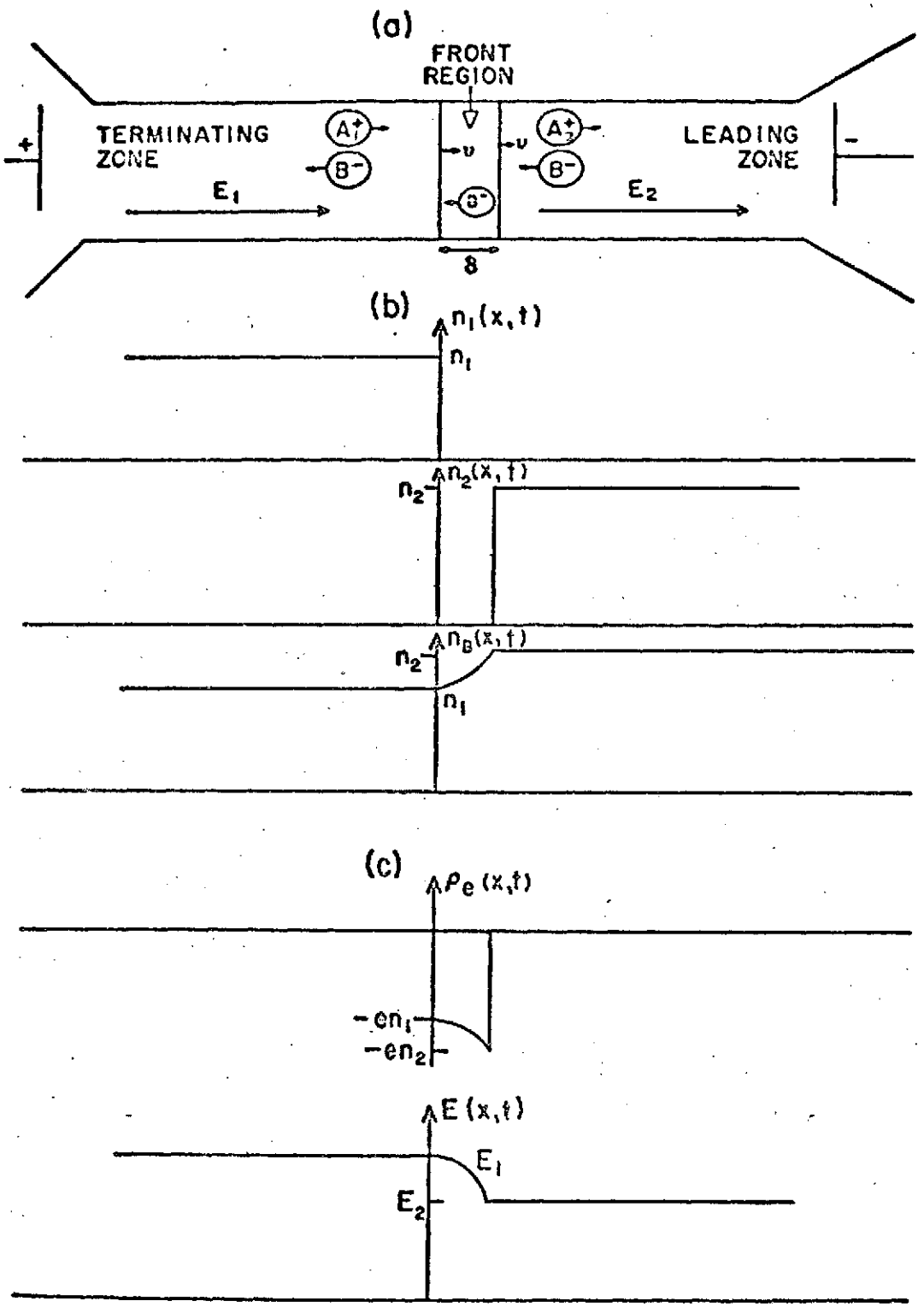
(a)
FRONT
REGION
TERMINATING
ZONE
LEADING
ZONE
+
-
A_1^+
B^-
A_2^+
B^-
v
v
δ^-
E_1
E_2
δ
(b)
$n_1(x,t)$
n_1
$n_2(x,t)$
n_2
$n_B(x,t)$
n_2
n_1
(c)
$\rho_e(x,t)$
$-en_1$
$-en_2$
$E(x,t)$
E_1
E_2

Fig. 2

ELECTROPHORETIC CRESCENT PHENOMENON*

T. W. Nee

Department of Physics and Optical Science Center
University of Arizona
Tucson, Arizona 85721

ABSTRACT

The crescent phenomenon in the electrophoresis experiment is due to the viscous fluid-dynamic mechanism of the system of charged particles with finite size in the solution. This phenomenon is enhanced if the charged particles are so big that become impermeable to the membranes at the ends of the cell.

*Work supported in part by U.S. National Aeronautics and Space Administration Contract NAS 8-29566.

In the electrophoresis experiments, it is frequently observed the so-called crescent phenomenon: the charged fluid under applied electric field which is parallel to the tube wall will move in different directions across the tube cross section. The fluid near the wall and that at center are moving in opposite directions i.e. the negative and positive flows (Fig. 1). This crescent phenomenon is further amplified in a tube with closed ends because of the liquid circulation in the form of a closed double loop (Fig. 2).[1,2] This phenomenon is also observed in the electrophoresis experiment in the Apollo 16 spacecraft during its flight mission to the moon.[1]

This phenomenon was characteristically explained by Fan[1] as a result of the simultaneous action of electrophoretic motion in the center of the tube and the electro-osmosis effect near the wall. Due to the existence of double layer[3] in a charged fluid, the charge distribution becomes non-uniform near the tube wall. Furthermore, the velocity will be correspondingly non-uniform due to the fluid shearing force. Therefore, there will be possible negative flow near the wall. This would be a satisfactory qualitative explanation of the crescent phenomenon if all the component charged particles in the solution have the same kind of charge (either positive or negative). However, in an electrophoresis experiment, there exist both positive and negative charged particles. The contributions of opposite ions to the double layer electrostatic potential are just opposite (Fig. 3). This cancellation effect will cause very small effect of charge non-uniformity

on the velocity non-uniformity. This greatly reduces the contribution of electroosmosis effect to the crescent phenomenon. Then it is interesting to see the other possibility to produce the crescent phenomenon. We shall show following that there is a purely viscous fluid-dynamic mechanism which never involve any electrostatic double layer effect.

There were two sets of electrophoretic experiments in the Apollo moon mission: Apollo 14[4] and Apollo 16[1]. They have the same experimental apparatus but different samples. The charged particles in the two samples have different sizes:

$$\frac{d}{\delta} < 0.1 \qquad \text{(Apollo 14)}$$
$$\frac{d}{\delta} > 100 \qquad \text{(Apollo 16)} \qquad (1)$$

where d is the diameter of the charged particle and δ is the surrounding double layer thickness. The charged fluid in Apollo 14 experiment is more like a continuous charged fluid whereas the charged particles in the sample of Apollo 16 experiment is rather big, and the continuous fluid will not be an appropriate picture. The motion of big particles must be taken into consideration.

According to the theory of Brownian motion, a particle moving in a fluid with velocity $\vec{v}_p$ is acted by the surrounding medium a force of the form

$$\vec{F}_m = -\zeta \vec{v}_p + \vec{F}_f \qquad (2)$$

where $\vec{F}_f$ is the fluctuation force which will vanish after averaging. ζ is the friction constant. The average force is called the frictional force

$$\langle \vec{F}_m \rangle = -\zeta \vec{v}_p$$

It is known that the bigger the particle the smaller the fluctuation force $\vec{F}_f$ in comparison with the frictional force $-\zeta \vec{v}_p$. Hence for a large particle (with size much greater than that of fluid molecules), it is good and reasonable approximation to neglect the fluctuation force and write

$$\vec{F}_m \simeq -\zeta \vec{v}_p \qquad (3)$$

With this approximation, we can derive the fluid-dynamic equation for a system of large charged particles in a solution:[5]

$$mn \frac{d}{dt} \vec{v} = -\zeta \left[\vec{J} \mp \mu n \vec{E} \right] - \nabla p + \eta \nabla^2 \vec{v} + \left(\eta + \frac{\nu}{3} \right) \nabla (\nabla \cdot \vec{v}) + \vec{F}_B^{ext} \qquad (4)$$

(positive / negative charge)

where m is the mass of the charged particle, μ the mobility, $\vec{E}$ the electric field. n is the charged particle density, $\vec{J} = n \vec{v}$ the charged particle circuit density, $\vec{v}$ the velocity field and p the partial pressure of the system of charged particle. η and ν are the two stress constant of the charged fluid. $\vec{F}_B^{ext}$ is the force density due to external forces in addition to the electric field $\vec{E}$.

Next, we shall consider the crescent phenomenon. For a simple demonstration we consider a charged system bounded by two planes at $y = \pm L$, the externally applied field $\vec{E}$ is in the x-direction. We assume the length of the cell Δx is so large that we can neglect the edge effect, i.e., we only consider the fluid behavior at where far away from the two ends. In steady state, the velocity is in x-direction and has spatial y-variation only. Furthermore, we neglect all the electrostatic screening effects, i.e. the existence of double layers. Then there is no spatial density, pressure or electric field variation in the y-direction. We have

$$\vec{E} = [\, E, 0, 0 \,] \tag{5}$$

$$\vec{v} = [\, v(y), 0, 0 \,] \tag{6}$$

$$\vec{J} = [\, n v(y), 0, 0 \,] \tag{7}$$

and

$$\vec{F}_B^{ext} = 0 \tag{8}$$

where E, n are constants. Then we have

$$\nabla \cdot \vec{v} = 0$$

and

$$\frac{d}{dt} \vec{v} = \left(\frac{\partial}{\partial t} + \vec{v} \cdot \nabla \right) \vec{v} = 0$$

The x-component of equation (4) gives

$$-5n\left[v(y) \mp \mu E\right] + \eta \frac{d^2}{dy^2} v(y) = 0 \qquad (9)$$

or

$$\left[\frac{d^2}{dy^2} - K^2\right] v(y) = \mp \mu K^2 E \qquad (9')$$

where

$$K = \sqrt{\frac{5n}{\eta}} \qquad (10)$$

is a characteristic constant with dimension of inverse length.

We consider the special case that the two ends of the cell is <u>impermeable</u> to the big charge particles. Because of the circulation due to mass conservation there exists negative flow (Fig. 2). The velocity will vanish at $y = \pm L_s$ ($L_s < L$).
Using this condition, we can get the velocity distribution by solving eq. (9').

$$v(y) = \pm \mu E \left\{ 1 - \frac{\cosh Ky}{\cosh KL_s} \right\} \qquad (11)$$

The typical curve of v(y) is shown in Fig. 4. The constant Ls is determined from the mass conservation, i. e. rate of positive flow equals the rate of negative flow.

$$\int_{-L_s}^{L_s} dy\, n v(y) = \int_{-L}^{-L_s} + \int_{L_s}^{L} dy\, n v(y) .$$

The result is

$$L_s = \frac{1}{K} \cosh^{-1}\left[\frac{\sinh KL}{KL}\right] . \qquad (12)$$

It is shown in Fig 5.

Substituting eq. (12) into (11), we can rewrite the velocity field as

$$v(y) = \pm \mu E \left\{ 1 - \frac{KL}{\sinh KL} \cosh Ky \right\} \qquad (11^1)$$

Then we have the velocities at the center

$$v(0) = \pm \mu E \left\{ 1 - \frac{KL}{\sinh KL} \right\} \qquad (13)$$

and at the wall

$$v(\pm L) = \pm \mu E \left\{ 1 - KL \coth KL \right\} \qquad (14)$$

The KL -dependence of center velocity $v(0)$ [Forward Flow] and Wall Velocity $v(\pm L)$ [Back Flow] are shown in Fig. 6. For a given L, the typical velocity fields at different value of K are shown in Fig. 7.

The characteristic effect of the shearing stress can be clearly seen from Figs. 5, 6 and 7. For given L, ζ ($\propto \mu$) , E, the smaller shearing stress constant η (the bigger value of K), the forward flow velocity will increase and approach the upper limit $\pm \mu E$, (the value in the absence of shearing stress). The back flow region will shrink to the wall and form a very strong surface backward current $V(\pm L)$ due to the mass conservation.

For bigger value of shearing constant η (K is smaller), due to the higher viscous force, both backward and forward velocities are smaller. Then the crescent phenomenon is reduced.

Equation (9) can be rewritten as

$$n\left[-\zeta v(y) \pm \mu E\right] + \eta \frac{d^2}{dy^2} v(y) = 0, \qquad (9'')$$

where q is the particle charge. In this paper, we have consider n as constant by neglecting the double layer effect. However, in case of system of small charge particles (of one kind of charge), this electrostatic screening double layer effect would be probably important because the system are more like continuous charge fluid. Then the charge density will have spatial y-variation, q n (y). From eq. (9'') there is corresponding y-variation in the velocity v(y). This is the electro-osmosis effect. In Fan's calculation[1], he neglected the term $-n\zeta v(y)$ in eq. (9''). This approximation is only reasonable where $|v(y)| \ll \mu E$. The calculation of electro-osmosis effect by using eq. (9'') would be interesting for further investigations.

As a conclusion, we have shown that, in addition to the electro-osmosis effect, the viscous fluid mechanism can contribute to the crescent phenomenon in the electrophoresis experiment. This is a result of viscous charged fluid with shearing stress force. The velocity will be non-uniform over the tube cross section: it is bigger at center and smaller at the wall. Then it is possible to have back flow near the wall. In a system with ends impermeable to the charged particles,

the back flow is very large because of the circulation of these particles. This will reduce the forward velocity from its maximum value μE which is the velocity in the absence of shearing force. [Eq (13)] For small particles which are permeable to the end walls, there will be no back flow and the crescent phenomenon will not be observed. This is a very possible reason that crescent phenomenon is observed in Apollo 16 experiment rather than the Apollo 14 experiment.

For mathematical simplicity, we consider here a system bounded by two planes $y = \pm L$. For a real experiment in circular tube, the cylindrical coordinates must be used. However, there will be no qualitative change.

REFERENCES

1. C. Fan, "Convection Phenomena in Electrophoresis Separation" IMSC-MREC TR D306300, Lockheed Missiles and Space Company, Huntsville, Ala., December, 1972.
2. A. Strickler and T. I. Sacks, "Continuous Free-Film Electrophoresis: The Crescent Phenomenon," Beckman Instruments, Inc., May 11, 1970.
3. J. Th. G. Overbeek and J. Lijklema: "Electric Potentials in Colloidal Systems," in M. Bier: "Electrophoresis" Vol. II.
4. E. C., McKannan, et al. "Electrophoresis Separation in Space - Apollo 14". NASA TMX-64611, Marshall Space Flight Center, Ala., August, 1971.
5. T. W. Nee, ~~in preparation, to be published.~~ and "Theory of Isotachophoresis (Displacement Electrophoresis, Transphoresis)" Submitted to "Journal of Chromatography".

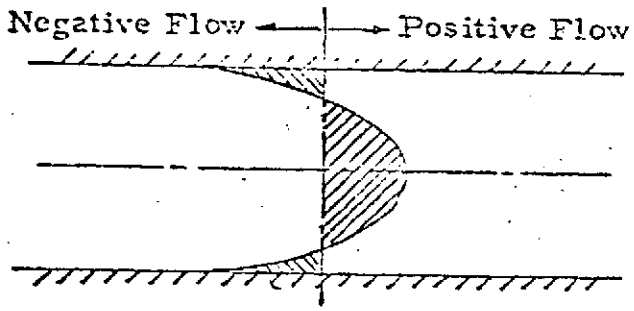

Fig. 1 – The Crescent Phenomenon

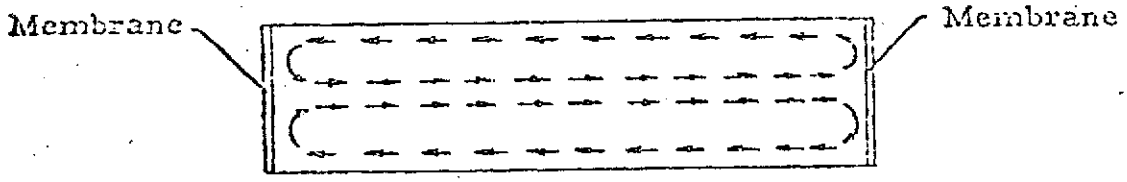

Fig. 2 – Liquid Circulation Due to Mass Conservation Inside a Cell

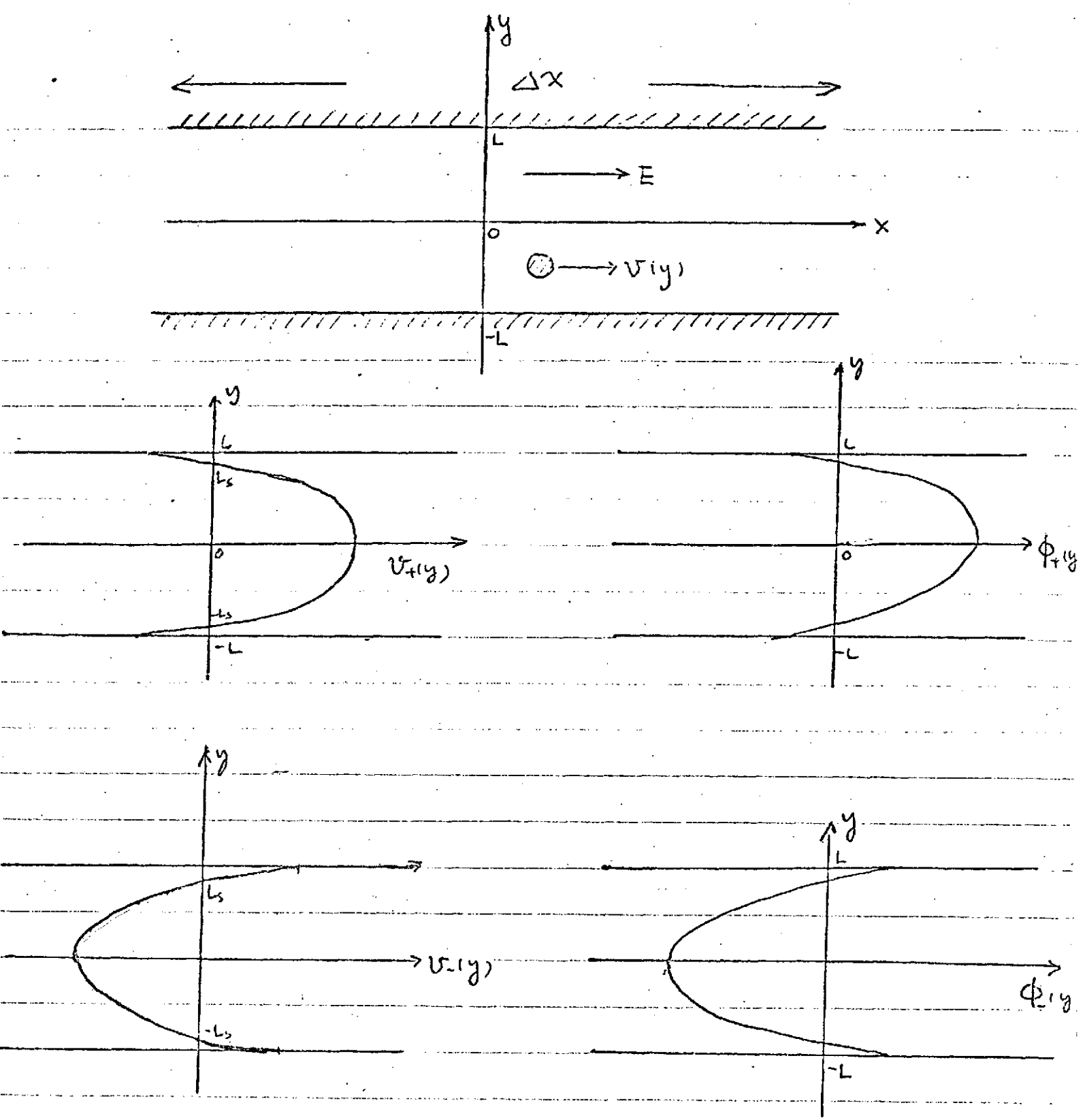

Fig. 3

Fig 4

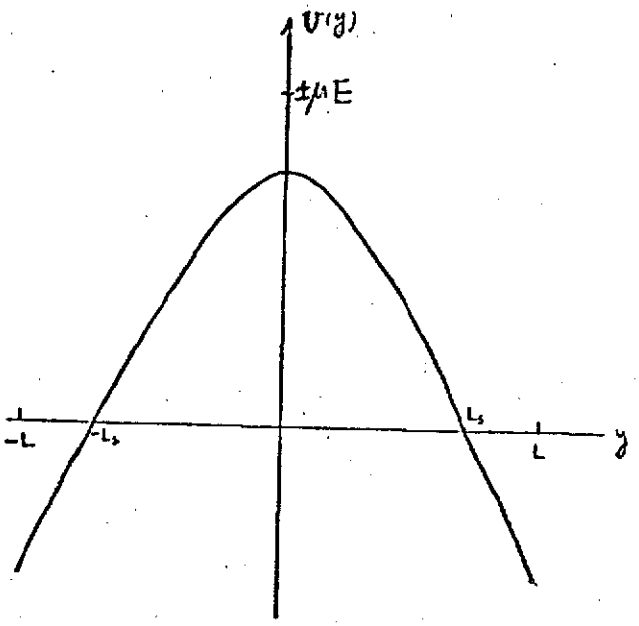

Fig 5

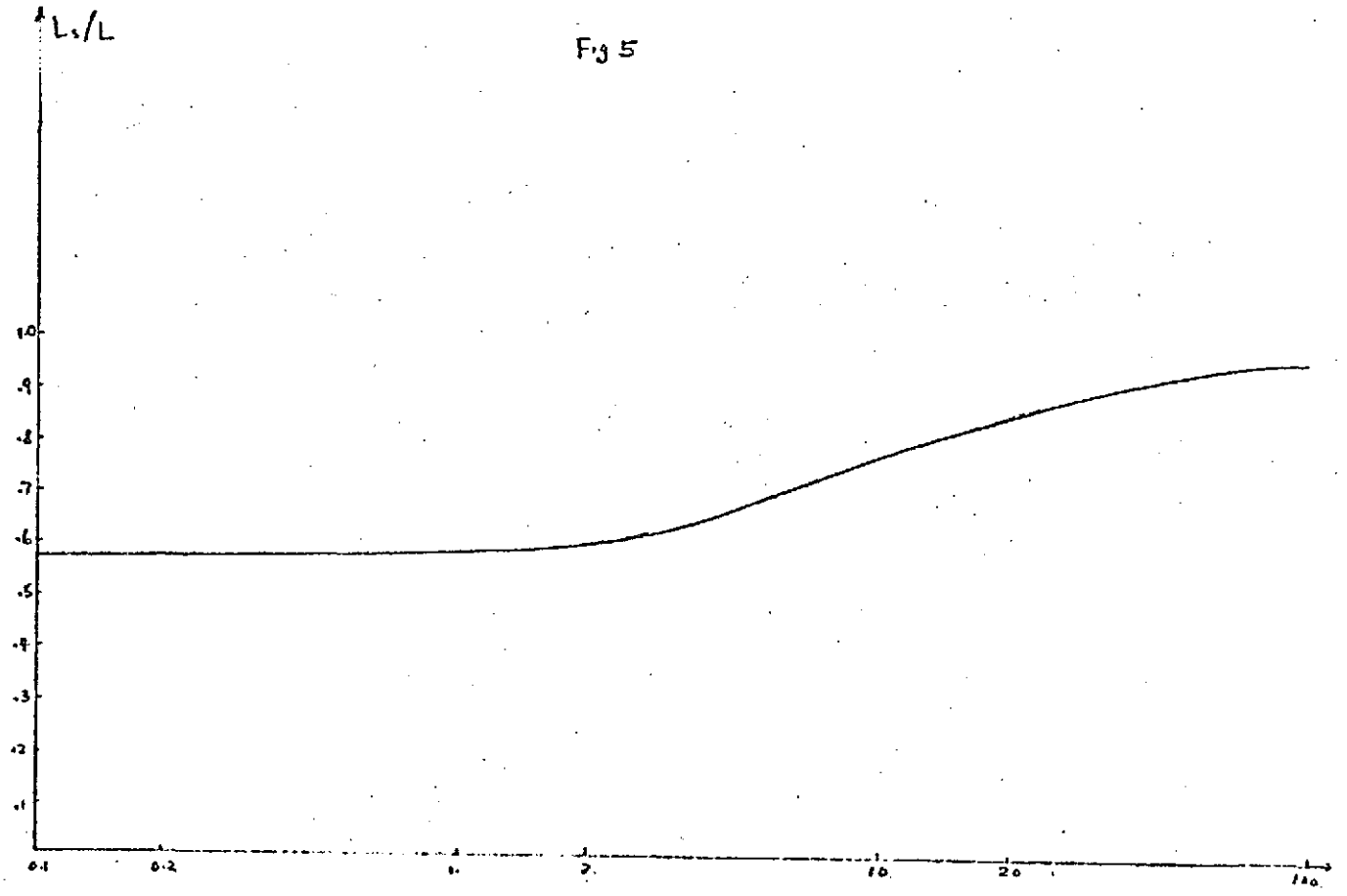

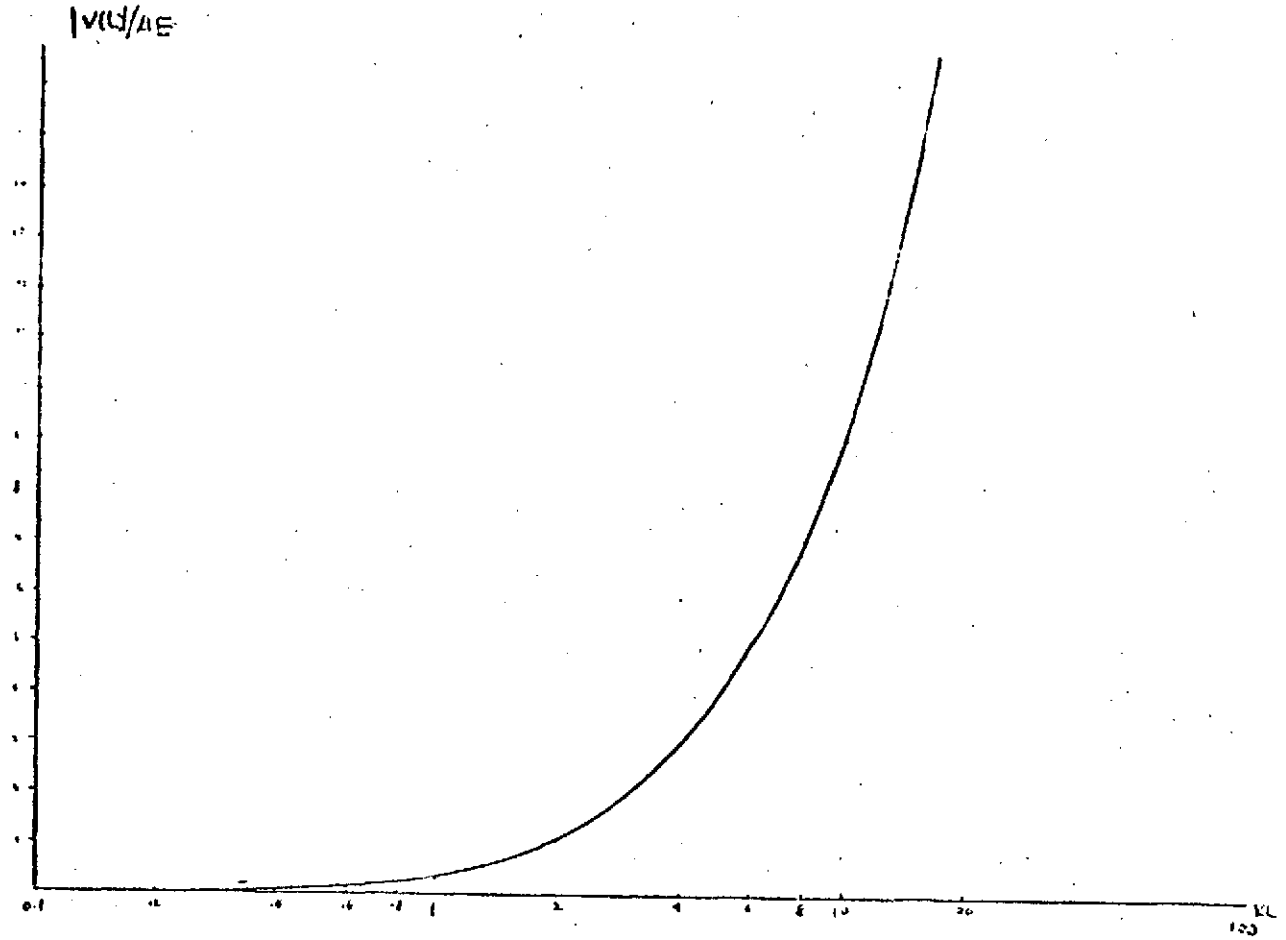

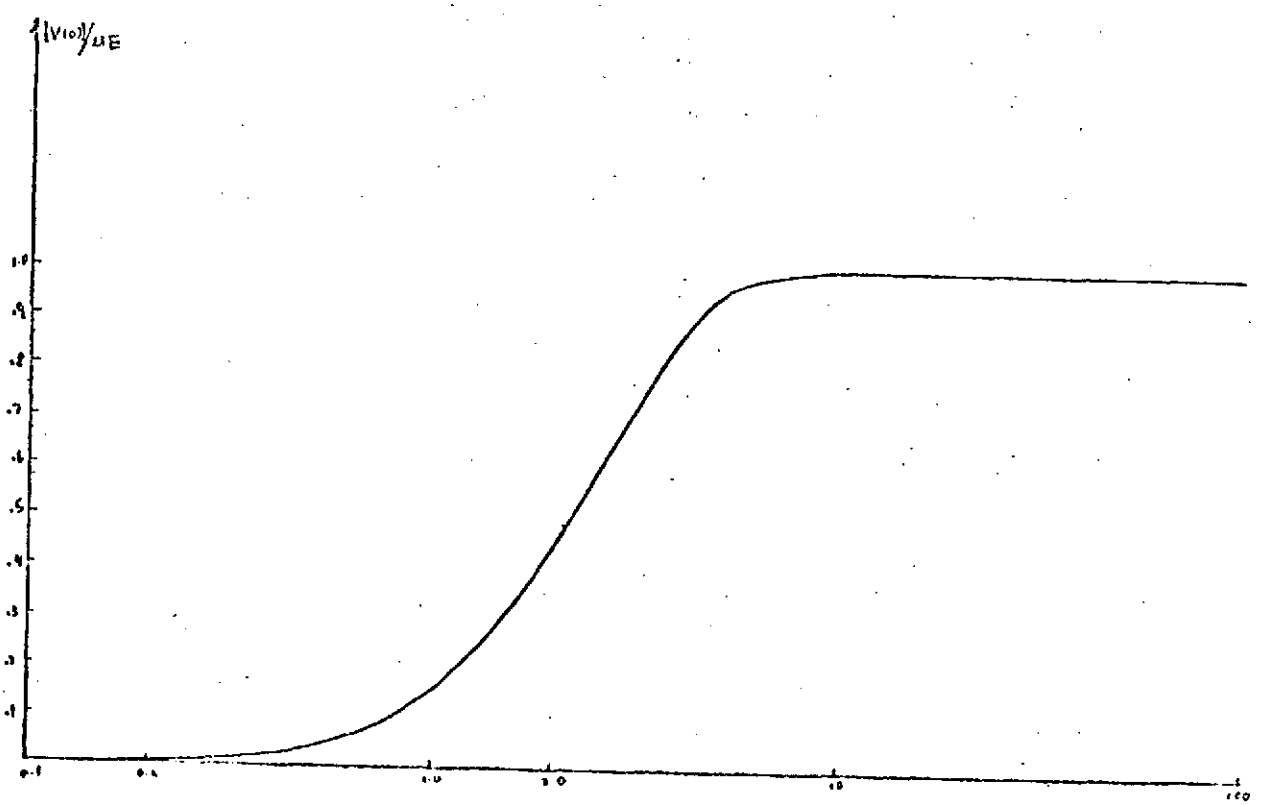

Fig. 6

B-40

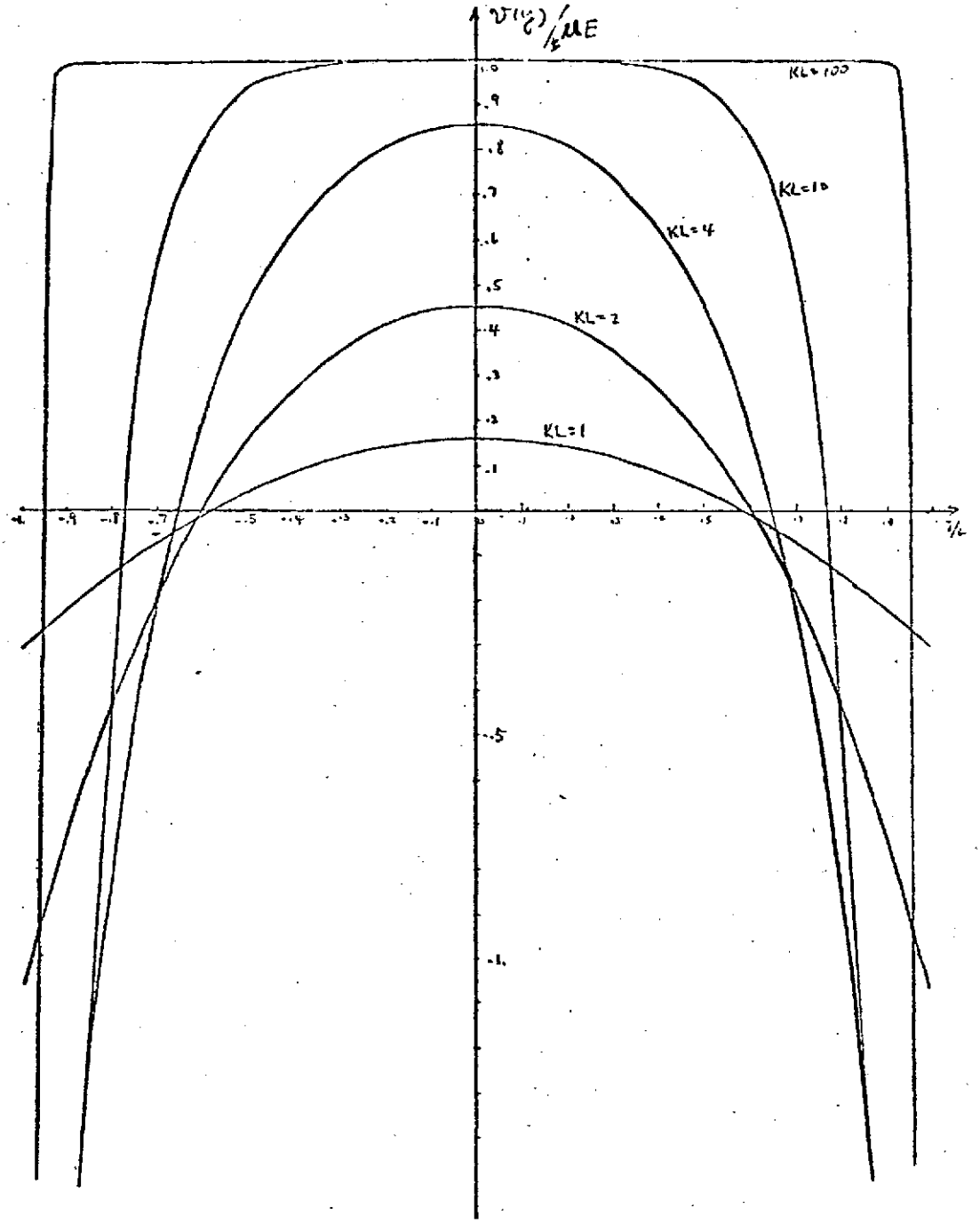

Fig. 7

Abstract of a Paper on the Theory of Isotachophoresis
Now in Preparation

by

Dr. Gerald T. Moore

Partial differential equations describing the migration of ions through a stationary medium under the influence of an electric field are developed and then applied to the analysis of steady-state and unsteady-state properties of isotachophoresis in one dimension. The original equations are three dimensional, contain terms describing ion diffusion, and also allow the possibility of arbitrary temperature and mobility distributions. It is shown that charge imbalance can be neglected to an excellent approximation, and that the electric field is determined in terms of the ion distributions by an equation similar to Poisson's equation. The solution of this equation is trivial for one-dimensional systems. Analysis of a one-dimensional system with constant temperature and mobilities shows that the transition region between the two ion species in the steady state has a finite thickness (typically 10^{-3} to 10^{-2} cm) determined by the effect of diffusion. The exact shape of the transition region is discussed. The steady state with an arbitrary number of ions present can be determined completely by solving one

ordinary first-order differential equation. The unsteady state is analyzed using a model in which the diffusion constants approach zero. The approach to the steady state from an arbitrary initial state is particularly simple if only a leader ion and a terminator ion are present. This is described using the method of characteristics. The nonlinear partial differential equation being solved is not by itself sufficient to determine the evolution of the system after the shock front (boundary between leader and terminator) becomes sharp, but must be supplemented by the relation between the instantaneous speed of the front and the discontinuity in ion density.

Studies on Possible Instabilities for Electrophoresis*

H.S.T. Shih, M. O. Scully and T. W. Nee

Department of Physics and Optical Science Center

University of Arizona, Tucson, Arizona 85721

*Work supported in part by U. S. National Aeronautics and Space Administration Contract NAS8-29566.

Studies On Possible Instabilities For Electrophoresis

Laminar flows are usually assumed in analytical studies for electrophoretic phenomena. Instabilities could arise however. One example is due to the combined effects of large electric fields and temperature variations in the charged fluids. It is analogous to the Benard instability (for a layer of fluid heated from below) in Hydrodynamics[1], with the electric field E playing now the role of gravity. In order to gain understanding to the effects of turbulence in electrophoretic problems, we set out, as a first step, to investigate the Benard problem by using techniques developed in the laser theory[2] and in the general theories of non-equilibrium statistical mechanics.

As a preliminary step we study the "Benard instability" in very much the same spirit as in the Lamb's semi-classical theory of "laser instability".[3] Corresponding to Maxwell equations, hydrodynamic equations are employed. By restricting our attention to the threshold region, the normal-mode method is used and an equation of the form

$$(R - R_c)\, V - \xi V^3 = 0$$

is obtained at steady state. R is the Rayleigh number and the mode amplitude V is the "order parameter". The saturation term ξV^3 is due, in our theory, not to the nonlinear constituent relations like in the laser case, but to the non-linearities inherent in the hydrodynamic equations themselves. In other words, the convective processes are responsible. A simple application of the result is given to explain the experimentally observed dependence of the Nusselt number on the Rayleigh number.

Langevin-type equations can then be obtained for the coupled modes involving both velocity and temperature variations.

[1] S. Chandrasekhar, "Hydrodynamic and Hydromagnetic Stability", Oxford University Press (1961).

[2] V. DeGiorgio and M.O. Scully, Phys. Rev. A2, 1170 (1970).

[3] W.E. Lamb, Jr., Phys. Rev. 134, A1429 (1964).

Following is a rough draft of some of the analysis carried out. It will be refined and included in the next report.

1. NL - Coupled equations on ∇_j and δT
2. Normal-mode approach and the threshold condition:

   A Review
3. Steady State solutions near threshold
4. Heat conduction

1. Nonlinear coupled equations on v_z and δ T

Let us start with the hydrodynamic equations in the following form[1],

$$\left.\begin{aligned} &\frac{\partial}{\partial t}\rho + \nabla\cdot(\rho\bar{v}) = 0 \\ &\rho\left(\frac{\partial}{\partial t} + \bar{v}\cdot\nabla\right)\bar{v} + \nabla\cdot\bar{\bar{P}} = \rho\bar{f} \\ &\rho\left(\frac{\partial}{\partial t} + \bar{v}\cdot\nabla\right)e + \nabla\cdot\bar{J}_q = -\bar{\bar{P}}:\nabla\bar{v} \end{aligned}\right\} \quad (1)$$

where

ρ = liquid density

$\bar{v}$ = fluid velocity

e = internal energy density

$\bar{f}$ = body force = $g\hat{z}$

$\bar{\bar{P}}$ = stress tensor

$\bar{J}_q$ = heat flux

For incompressible fluid, internal energy e and density ρ can be expressed in terms of the temperature T as,

$$\delta e = c_v \delta T \quad (2)$$

$$\rho \cong \rho_0(1 - \alpha T') \quad (3)$$

where

$$T' = T - T_{ref}$$

In addition, let us take the linear flux - force relations,

$$\bar{\bar{P}} = p\,\bar{\bar{I}} - \eta(\nabla\bar{v})_s \tag{4}$$

$$\bar{J}_q = -\lambda \nabla T \tag{5}$$

where

p = (isotropic) pressure

$(\nabla\bar{v})_s$ = velocity strain = $\vec{\nabla}\bar{v} + \bar{v}\overleftarrow{\nabla}$ $\left(= \partial_i v_j + \partial_j v_i\right)$

η = viscosity

λ = thermal conductivity

Substitute Eq.s (2-5) into (1), we obtain

$$\nabla\cdot\bar{v} = -\frac{\alpha}{1-\alpha T}\left(\frac{\partial}{\partial t} + \bar{v}\cdot\nabla\right)T'$$

$$\rho\frac{\partial}{\partial t}\bar{v} + \rho\,\bar{v}\cdot\nabla\bar{v} - \eta(\nabla^2\bar{v} + \nabla\nabla\cdot\bar{v}) + \nabla p = \hat{z}\rho g \tag{6}$$

$$\left(C_v\rho\frac{\partial}{\partial t} + C_v\rho\,\bar{v}\cdot\nabla - \lambda\nabla^2\right)T' = -p\nabla\cdot\bar{v} + \eta(\nabla\bar{v})_s:\nabla\bar{v}$$

Note that we have assumed <u>linear</u> constituent relations (Eq.s 3-5), and that nonlinear efforts are due solely to the nonlinearities of the hydrodynamic equations (1). Especially, the convection terms ($\rho\bar{v}\cdot\nabla\bar{v}$ and $C_v\rho\bar{v}\cdot\nabla$)

in Eq. (1) are mainly responsible for the saturation effect as will be shown later.

Using the small "expansion coefficient" α as the perturbation parameter in the same spirit as in the so-called Boussinez approximation[2], we obtain from Eq. (6),

$$\left.\begin{aligned} &\nabla\cdot\bar{v}=0 \\ &(\partial_t-\nu\nabla^2)\,\bar{v}+\bar{v}\cdot\nabla\bar{v}+\frac{1}{\rho_0}\nabla p=\hat{\zeta}\,(g-\alpha g T') \\ &(\partial_t-\kappa\nabla^2)\,T'+\bar{v}\cdot\nabla T'=\kappa\frac{\eta}{\lambda}\left[\nabla^2 v^2+(\partial_j v_i)(\partial_i v_j)\right] \end{aligned}\right\} \quad (7)$$

where

ν = Kinematic viscosity = η/ρ_0

κ = coefficient of thermometric conductivity = $\frac{\lambda}{\rho_0 C_v}$

Eq. (7) is easily solved if $\alpha = 0$:

$$\bar{v} = \bar{v}^{(0)} = 0$$

and, $p = p^{(0)}$, $T' = T^{(0)}$ are simply solvable through,

$$\frac{1}{\rho_0}\nabla p^{(0)} = \hat{\zeta} g$$

$$-\kappa\nabla^2 T^{(0)} = 0$$

i.e.,

$$\left.\begin{aligned} T^{(0)} &= \hat{\zeta}\,(T_1-\beta z) \\ p^{(0)} &= p_1^{(0)}+\rho_0 g z \end{aligned}\right\} \quad (8)$$

Let us now write, for $\alpha \neq 0$,

$$\left.\begin{aligned} T' &= T^{(0)} + \delta T \\ \bar{v} &= \bar{v}^{(0)} + \delta \bar{v} = \bar{v} \\ p &= p^{(0)} + \delta p \end{aligned}\right\} \qquad (9)$$

Eq. (7) now gives,

$$\nabla \cdot \bar{v} = 0 \qquad (10)$$

$$(\partial_t - \nu \nabla^2 + \bar{v} \cdot \nabla)\bar{v} + \frac{1}{\rho_0} \nabla \delta p = -\hat{z} \alpha g \delta T \qquad (11a)$$

$$(\partial_t - \kappa \nabla^2 + \bar{v} \cdot \nabla) \delta T = -\beta \hat{z} \cdot \bar{v} + \kappa \left(\frac{\eta}{\lambda}\right)[\nabla^2 v^2 + (\partial_j v_i)(\partial_i v_j)] \qquad (11b)$$

With the aid of the identity,

$$\nabla \times \nabla \phi = 0$$

We eliminate the presence of δp by taking curl of the Eq. (11a) which gives,

$$(\partial_t - \nu \nabla^2)(\nabla \times \bar{v}) + \nabla \times (\bar{v} \cdot \nabla \bar{v}) = -\nabla \times (\hat{z} \alpha g \delta T) \qquad (12)$$

Note that, subject to the divergenceless condition of Eq. (10), the velocity vector $\bar{v}$ may be equivalently specified by two independent scalars, e.g., $\bar{v} \cdot \hat{z} = v_z$ and $(\nabla \times \bar{v}) \cdot \hat{z} \triangleq \zeta$.

From Eq.s (11b) and (12), we see that ζ obeys the following equation,

$$(\partial_t - \nu\nabla^2)\underbrace{(\nabla\times\bar{v})_z}_{\zeta} = -\hat{z}\cdot[\nabla\times(\bar{v}\cdot\nabla)\bar{v}] \tag{13}$$

It states that, to 1st order in $\bar{v}$, $\hat{z}\cdot(\nabla\times\bar{v})$ is not affected by gravity and is purely dissipative. We therefore will concentrate on the behavior of v_z alone from now on.

Taking Curl once more on Eq. (12) and retain its $\hat{z}$-component, we see that v_z satisfies the coupled-equations with δT as,

$$(\partial_t - \nu\nabla^2)\nabla^2 v_z + \hat{z}\cdot\{(\nabla^2 - \nabla\nabla\cdot)[(\bar{v}\cdot\nabla)\bar{v}]\} = \alpha g \nabla_\perp^2 \delta T$$

$$(\partial_t - \kappa\nabla^2)\delta T + \bar{v}\cdot\nabla\delta T = \beta v_z + \kappa\frac{\eta}{\lambda}[\nabla^2\bar{v}^2 + (\partial_j v_i)(\partial_i v_j)] \tag{14}$$

where $\bar{v}$ can be expressed in terms of v_z as,

$$\bar{v} = \hat{z}v_z + \bar{v}_\perp$$

$$= \left[\hat{z} + (\nabla_\perp^2)^{-1}(-\nabla_\perp\partial_z)\right]v_z \tag{15}$$

This is obtained[+] easily from Eq. (10)

$$\nabla\cdot\bar{v} = 0$$

and assuming [consistent with Eq. (13)],

$$\hat{z}\cdot(\nabla\times\bar{v}) = 0$$

+ See Appendix A.

2. Normal mode approach and the threshold condition - A Review

In the limit of diminishingly small $\bar{v}$ and δT, nonlinear terms in Eq. (14) may be dropped to give

$$\left.\begin{aligned}(\partial_t - \nu\nabla^2)\nabla^2 v_z &= \alpha g \nabla_\perp^2 \delta T \\ (\partial_t - \kappa\nabla^2)\delta T &= \beta v_z\end{aligned}\right\} \qquad (2\text{-}1)$$

For steady state solutions, they combine to yield a single equation on , in the following simple form,

$$[(\partial_z^2 + \nabla_\perp^2)^3 - R'\nabla_\perp^2]\, v_z = 0 \qquad (2\text{-}2)$$

where

$$R' = \frac{\alpha g \beta}{\kappa \nu} = R/k^4$$

$$R = \text{Rayleigh number} = \frac{\alpha g \beta}{\kappa \nu} l^4$$

For simplicity we restrict our attention to the case of free boundaries at $z = 0, h$. It can be shown[2] that as a consequence of the incompressible fluid,

$$\nabla \cdot \bar{v} = 0$$

at the boundaries, we have for the present case the following boundary conditions on v_z ,

$$\left.\begin{aligned} v_z &= 0 \\ \partial_z^2 v_z &= 0 \end{aligned}\right\} \qquad (2\text{-}3)$$

Together with Eq. (2-2), it demands, first of all,

$$v_z = \sum_{n=1}^{\infty} \left(\sin \frac{n\pi}{h} z\right) f^{(n)}(\underline{r}_\perp) .$$

or, expressed in terms of "normal modes":

$$v_z = \sum_{n=1}^{\infty} \int d^2\underline{k}_\perp \, A_{(n)}(\underline{k}_\perp) \, \varphi_{n,\underline{k}_\perp}(\underline{r}) \qquad (2\text{-}4)$$

where

$$\varphi_{n,\underline{k}_\perp}(\underline{r}) = \left(\sin \frac{n\pi}{h} z\right) e^{i \underline{k}_\perp \cdot \underline{r}_\perp} \qquad (2\text{-}5)$$

For each of the normal modes specified by Eq. (2-5), Eq. (2-2) for the onset of the instability demands also

$$\left[\left(\frac{n\pi}{h}\right)^2 + k_\perp^2\right]^3 - R' k_\perp^2 = 0 \qquad (2\text{-}6)$$

Graphically, this equation is represented in Fig. 1. The minimum value of such R' which is the instability threshold is then easily found,[2]

$$R_c' = \frac{\left(\frac{3}{2}\pi^2\right)^3}{\frac{1}{2}\pi^2} \times \frac{1}{h^4} \simeq 657.541\, h^{-4} \qquad (2\text{-}7)$$

for n = 1, and

$$\sqrt{k_\perp^2} = k_\perp^c = \frac{\pi}{\sqrt{2}\,h} \cong \frac{2.2214}{h} \qquad (2\text{-}8)$$

.

3. Steady State Solution near threshold.

Let us further restrict our attention to a small region near the threshold,

$$R' = R_c'(1+\epsilon)$$
$$0 < \epsilon \ll 1 \qquad (3\text{-}1)$$

Following the discussion of § 2, it is clear that even in this limit, it will not be a good approximation to treat the Bénard instability as consisting of a single "normal mode". Indeed, all the modes with $n = 1$ and $|\vec{k}_\perp| = k_\perp^c$ will be "excited". We thus write approximately

$$v_z \cong (\sin \tfrac{\pi}{h} z) \int_0^\pi \frac{d\varphi}{\pi} V(\varphi) \left[e^{i k_\perp^c \hat{\varphi} \cdot \vec{r}_\perp} + c.c. \right] \qquad (3\text{-}2)$$

and

$$\delta T \cong (\sin \tfrac{\pi}{h} z) \int_0^\pi \frac{d\varphi}{\pi} \Pi(\varphi) \left[e^{i k_\perp^c \hat{\varphi} \cdot \vec{r}_\perp} + c.c. \right] \qquad (3\text{-}3)$$

where $\hat{\varphi}$ = unit directional vector which lies in the transverse (x-y) plane and makes angle φ with say the x-axis.

Eq.s (14, 15) now become, in the steady state ($\partial_t = 0$)

$$-\nu k_c^4 v_z + f_v^{(2)} \cong -\alpha g (k_\perp^c)^2 \delta T \qquad (3\text{-}4)$$

$$(K k_c^2 + \bar{v}\cdot\nabla)\,\delta T \cong \beta v_z \tag{3-5}$$

and,

$$\bar{v} = \left[\hat{z} + \frac{1}{(k_\perp^c)^2}\,\nabla_\perp \partial_z\right] v_z \tag{3-6}$$

where

$$f_v^{(2)} = \hat{z}\cdot\left[(\nabla^2 - \nabla\nabla\cdot)(\bar{v}\cdot\nabla\bar{v})\right]$$

$$k_c^2 = \left(\frac{\pi}{h}\right)^2 + (k_\perp^c)^2 \tag{3-7}$$

Combining Eq.s (3-4) and (3-5), we deduce,

$$(k_\perp^c)^2 (R' - R_c') v_z + M_v^{(2)} + \frac{1}{K\nu}\,\bar{v}\cdot\nabla f_v^{(2)} = 0 \tag{3-8}$$

where

$$M_v^{(2)} = \frac{1}{K\nu}\left[K k_c^2 f_v^{(2)} - \nu k^4 \bar{v}\cdot\nabla v_z\right] \tag{3-9}$$

$$R_c' = (k_c)^6 / (k_\perp^c)^2$$

Let us further assume that the transverse dimensions are infinitely large so that Eq.'s (3-2), (3-3) simplify as

$$v_z \cong V(\sin \tfrac{\pi}{h} z) \int_0^{\pi} \frac{d\varphi}{\pi} \left[e^{i\eta(\varphi) + i k_\perp^c \hat{\varphi} \cdot \bar{r}_\perp} + c.c. \right] \tag{3-10}$$

$$\delta T \cong \Pi (\sin \tfrac{\pi}{h} z) \int_0^{\pi} \frac{d\varphi}{\pi} \left[e^{i\eta(\varphi) + i k_\perp^c \hat{\varphi} \cdot \bar{r}_\perp} + c.c. \right] \tag{3-11}$$

Inserting Eq. (3-10) into Eq.'s (3-8), (3-9) and (3-7), and multiply the resultant equation by $(\sin \frac{\pi}{h} z) \cos(k_\perp^c \hat{\varphi} \cdot \bar{r}_\perp)$ and then integrated over z and $\bar{r}_\perp$, we obtain,

$$(R - R_c) V - \mathcal{F} V^3 = 0 \tag{3-12}$$

where

$$R = \frac{\alpha g \beta}{\kappa \nu} h^4 = R' h^4 \quad = \text{Rayleigh number}$$

$$R_c = R_c' h^4 = \frac{(k_c)^6}{(k_\perp^c)^2} h^4 \quad = \text{Critical Rayleigh number}$$

and

$$\mathcal{F} = \frac{h^4}{(k_\perp^c)^2} \frac{1}{\kappa \nu} \times \left(\frac{-1}{V^3}\right) \times \int_0^h \frac{2\,dz}{h} \int dx (\sin \tfrac{\pi}{h} z)(\cos k_\perp^c x)\, \bar{v} \cdot \nabla f_v \Big|_{v=1}$$

The evaluation of ξ is cumbersome and will (?) be pursued later.+

From Eq. (3-12) it follows

$$V^2 \simeq (R - R_c)/\xi \qquad (3\text{-}13)$$

+ Need to confer with M.O.S.

4. Heat Conduction

We shall now apply the results obtained in the previous sections to explain the experiments of Silverston on the measurements of heat transfers in various liquids.[2,3] Silverston's result is shown in Fig. 2.

The heat conduction rate measured is,

$$\frac{d}{dt}Q = \iint d^2\vec{a}\cdot\bar{\bar{J}}_q$$

$$= -\iint dx\,dy\ (\bar{\bar{J}}_q\,\hat{z})_{z=0} \qquad (4\text{-}1)$$

In our approximation the heat flux $\bar{\bar{J}}_q$ is linear on the gradient of T,

$$\bar{\bar{J}}_q = -\lambda\nabla T$$

Combining it with Eq.'s (9) and (8), we see

$$\bar{\bar{J}}_q = -\lambda(\nabla T^{(0)} + \nabla\delta T)$$

$$= \lambda\beta\hat{z} - \lambda\nabla\delta T$$

Therefore,

$$\frac{d}{dt}Q = \lambda\beta A - \lambda\iint dx\,dy\ \frac{\partial}{\partial z}\delta T \qquad (4\text{-}2)$$

where A = area of the heat conducting plates.

The Nusselt number N_u is defined as,

$$N_u \equiv \frac{\frac{dQ}{dt}}{\lambda \beta A}$$

Thus,

$$N_u = 1 + \frac{-\lambda \iint q_x \, dy \, \frac{\partial}{\partial z} \delta T}{\lambda \beta A} \qquad (4\text{-}3)$$

$$= 1 - \frac{1}{\beta} \iint \frac{dx\,dy}{A} \, \partial_z \, \delta T$$

For the region near the threshold, Eq. (3-4) implies,

$$\delta T \cong \frac{\nu k_c^4}{\alpha g (k_1^c)^2} v_z - \frac{f_v^{(2)}}{\alpha g (k_1^c)^2}$$

and thus,

$$N_u = 1 - \frac{1}{\beta} \iint \frac{dx\,dy}{A} \frac{\nu k_c^4}{\alpha g (k_1^c)^2} \partial_z v_z + \frac{1}{\beta} \iint \frac{dx\,dy}{A} \frac{1}{\alpha g (k_1^c)^2} \partial_z f_v^{(2)}$$

With v_z given by Eq. (3-10), it is obvious that the 2nd-term here vanishes. We thus conclude, using Eq. (3-13),

$$N_u = 1 + \frac{\alpha V^2}{\beta} = 1 + \frac{\alpha}{\beta \mathcal{F}} (R - R_c) \qquad (4\text{-}4)$$

where

$$\alpha = \int \frac{dx\,dy}{A} \frac{1}{\alpha g (k_\perp^c)^2} \partial_z \frac{f_v^{(2)}}{V^2}$$

$$= \text{Constant} \quad (\text{independent of } V)$$

The dependence of the Nusselt number or the Rayleigh number R as given by Eq. (4-4) compares favorably with the experiment of Fig. 1.

References

1. S.R. De Groot and P. Maxur, "Non-equilibrium Thermodynamics", North-Holland (1962).
2. S. Chandrasekhar, "Hydrodynamic and Hydromagnetic Stability", Oxford University Press (1961).
3. P.L. Silverston, Forsch. Ing. Wes. 24, 29-32 and 59-69 (1958).

Appendix A - Derivation of Eq. (15)

Eq. (15) will now be shown as a consequence of

$$\nabla \cdot \bar{V} = 0 \tag{A.1}$$

$$(\nabla \times \bar{V}) \cdot \hat{z} = 0 \; . \tag{A.2}$$

Rewrite Eq.'s (A.1) and (A.2) in Cartesian co-orders as

$$\partial_z V_z + \partial_x V_x + \partial_y V_y = 0 \tag{A.3}$$

$$\partial_x V_y - \partial_y V_x = 0 \tag{A.4}$$

Using Eq. (A.4), we may eliminate V_y in Eq. (A.3) to give

$$\partial_x \partial_z V_z + (\partial_x^2 + \partial_y^2) V_x = 0$$

or,

$$\nabla_\perp^2 V_x = -\partial_x \partial_z V_z \tag{A.5}$$

And similarly, V_x may be eliminated:

$$\nabla_\perp^2 V_y = -\partial_y \partial_z V_z \tag{A.6}$$

Equations (A.5) and (A.6) may be combined into one vector-equation,

$$\nabla_\perp^2 \bar{v}_\perp = -\nabla_\perp \partial_z v_z$$

or, symbolically,

$$\bar{v}_\perp = -(\nabla_\perp^2)^{-1} \nabla_\perp \partial_z v_z$$

Eq. (15) thus follows immediately.

SECTION C

REPORT BY THE ENGINEERING GROUP

by

M. Coxon and M. J. Binder

INTRODUCTION

1. Introduction.

The first several months of the year, whose activities are the subject of this report, were necessarily spent in reviewing previous work in the field of electrophoresis. Coming to this field without previous experience, our learning process was greatly assisted by discussions with our colleagues in the other groups particularly Dr. M. Bier and Mr. J. O. N. Hinckley of the experimental group.

As a result of these early studies we have become particularly attracted to the possibilities of Isotachophoresis. In consequence the main thrust of our effort has been directed towards a better understanding of the many complex factors affecting the performance of Isotachophoretic devices.

The philosophy underlying our approach has been deliberate and we believe sound. The problems attacked so far have been simplified as far as possible consistent with the retention of the dominant physical characteristics of the system. It is our intention to proceed through a series of successively more realistic models until we arrive at a reasonably complete description of the process of Isotachophoresis for a system involving only simple ions. Until this point in the development of the theory is reached it is unlikely that any meaningful treatment can be attempted of the various anomalous behaviours observed in the separations of macromolecules and living cells.

Specifically our accomplishments to date have been (i) the development of an approximate solution for the structure of an ideal plane front in Isotachophoresis and (ii) preliminary investigations with regard to heat conduction, heat generation and determination of the non-uniform temperature field in an Isotachophoresis column.

This work is discussed in general terms in the succeeding sections of the report while more technical details are given in (Sections 2-5)

2. Isotachophoresis Theory - Structure of the Ionic Species Interface.

An approximate solution has been obtained for the equations governing the structure of the inter-species ionic interface in discrete sample Isotachophoresis in an ideal one-dimensional system, in the presence of a common counterion and in the absence of continuous mobility spectrum spacer ampholytes.

The approximation is reasonably good for values of the Kohlrausch-regulated terminator/leader concentration ratio greater than 0.5. The dependence of interface thickness on mobility and concentration ratios is discussed and results are compared to those of previous workers. Interface thickness is found to be inversely proportional to leader voltage gradient.

The estimates of frontal thicknesses and the details of concentration and electric field gradients in the interface obtained in this work are believed to be superior to those given elsewhere.

This work has been submitted for publication to the Journal of Chromatography and the paper (as submitted) is reproduced in its entirety as Section 2 of this report.

3. Preliminary Investigations of the Temperature Distribution in Isotachophoresis Columns.

We consider the Isotachophoresis to occur in a glass walled column of circular cross-section. The voltage drop along the column is assumed to be independent of the temperature and hence of the radial location. It follows that the current density is then a function of radial location because of the temperature dependence of the electrical conductivity.

For the application which we have in mind (ultimately; e.g. separations involving living cells) relatively small temperature changes can be tolerated over the cross-section of the column. In the case of living cells the permissible temperature range must certainly be between 0°C and 37°C if cell damage is to be avoided. This in turn implies a restriction on the heat generated in either the free solution or supporting medium in the column due to the passage of the electric current.

Present calculations have been based on the following assumptions:

(1) Operation occurs in a gravity free environment

(2) Convective effects may be ignored

(3) The fluid or supporting medium is essentially at rest with the various ionic species drifting through it in the axial direction

(4) The thermal properties (density, specific heat and thermal conductivity) are independent of temperature

(5) The electrical conductivity is a linear function of the temperature over the range of temperatures of interest

(6) The temperature distribution may be obtained as the solution of a conduction problem involving only the radial coordinate and time.

Some further comments are in order with respect to these assumptions.

Assumption (6) will be a good approximation in any longitudinal (axial) region sufficiently far away from any fronts where it is obvious that strong longitudinal temperature gradients must exist. It may be argued that it is precisely in the region of the fronts that we wish to determine the effects of non-uniformities in the temperature distribution. However, the present approach is a legitimate first step towards the more general problem and certainly should permit a first order estimate of the temperature dependence of the species migration velocity profile to be determined. Furthermore it is clear that there is always one region (the terminator) where the heat generation is a maximum and this region is not a sample region. Thus if the maximum design temperature is specified in this region there will be no danger of the sample species becoming overheated. Present calculations will permit the determination of the time taken to reach maximum design temperature and the corresponding maximum electric field strength.

Assumption (2) has been thought to be reasonable in view of assumption (1). However there remains the possibility of electroconvection and further work must be done to determine whether this will be an important factor.

In view of assumption (3) the present results will not apply to any system using a free solution with counterflow.

Assumption (4) has been checked by comparing the "exact" steady-state constant properties solution with the results of a steady-state perturbation analysis which permits variation in the thermal properties with temperature. It appears that the effect of neglecting thermal property variations is very small and that the results of a constant property analysis are conservative. Details of this particular point are discussed in Section 5 of this report.

The problem discussed here appears to have been considered first by Hinckley, Brown and Jones (1972). They considered only a steady-state solution with a constant temperature boundary condition at the outside wall of the column, whereas here we treat the transient problem and use a more general external boundary condition. Details of our solution, based on the method of Tittle (1965), are given in Section 3 of this report.

In addition to the above we have considered the corresponding problem for a column formed between parallel flat plates, the side walls of the column being perfectly insulated.

The motivation here is as follows. There is an obvious limitation on the size (radial) of a circular column due to the fact that the cross-section area increases as the square of the radius while the external perimeter increases only directly with the radius. Thus the volume in which heat generation occurs grows faster than the area available for surface cooling. With a parallel plates system however the volume may be increased indefinitely while maintaining a fixed ratio of volume to surface area simply by increasing the width of the plates. Thus the rectangular geometry offers the possibility of increased sample production.

Details of the solution for this case are given in Section 4

At the present time we are only beginning numerical calculations of various cases and attempting to assess the fuller implications of the work. Thus this part of our report should be considered as a statement of progress only and not as a final communication.

4. Conclusion

In conclusion it is desirable to say something of future objectives. It is our intention to generalize the thermal analyses presented here so that details of the mechanics of the frontal regions may be further explored.

In addition it will be necessary to investigate the possibility of electro-convection effects. Other factors such as electroosmosis must also be included before the complete process is well understood and a rational design procedure established for a productive piece of equipment--even for cases involving only simple ionic species.

Eventually, the investigation of sample behaviour when the sample contains macro-molecules or living cells is the goal.

M. COXON

M. J. BINDER

February, 1974

References:

Hinckley, J. O. N., Brown, J. and Jones, D. (1972) written communication.

Tittle, C. W. (1965) "Boundary Value Problems in Composite Media; Quasi--Orthogonal Functions." J. Appl. Physics, Vol. 36. #4, pp 1486-1488.

ISOTACHOPHORESIS (DISPLACEMENT ELECTROPHORESIS, TRANSPHORESIS)

THEORY - STRUCTURE OF THE IONIC SPECIES INTERFACE

(Submitted to the Journal of Chromatography)

Authors:

M. Coxon
M. J. Binder
Aerospace and Mechanical Engineering Department
University of Arizona
Tucson, Arizona 85721, USA

Mail Proofs To:

Dr. M. Coxon at the above address.

Running Title:

Structure of the Interface in Isotachophoresis

SUMMARY

An approximate solution is given for the equations governing the structure of the inter-species ionic interface in discrete sample isotachophoresis (displacement electrophoresis, transphoresis) in an ideal one-dimensional system, in the presence of a common counterion and in the absence of continuous mobility spectrum spacer ampholytes. It is shown that the approximation is reasonably good for values of the Kohlrausch-regulated terminator/leader concentration ratio greater than 0.5. The dependence of interface thickness on mobility and concentration ratios is discussed and results are compared to those in previous literature. Interface thickness is found to be inversely proportional to leader voltage gradient.

INTRODUCTION

Isotachophoresis[1] (displacement electrophoresis,[2] transphoresis[3]) is an electrophoretic separation method characterized by equal velocities for all ions migrating in the system once equilibrium has been attained. The sample to be separated is placed in a tube between leader and terminator electrolyte solutions whose ions are of the same sign as the sample ions, and whose mobilities are respectively higher and lower than the mobilities of any of the sample ions. In the absence of co-moving continuous mobility spectrum spacer ampholytes[1], the sample ions separate into a number of contiguous compartments arranged in the order of their mobilities, each compartment being of uniform characteristic concentration governed by the Kohlrausch regulating function[4] (see equation 33) except in the vicinity of the interfaces.

The system was first described by Kendall[5], and subsequent work, including direct method transport number determinations, has been partly reviewed elsewhere[1,3,6-10].

Because of diffusion effects, the interfaces between the compartments are not sharp (although in most cases they are much sharper than ionic discontinuities in other forms of electrophoresis), but rather, a continuous distribution of all ions exists throughout the entire tube. However, in discrete sample (as opposed to continuous frontal) separations, the bulk of the concentration change of the individual ion species occurs in a very short length of tube if the mobility differences are not excessively small. We refer to the distance over which the concentration changes from 99% to 1% as the

interface thickness, Δ. This paper presents an approximate method for determining the structure of the concentration and potential gradient profiles and the interface thicknesses based on a one-dimensional analysis of the interface which would exist between leader and terminator in a sample-free model.

Such a one-dimensional system has no physical existence, but may approximate isotachophoretic behaviour under ideal conditions. It is, therefore, a first step in the theory from which the three-dimensional case may follow if the radial and longitudinal non-uniformities of real systems can be estimated. Such non-uniformities include the effects of radial and longitudinal temperature gradients and the various property variations which result from them, electro-osmosis, electro-convection, and gravity-dependent phenomena such as sedimentation and thermal convection. Further corrections are also required for partly ionized compounds and macromolecules.

A theoretical prediction of the thickness of isotachophoretic interfaces is of importance in evaluating the maximum resolution of the method for preparative applications, and in determining in what ways experimental parameters may be varied to achieve optimal performance.

A list of symbols is printed at the end of the paper.

PREVIOUS WORK

Previous work concerning the determination of the interface thickness has been restricted for the most part to one-dimensional interfaces (i.e. no variations in a radial direction, steady state

conditions) between two essentially 100% dissociated electrolyte solutions having a common counterion. The effects of electro-osmosis and temperature gradients have been dealt with only in a qualitative manner. The basic differences between the various analyses to date lie in the additional assumptions made in each case to render the problem tractable.

Longsworth[11] obtained solutions for the concentration profiles of leader, terminator, and counterion for the case in which the mobilities of leader and counterion were equal and twice the mobility of the terminator. In his analysis he imposed the condition of electrical neutrality throughout the entire system. While this is certainly true for points removed from the interface region, Gauss's law requires some net charge to exist (however small) in the interface region in order that an electric field gradient exist there.

Martin and Everaerts[2] consider the case where leader and terminator mobilities are approximately equal and assume that diffusion effects can be characterized by a single diffusion coefficient for all three ion species. Their results do not show a dependence of front thickness on counterion mobility. They and Routs[12] rewrite the Kohlrausch regulating function to account for partial ionization and compartmental pH differences, with attendant mobility and concentration differences.

Westhaver[13] considers the case of a very thick interface where there is a small mobility difference, the interface representing a form of frontal enrichment.

Konstantinov and Oshurkova[14] consider only the species continuity equations for leader and terminator and obtain solutions for the ratio of either leader or terminator concentration to the sum of the leader and terminator concentrations. A similar solution is obtained by Routs[15] for the ratio of leader concentration to terminator concentration.

Hall and Hinckley[16] obtain solutions valid at points removed from the vicinity of the interface and then estimate interface thicknesses for all three ion species from this. Hinckley[17] has predicted that the interface thickness should be inversely proportional to the leader voltage gradient on the basis that diffusion depends on both mobility and concentration gradient, and the latter increases with reduction of interface thickness (cf. Routs[15]).

Brouwer and Postema[18] consider the unsteady problem but neglect diffusion, thus arriving at a steady state in which all components are separated into distinct compartments, each compartment containing only one component, and hence do not obtain estimates of interface thickness.

GOVERNING EQUATIONS FOR THE ONE-DIMENSIONAL INTERFACE

The governing equations for the one-dimensional interface in isotachophoresis are the species continuity equations for the leader, terminator, and common counterion, and Gauss's law. These may be written as

$$\frac{\partial n_1^*}{\partial t} + \nabla\cdot(\mu_1 n_1^* \vec{E}^*) = D_1 \nabla^2 n_1^* \qquad (1)$$

$$\frac{\partial n_2^*}{\partial t} + \nabla\cdot(\mu_2 n_2^* \vec{E}^*) = D_2 \nabla^2 n_2^* \qquad (2)$$

$$\frac{\partial n_3^*}{\partial t} - \nabla\cdot(\mu_3 n_3^* \vec{E}^*) = D_3 \nabla^2 n_3^* \qquad (3)$$

$$\nabla\cdot\vec{E}^* = \frac{q}{\epsilon^*}(n_1^* + n_2^* - n_3^*) \quad . \qquad (4)$$

If variations in properties over the cross-section of the tube are neglected, then the above equations may be simplified to give

$$\frac{\partial n_1^*}{\partial t} + \mu_1 \frac{\partial (n_1^* E^*)}{\partial x^*} = D_1 \frac{\partial^2 n_1^*}{\partial x^{*2}} \qquad (5)$$

$$\frac{\partial n_2^*}{\partial t} + \mu_2 \frac{\partial (n_2^* E^*)}{\partial x^*} = D_2 \frac{\partial^2 n_2^*}{\partial x^{*2}} \qquad (6)$$

$$\frac{\partial n_3^*}{\partial t} - \mu_3 \frac{\partial (n_3^* E^*)}{\partial x^*} = D_3 \frac{\partial^2 n_3^*}{\partial x^{*2}} \qquad (7)$$

$$\frac{\partial E^*}{\partial x^*} = \frac{q}{\epsilon^*}(n_1^* + n_2^* - n_3^*) \quad . \qquad (8)$$

Transforming the problem to a coordinate system moving with the interface by putting $\tilde{x} = x^* - Ut$, the following is obtained:

$$D_1 \frac{d^2 n_1^*}{d\tilde{x}^2} = \mu_1 \frac{d}{d\tilde{x}}(n_1^* E^*) - U \frac{dn_1^*}{d\tilde{x}} \qquad (9)$$

$$D_2 \frac{d^2 n_2^*}{d\tilde{x}^2} = \mu_2 \frac{d}{d\tilde{x}}(n_2^* E^*) - U \frac{dn_2^*}{d\tilde{x}} \qquad (10)$$

$$D_3 \frac{d^2 n_3^*}{d\tilde{x}^2} = -\mu_3 \frac{d}{d\tilde{x}} (n_3^* E^*) - U \frac{dn_3^*}{d\tilde{x}} \tag{11}$$

$$\frac{dE^*}{d\tilde{x}} = \frac{q}{\varepsilon^*} (n_1^* + n_2^* - n_3^*) \quad . \tag{12}$$

Equations (9), (10), and (11) may be integrated once to obtain

$$D_1 \frac{dn_1^*}{d\tilde{x}} = \mu_1 n_1^* E^* - U n_1^* + C_1 \tag{13}$$

$$D_2 \frac{dn_2^*}{d\tilde{x}} = \mu_2 n_2^* E^* - U n_2^* + C_2 \tag{14}$$

$$D_3 \frac{dn_3^*}{d\tilde{x}} = -\mu_3 n_3^* E^* - U n_3^* + C_3 \quad . \tag{15}$$

The boundary conditions are:

$\underline{\tilde{x} \to -\infty}$

$$\begin{aligned} n_1^* &\to N \\ n_2^* &\to 0 \\ n_3^* &\to N \\ E^* &\to E_A \end{aligned} \tag{16}$$

$\underline{\tilde{x} \to +\infty}$

$$\begin{aligned} n_1^* &\to 0 \\ n_2^* &\to M \\ n_3^* &\to M \\ E^* &\to E_B \quad . \end{aligned} \tag{17}$$

Applying boundary conditions (16), and noting that $\mu_1 E_A = \mu_2 E_B = U$, equations (13), (14), and (15) become

$$D_1 \frac{dn_1^*}{d\tilde{x}} = \mu_1 n_1^* E^* - U n_1^* \tag{18}$$

$$D_2 \frac{dn_2^*}{d\tilde{x}} = \mu_2 n_2^* E^* - U n_2^* \tag{19}$$

$$D_3 \frac{dn_3^*}{d\tilde{x}} = -\mu_3 n_3^* E^* - U n_3^* + E_A N(\mu_1 + \mu_3) \ . \tag{20}$$

According to the Einstein relation $D = \frac{\mu kT}{e}$. For monovalent ions, this is equivalent to $D = \frac{\mu kT}{q}$. Using this, and introducing the dimensionless variables n, E, and x, equations (18), (19), (20), and (12) become

$$\frac{dn_1}{dx} = n_1 E - n_1 \tag{21}$$

$$\frac{dn_2}{dx} = n_2 E - \frac{n_2}{b_2} \tag{22}$$

$$\frac{dn_3}{dx} = -n_3 E - \frac{n_3}{b_3} + \theta_2(1 + 1/b_3) \tag{23}$$

$$\epsilon \frac{dE}{dx} = n_1 + n_2 - n_3 \ . \tag{24}$$

In non-dimensional terms, the boundary conditions become

$\underline{x \to -\infty}$

$$n_1 \to \theta_2$$
$$n_2 \to 0$$
$$n_3 \to \theta_2$$
$$E \to 1 \qquad \text{(25 a,b,c,d)}$$

$\underline{x \to +\infty}$

$$n_1 \to 0$$
$$n_2 \to 1$$
$$n_3 \to 1 \qquad (26\ a,b,c,d)$$
$$E \to \theta_1 \quad .$$

Eliminating E from equations (21) and (22) gives

$$n_2 = n_1 C e^{\alpha x} \quad .$$

Choosing the origin at the point where $n_1 = n_2$ gives $C = 1$, thus

$$n_2 = n_1 e^{\alpha x} \quad . \qquad (27)$$

From equation (21)

$$E = 1 + 1/n_1 \frac{dn_1}{dx} \quad . \qquad (28)$$

Thus

$$\frac{dE}{dx} = \frac{1}{n_1^2} \left[n_1 \frac{d^2 n_1}{dx^2} - \left(\frac{dn_1}{dx}\right)^2 \right] . \qquad (29)$$

Substitution of (27) and (29) in (24) yields

$$n_3 = n_1(1 + e^{\alpha x}) - \varepsilon \frac{n_1''}{n_1} + \varepsilon \left(\frac{n_1'}{n_1}\right)^2 \quad . \qquad (30)$$

where $n_1' = \frac{dn_1}{dx}$, etc.

Thus

$$n_3' = n_1 \alpha e^{\alpha x} + n_1'(1 + e^{\alpha x}) - \varepsilon \left(\frac{n_1 n_1''' - n_1' n_1''}{n_1^2}\right)$$

$$+ \varepsilon \left(\frac{2n_1^2 n_1' n_1'' - 2n_1 n_1'^3}{n_1^4}\right) \quad . \qquad (31)$$

Substitution of (28), (30), and (31) in (23) gives

$$2n_1^3 n_1'(1 + e^{\alpha x}) + n_1^4 \alpha e^{\alpha x} - \varepsilon n_1^2 n_1''' + \varepsilon n_1^2 n_1''(3 - \beta)$$

$$- \varepsilon n_1'^3 - \varepsilon n_1 n_1' n_1'' + \beta \varepsilon n_1 n_1'^2 + \beta n_1^4 (1 + e^{\alpha x})$$

$$- \frac{\alpha \theta_2}{1-\theta_2} n_1^3 = 0 \quad . \tag{32}$$

The last term in equation (32) is obtained by using the relationship

$$\beta = (1 + 1/b_3) = \alpha/(1-\theta_2) \quad . \tag{33}$$

This may be obtained by applying boundary conditions (25) and (26) to equation (15) after it has been put in dimensionless form. Boundary condition (25) yields as before

$$\bar{C}_3 = \theta_2(1 + 1/b_3) \ .$$

Boundary condition (26) gives

$$\bar{C}_3 = \theta_1 + 1/b_3 \ .$$

Equating the two expressions for $\bar{C}_3$ gives

$$\theta_2(1 + 1/b_3) = \theta_1 + 1/b_3 \ .$$

Noting that $b_2\theta_1 = 1$, equation (33) is obtained by algebraic manipulation. Equation (33) has been described by Kohlrausch[4] and Weber[19] and is known as the Kohlrausch regulating function.

Equation (32) may be rearranged to give

$$2n_1'(1 + e^{\alpha x}) + n_1\alpha e^{\alpha x} - \varepsilon\frac{n_1'''}{n_1} + \varepsilon\frac{n_1''}{n_1}(3-\beta) - \varepsilon\left(\frac{n_1'}{n_1}\right)^3$$

$$- \varepsilon\frac{n_1'n_1''}{n_1^2} + \beta\varepsilon\left(\frac{n_1'}{n_1}\right)^2 + \beta n_1(1 + e^{\alpha x}) = \frac{\alpha\theta_2}{(1-\theta_2)} \quad . \quad (34)$$

SOLUTION OF THE PROBLEM

The problem consists of finding a solution for equation (34) which satisfies the boundary conditions (25) and (26). The nature of the problem and the boundary conditions indicate the general shape of the solution curve (it might be referred to as a distorted sigmoid). The results of the aforementioned references tend to confirm this statement. Hence we assume a solution of the form

$$n_1 = \frac{\theta_2}{(1 + \psi(x)e^{\phi(x)})^{N_1}} \quad . \quad (35)$$

Hence

$$n_2 = \frac{\theta_2 e^{\alpha x}}{(1 + \psi(x)e^{\phi(x)})^{N_1}} \quad .$$

It is seen that boundary condition (25 b) is satisfied if

$$\phi(x) \leq (\alpha/N_1)x \quad .$$

Boundary condition (26 b) is satisfied only if the following conditions are met:

(1) $\phi(x) = (\alpha/N_1)x$

(2) $\psi(x) = K$ (a constant)

(3) $\frac{K^{N_1}}{\theta_2} = 1$.

Hence the assumed solution for n_1 becomes

$$n_1 = \frac{\theta_2}{(1 + Ke^{\alpha x/N_1})^{N_1}} \tag{36}$$

where

$$K = \theta_2^{1/N_1} \ . \tag{37}$$

It is easily seen that equation (35) also satisfies the other boundary conditions.

Substitution of equation (36) into equation (34) yields an equation of the form

$$f(x) = \beta\theta_2 \ . \tag{38}$$

As an indication of how well our assumed solution satisfies equation (38), we define the error in the system to be

$$\text{Error } (\%) = \left| \frac{100[f(x) - \beta\theta_2]}{\beta\theta_2} \right| \ .$$

In general, the error will be a function of x, and the exponent N_1 must be chosen in such a way as to minimize the maximum error for each set of experimental conditions considered.

RESULTS

A numerical search routine was employed to determine the optimum value of N_1 for each set of parameters considered, the calculations being performed on the CDC-6400 computer at the University of Arizona Computer Center. The optimum value of N_1 and the resulting maximum error were found to be highly dependent on θ_2 but essentially inde-

pendent of α and ε. The variations of N_1 and the maximum error with θ_2 are shown in figures 1 and 2 respectively.

The values of interface thickness for leader and terminator ions were found to be equal and highly dependent on α and θ_2, but independent of ε. This same parameter dependency was found to be true for the counterion and electric field interface thicknesses. The variations of interface thickness with α and θ_2 are shown in figures 3, 4, and 5.

DISCUSSION

As can be seen from figure 2, the assumed solution satisfies the governing equations with negligible error for $\theta_2 > 0.75$. The error increases rapidly for decreasing θ_2. At $\theta_2 = 0.5$ the maximum error is about 7.5%.

A comparison of figures 3 and 4 shows that δ_3 is less than δ_1 and δ_2. This result was also predicted by Hall and Hinckley[16].

A comparison of figures 3 and 5 shows that for large values of θ_2, δ_E is approximately equal to δ_1, but that for small values of θ_2, δ_E is considerably greater than δ_1. Since a common means of determining δ_1 experimentally is to measure δ_E, it would appear that at low values of θ_2 this method would give values of δ_1 which are larger than they should be. However, since it is for low values of θ_2 that the error in our calculations is very large, this may not actually be the case.

As a numerical example for use in comparison with the results of previous analyses we consider the conditions given in Table 1. For the parameters given, figure 3 gives $\delta_1 = 27.68$. This is a

dimensionless interface thickness, and it may be put back into dimensional form by employing the definition of the dimensionless distance x given in the symbol table. Thus

$$\Delta = \frac{\delta_1 kT}{qE_A} .$$

For the conditions given this yields an interface thickness Δ of 0.027 mm.

Martin and Everaerts[2] predict an interface thickness of 1.2 mm. from the results of their analysis. Applying the data of Table 1 to the formulations of Hall and Hinckley[16] and Konstantinov and Oshurkova[14] gives values of 0.0038 mm. and 0.0115 mm. respectively, although the latter is based on a definition of interface thickness different to that used here.

Arlinger and Routs[20] using an UV detector detected interface thicknesses of less than 1 mm., and Hinckley[17] has detected alkali metal interfaces of 0.2 mm. or less with a D.C. Electrometric detector, although exact measurement is difficult because of the short distances involved.

The concentration and electric field profiles for the conditions of Table 1 are shown in figure 6.

Since the non-dimensional interface thickness is seen to be independent of ε, the variation of dimensional interface thickness with terminator voltage gradient (and hence leader voltage gradient since they are proportional) may be determined directly from the definition of x. Thus

$$\Delta = \frac{\delta_1 kT}{qE_A} = \frac{\delta_1 (1-\alpha) kT}{qE_B} \quad .$$

Interface thickness is seen to be inversely proportional to the terminator or leader voltage gradients with the temperature of the system as a parameter for a given δ_1. This variation is depicted in figure 7 for a value of δ_1 equal to 30, and is of the form predicted by Hinckley[17] on the grounds previously mentioned.

CONCLUSIONS

The approximate solution given is seen to satisfy the governing equations for the one-dimensional interface in Isotachophoresis with a maximum error of 7.5% for values of terminator to leader concentration ratio greater than 0.5. It yields values of interface thickness which are less than those of previous analyses, and this prediction seems to be in line with experimental observations. It is seen that the sum of the concentrations of leader, terminator, and counterion in the region of the interface is very small but not zero, in accordance with Gauss's law. The interface thickness is found to be inversely proportional to the leader voltage gradient as predicted by Hinckley[17].

ACKNOWLEDGEMENTS

The authors wish to express their gratitude to Dr. Milan Bier for his interest and comments in discussion. Thanks are also due to J. O. N. Hinckley for suggesting this study and for providing us with previous publications and unpublished material related to the problem.

LIST OF SYMBOLS

SYMBOL	MEANING	UNITS
b_2	Dimensionless mobility $= \mu_2/\mu_1$	———
b_3	Dimensionless mobility $= \mu_3/\mu_1$	———
C	Integration Constant	———
C_1	Integration Constant	$\frac{\text{ions}}{\text{cm}^2\text{sec}}$
C_2	Integration Constant	$\frac{\text{ions}}{\text{cm}^2\text{sec}}$
C_3	Integration Constant	$\frac{\text{ions}}{\text{cm}^2\text{sec}}$
$\overline{C}_3$	Integration Constant	———
D_1	Terminator Diffusion Coefficient	cm^2/sec
D_2	Leader Diffusion Coefficient	cm^2/sec
D_3	Counterion Diffusion Coefficient	cm^2/sec
E^*	Electric Field	volts/cm
E	Dimensionless Electric Field $= E/E_A$	———
E_A	Electric Field In Terminator Zone	volts/cm
E_B	Electric Field In Leader Zone	volts/cm
e	Electronic Charge	coulombs/electron
K	Constant	———
k	Boltzmann's Constant	erg/°K

M	Ionic Number Density In Leader Zone	ions/cm^3
N	Ionic Number Density In Terminator Zone	ions/cm^3
N_1	Constant, Exponent in Assumed n_1 Solution	————
n_1^*	Terminator Ionic Number Density	ions/cm^3
n_2^*	Leader Ionic Number Density	ions/cm^3
n_3^*	Counterion Ionic Number Density	ions/cm^3
n_1	Dimensionless Terminator Ionic Number Density	————
n_2	Dimensionless Leader Ionic Number Density	————
n_3	Dimensionless Counterion Ionic Number Density	————
q	Ionic Charge	coulombs/ion
T	Temperature	°K
t	Time	sec.
U	Speed of migrating ions	cm/sec
x^*	Distance Along Axis Of Tube Refered To A Fixed Coordinate System	cm.
$\bar{x}$	Distance Along Axis Of Tube Refered To A Moving Coordinate System	cm.
x	Dimensionless Distance Along Axis Of Tube Refered To A Moving Coordinate System $= \frac{\bar{x}qE_A}{kT}$	————
α	Dimensionless Parameter $= \frac{b_2-1}{b_2} = 1-\theta_1$	————

β	Dimensionless Parameter $= \frac{b_3 + 1}{b_3}$	———
δ_1	Dimensionless Terminator Interface Thickness	———
δ_2	Dimensionless Leader Interface Thickness	———
δ_3	Dimensionless Counterion Interface Thickness	———
δ_E	Dimensionless Electric Field Interface Thickness	———
Δ	Dimensional Leader or Terminator Interface Thickness	mm.
ϵ^*	Dielectric Constant of the Medium	Farad/meter
ϵ	Dimensionless Dielectric Constant $= \frac{E_A^2 \epsilon^*}{kTM}$	———
θ_1	Dimensionless Electric Field In Leader Zone $= E_B/E_A = 1-\alpha$	———
θ_2	Dimensionless Number Density In Terminator Zone $= N/M = \frac{b_3\theta_1 + 1}{b_3 + 1}$	———
μ_1	Mobility of Terminator Ion	$cm^2/(volt\ sec)$
μ_2	Mobility of Leader Ion	$cm^2/(volt\ sec)$
μ_3	Mobility of Counterion	$cm^2/(volt\ sec)$
ϕ	Function of x in Assumed n_1 Solution	———
ψ	Function of x in Assumed n_1 Solution	———

REFERENCES

1. H. Haglund, *Science Tools*, 17 (1970) 2.

2. A.J.P.Martin and F.M.Everaerts, *Proc.Roy.Soc.Lond.*A., 316 (1970) 493.

3. J.O.N.Hinckley, in E. Reid (Editor), *Methodological Developments in Biochemistry*, Vol. 2, Longman, London, 1973, p.207.

4. F. Kohlrausch, *Ann. Phys. Leipzig*, 62 (1897) 209.

5. J. Kendall, *Phys. Rev.*, 21 (1923) 389.

6. D. Peel, in E. Reid (Editor), *Methodological Developments in Biochemistry*, Vol. 2, Longman, London, 1973, p. 205.

7. M. Gazith and A. Roy, *Electrochem.Technol.*, 2 (1964) 85.

8. H.D.Freyer and K.Wagener, *Angew.Chem.Int.Ed.Engl.*, 6 (1967) 757.

9. J.O.N.Hinckley, *Abstr.Analysis 72 Symp.Imperial College London* (1972).

10. D.A.MacInnes and L.G.Longsworth, *Chem.Rev.*, 11 (1932) 171.

11. L.G.Longsworth, *J.Am.Chem.Soc.*, 66 (1944) 449.

12. R.J.Routs, Doctoral Thesis, Eindhoven Technological University (1971).

13. J.W.Westhaver, *J.Res.Nat.Bur.Stand.*, 38 (1947) 169.

14. B.P.Konstantinov and O.V.Oshurkova, *Sov.Phys.Tech.Phys.*, 11 (1966) 693.

15. R.J.Routs, *Electrolyte Systems in Isotachophoresis and Their Application To Some Protein Separations*, Solna Skriv- & Stenograftjanst AB, Solna, Sweden, 1971, p. 37.

16. R.Hall and J.O.N.Hinckley, written communication (1971).

17. J.O.N.Hinckley, written communication (1973).

18. G.Brouwer and G.A.Postema, *J.Electrochem.Soc.*, 117 (1970) 874.

19. H. Weber, *Sitz.Preuss.Akad.Wiss.Berl.Sitzungsber.*, (1897) 936.

20. L.Arlinger and R.Routs, *Science Tools*, 17 (1970) 21.

TABLE 1

EXPERIMENTAL PARAMETERS

n_1^* = Sodium

n_2^* = Potassium

n_3^* = Chloride

$T = 283\ ^\circ K$

$\mu_1 = 35.98 \times 10^{-5}\ cm^2/(volt\ sec)$

$\mu_2 = 54.4 \times 10^{-5}\ cm^2/(volt\ sec)$

$\mu_3 = 55.25 \times 10^{-5}\ cm^2/(volt\ sec)$

$E_A = 250\ volts/cm$

$M = 1$ millimolar

$\epsilon^* = 7.4471 \times 10^{-10}$ farad/meter

$\alpha = 0.3386$

$\theta_2 = 0.79494$

$\epsilon = 1.98 \times 10^{-4}$

FIGURE LEGENDS

Figure 1 Variation of N_1 with ϑ_2 .

Figure 2 Variation of Maximum Error with θ_2.

Figure 3 Leader and Terminator Interface Thickness.

Figure 4 Counterion Interface Thickness.

Figure 5 Electric Field Interface Thickness.

Figure 6 Concentration and Electric Field Profiles.

Figure 7 Variation of Interface Thickness with Terminator Voltage Gradient.

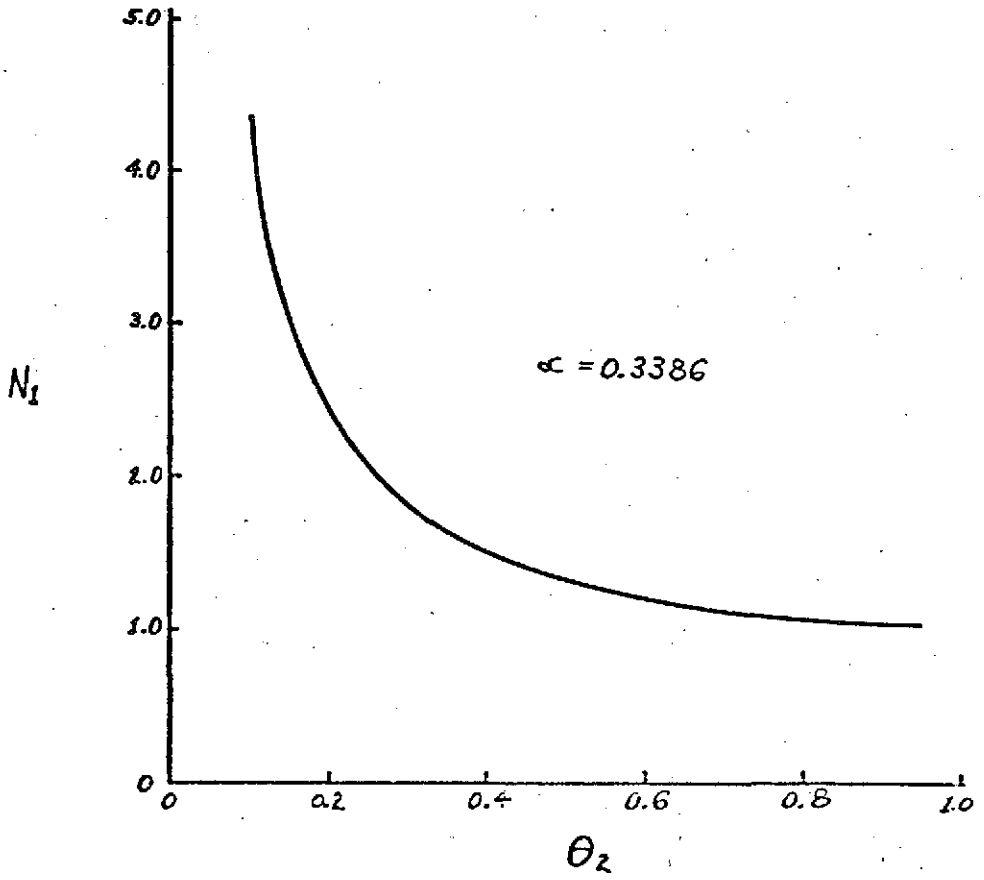

FIG. 1

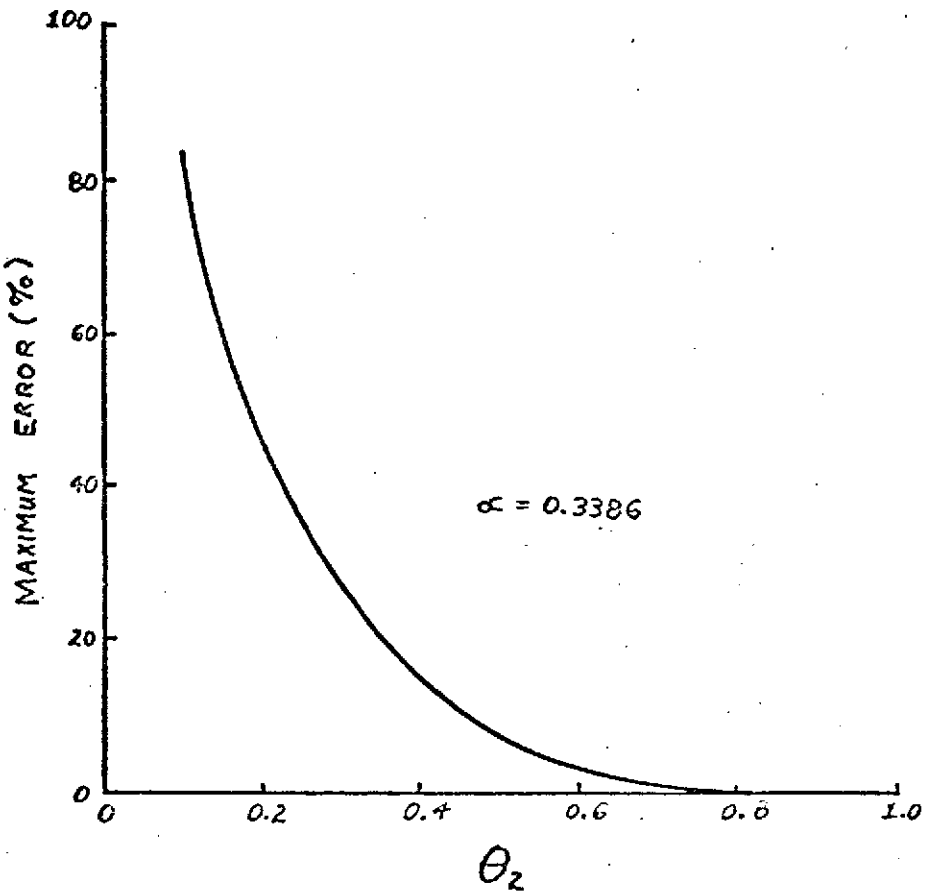

FIG. 2

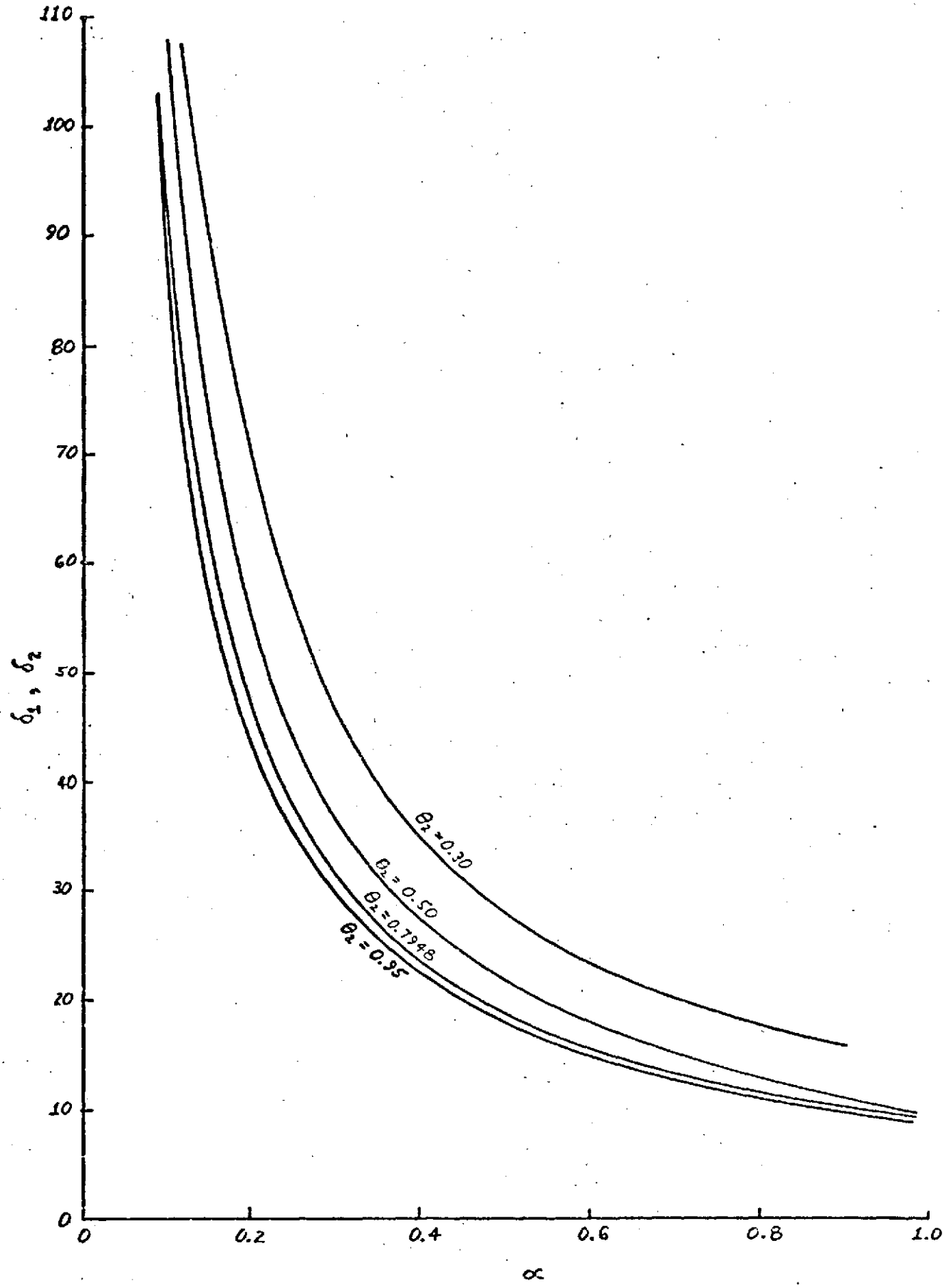
110
100
90
80
70
60
50
40
30
20
10
0
0
0.2
0.4
0.6
0.8
1.0
δ_1, δ_2
α
$\theta_2 = 0.30$
$\theta_2 = 0.50$
$\theta_2 = 0.7948$
$\theta_2 = 0.95$

FIG. 3

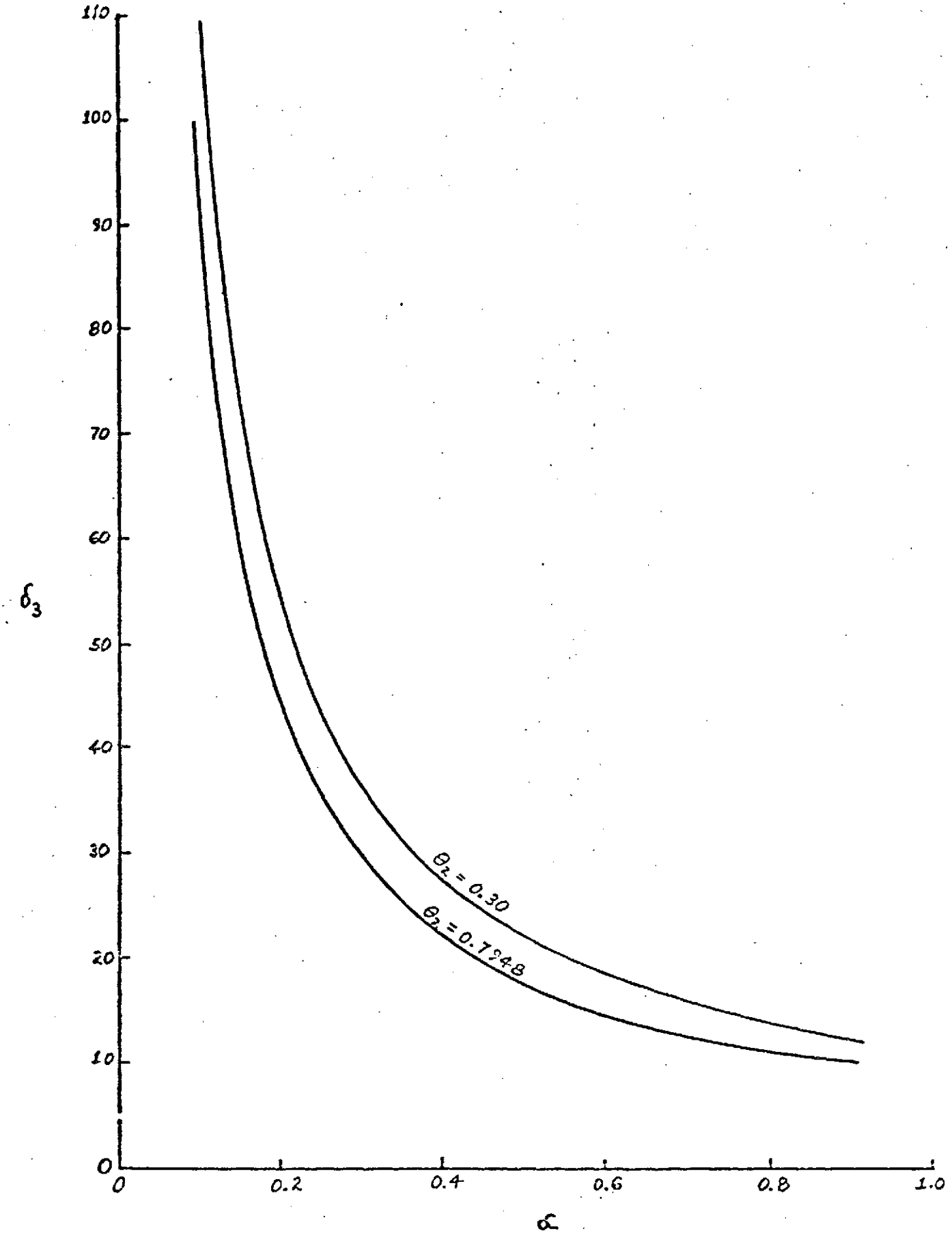
110
100
90
80
70
60
δ_3
50
40
30
20
10
0
0
0.2
0.4
0.6
0.8
1.0
α
$\theta_2 = 0.30$
$\theta_2 = 0.7948$

C-31

FIG. 4

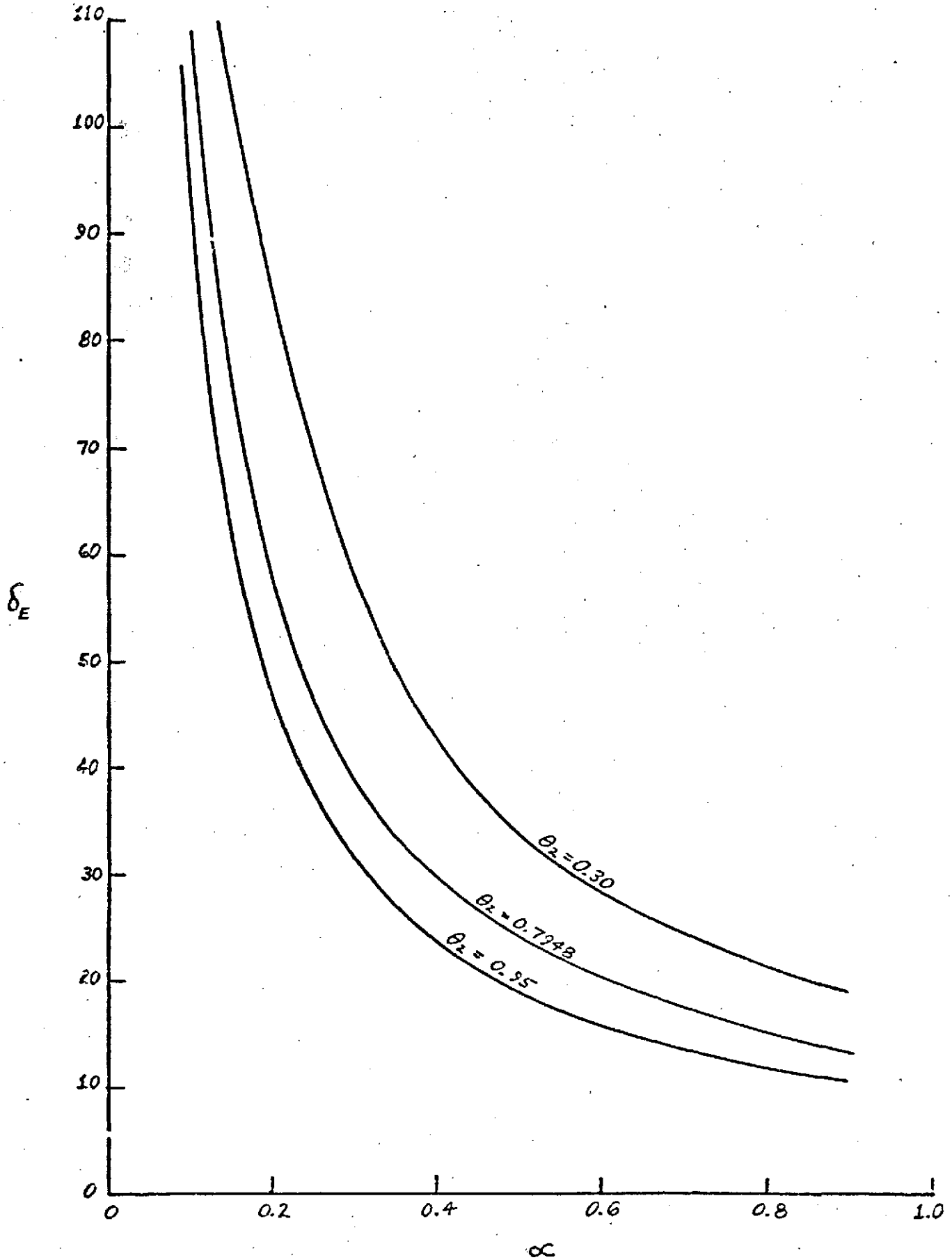
110
100
90
80
70
60
50
40
30
20
10
0
δ_E
0
0.2
0.4
0.6
0.8
1.0
α
$\theta_2 = 0.30$
$\theta_2 = 0.7348$
$\theta_2 = 0.95$

FIG 5

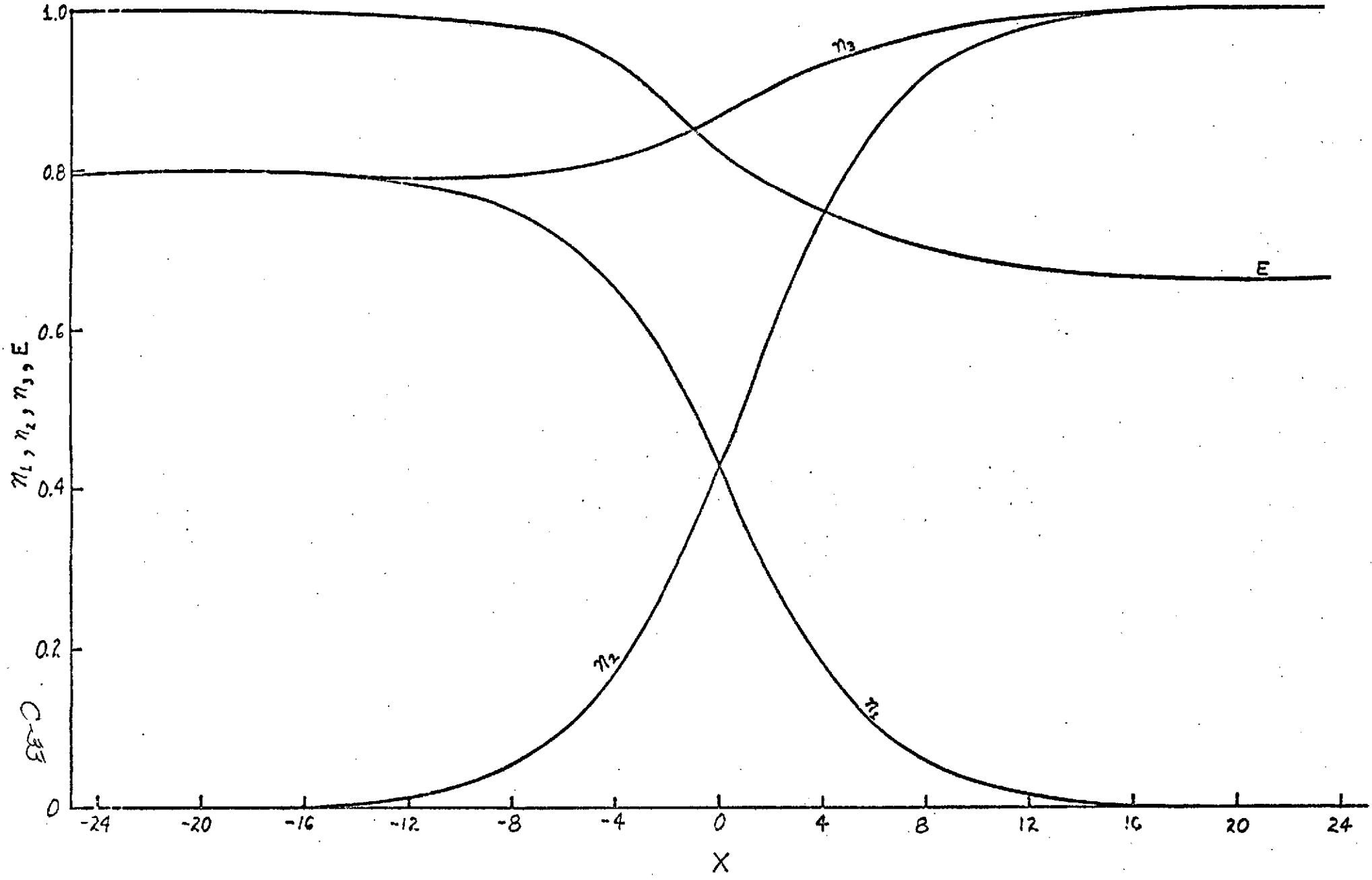
1.0
0.8
0.6
0.4
0.2
0
n_1, n_2, n_3, E
n_3
E
n_2
n_1
-24
-20
-16
-12
-8
-4
0
4
8
12
16
20
24
X

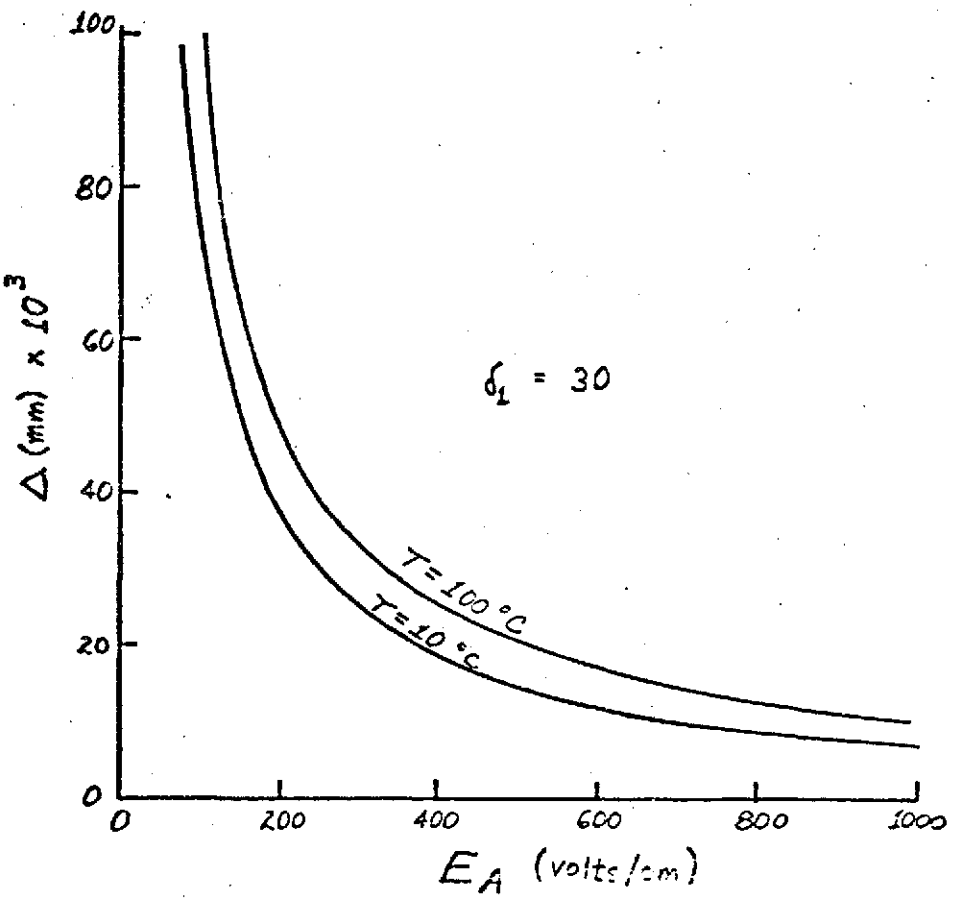
100
80
60
40
20
0
Δ (mm) x 10³
δ₁ = 30
T = 100 °C
T = 10 °C
0
200
400
600
800
1000
E_A (volts/cm)

FIG. 7

RADIAL TEMPERATURE DISTRIBUTION IN ISOTACHOPHORESIS COLUMNS OF CIRCULAR CROSS-SECTION

1. Statement of the Problem

The assumptions given in section 3 of the main report are made. Mathematically the problem may then be stated as follows:

$$K_1\left\{\frac{1}{r}\frac{\partial}{\partial r}\left(r\frac{\partial T_1}{\partial r}\right)\right\} = \frac{\partial T_1}{\partial t} - \frac{Q_e}{\rho_1 c_1}, \quad 0 \le r \le R_1$$

$$K_2\left\{\frac{1}{r}\frac{\partial}{\partial r}\left(r\frac{\partial T_2}{\partial r}\right)\right\} = \frac{\partial T_2}{\partial t}, \quad R_1 \le r \le R_2$$

$$T_1 = T_2 \qquad \text{at } r = R_1, \quad t>0$$

$$k_1\frac{\partial T_1}{\partial r} = k_2\frac{\partial T_2}{\partial r} \quad \text{at } r = R_1, \ t>0$$

$$T_1 \text{ finite at } r = 0.$$

$$k_2\frac{\partial T_2}{\partial r} + h(T_2 - T_\infty) = 0 \text{ at } r = R_2, \ t>0$$

$$T_1 = T_\infty \text{ in } 0 \le r \le R_1, \ t = 0$$

$$T_2 = T_\infty \text{ in } R_1 \le r \le R_2, \ t = 0$$

The symbols have their customary and/or obvious meaning.

We introduce the dimensionless variables

$$\theta = \frac{T-T_\infty}{T_\infty}, \qquad \xi = \frac{r}{R_2}, \qquad \tau = \frac{K_1 t}{R_2^2}$$

and assume that

$$Q_e = Q_o(1 + \alpha\theta) = JE^2\sigma = JE^2\sigma_o(1 + \alpha\theta)$$

where the heat generation per unit volume and the electrical conductivity are denoted by Q_o and σ_o respectively when evaluated at $\theta = 0$.

We also denote $S = \dfrac{Q_o R_2^2}{k_1 T_\infty}$

and $\gamma = \dfrac{hR_2}{k_2}$

and $\xi_1 = R_1/R_2$.

Then the statement of the problem in dimensionless variables is:

$$\frac{1}{\xi}\frac{\partial}{\partial\xi}\left(\xi\frac{\partial\theta_1}{\partial\xi}\right) = \frac{\partial\theta_1}{\partial\tau} - S(1+\alpha\theta_1) \quad , \quad 0 \le \xi \le \xi_1$$

$$\frac{1}{\xi}\frac{\partial}{\partial\xi}\left(\xi\frac{\partial\theta_2}{\partial\xi}\right) = \frac{K_1}{K_2}\frac{\partial\theta_2}{\partial\tau} \quad , \quad \xi_1 \le \xi \le 1$$

$\theta_1 = \theta_2$ at $\xi = \xi_1$

$k_1\dfrac{\partial\theta_1}{\partial\xi} = k_2\dfrac{\partial\theta_2}{\partial\xi}$ at $\xi = \xi_1$

θ_1 finite at $= 0$

$\dfrac{\partial\theta_2}{\partial\xi} + \gamma\theta_2 = 0$ at $\xi = 1$

$\theta_1 = 0$ in $0 \le \xi \le \xi_1$, $\tau = 0$

$\theta_2 = 0$ in $\xi_1 \le \xi \le 1$, $\tau = 0$

This problem is split into steady state and transient parts by writing

$$\theta(\xi,\tau) = \theta^s(\xi) + \theta^t(\xi,\tau) \ .$$

2. Steady State Problem

$$\frac{1}{\xi}\frac{d}{d\xi}\left(\xi\frac{d\theta_1^s}{d\xi}\right) = -S\left(1+\alpha\theta_1^s\right) \quad , \quad 0 \le \xi \le \xi_1$$

$$\frac{1}{\xi}\frac{d}{d\xi}\left(\xi\frac{d\theta_2^s}{d\xi}\right) = 0 \quad , \quad \xi_1 \le \xi \le 1$$

$\theta_1^s = \theta_2^s$ at $\xi = \xi_1$; θ_1^s finite at $\xi = 0$

$$k_1\frac{d\theta_1^s}{d\xi} = k_2\frac{d\theta_2^s}{d\xi} \quad \text{at } \xi = \xi_1$$

$$\frac{d\theta_2^s}{d\xi} + \gamma\theta_2^s = 0 \quad \text{at } \xi = 1$$

The solutions are

$$\theta_1^s = A_1 J_0(\beta\xi) - \frac{1}{\alpha} \quad , \quad \beta^2 = \alpha S$$

$$\theta_2^s = A_2\left[\ln\xi - \frac{1}{\gamma}\right]$$

where,

$$A_1 = \frac{1}{\alpha\left[J_0(\beta\xi_1) + \frac{k_1}{k_2}\beta\xi_1 J_1(\beta\xi_1)\left\{\ln\xi_1 - \frac{1}{\gamma}\right\}\right]}$$

and

$$A_2 = \frac{-\frac{k_1}{k_2}\beta\xi_1 J_1(\beta\xi_1)}{\alpha\left[J_0(\beta\xi_1) + \frac{k_1}{k_2}\beta\xi_1 J_1(\beta\xi_1)\left\{\ln\xi_1 - \frac{1}{\gamma}\right\}\right]}$$

3. Transient Problem

$$\frac{1}{\xi}\frac{\partial}{\partial \xi}\left(\xi \frac{\partial \theta_1^t}{\partial \xi}\right) = \frac{\partial \theta_1^t}{\partial \tau} - \alpha S \theta_1^t \quad , \quad 0 \le \xi \le \xi_1$$

$$\frac{1}{\xi}\frac{\partial}{\partial \xi}\left(\xi \frac{\partial \theta_2^t}{\partial \xi}\right) = \frac{K_1}{K_2}\frac{\partial \theta_2^t}{\partial \tau} \quad , \quad \xi_1 \le \xi \le 1$$

θ_1^t finite at $\xi = 0$

$\theta_1^t = \theta_2^t$ at $\xi = \xi_1$, $\tau > 0$

$k_1 \frac{\partial \theta_1^t}{\partial \xi} = k_2 \frac{\partial \theta_2^t}{\partial \xi}$ at $\xi = \xi_1$, $\tau > 0$

$\frac{\partial \theta_2^t}{\partial \xi} + \gamma \theta_2^t = 0$ at $\xi = 1$, $\tau > 0$

$\theta_1^t = -\theta_1^s$ in $0 \le \xi \le \xi_1$, $\tau = 0$

$\theta_2^t = -\theta_2^s$ in $\xi_1 \le \xi \le 1$, $\tau = 0$

This problem is solved by the method of Tittle*.

We seek a solution of the form

$$\theta_j^t(\xi, \tau) = \sum_{n=1}^{\infty} A_n X_{jn} e^{-\alpha_j \beta_{jn}^2 \tau}$$ in region j; j = 1,2.

It is easily shown that for region 1 we must have

$$X_{1_n}(\xi) = J_o(\lambda_{1_n} \xi)$$

---

*Tittle, C.W., "Boundary Value Problems in Composite Media; Quasi-Orthogonal Functions", J.Appl.Phys.,Vol.36,No.4(1965),pp. 1486-1488.

where $\lambda_{1_n}^2 = \beta^2 + \beta_{1_n}^2$ and β_{1_n} are the eigenvalues and $\alpha_1 = 1$. Similarly for region 2 we obtain

$$X_{2_n} = B_n[J_o(\beta_{2_n}\xi) + C_n Y_o(\beta_{2_n}\xi)]$$

and $\alpha_2 = K_2/K_1$.

The eigenvalues β_{2_n} are related to β_{1_n} by

$$\beta_{1_n}^2 = \alpha_2 \beta_{2_n}^2 .$$

The boundary condition at $\xi = 1$ leads to

$$C_n = \frac{\gamma J_o(\beta_{2n}) - \beta_{2n} J_1(\beta_{2n})}{\beta_{2n} Y_1(\beta_{2n}) - \gamma Y_o(\beta_{2n})}$$

Then equating θ_1^t and θ_2^t at $\xi = \xi_1$ gives

$$B_n = \frac{J_o(\lambda_{1n}\xi_1)}{[J_o(\beta_{2n}\xi_1) + C_n Y_o(\beta_{2n}\xi_1)]}$$

Finally equating $k_1 \frac{\partial \theta_1^t}{\partial \xi} = k_2 \frac{\partial \theta_2^t}{\partial \xi}$ at $\xi = \xi_1$ gives

$$k_1 \lambda_{1_n} J_1(\lambda_{1_n}\xi_1) = k_2 \beta_{2_n} B_n [J_1(\beta_{2_n}\xi_1) + C_n Y_1(\beta_{2_n}\xi_1)]$$

as the transcendental equation to be solved for the eigenvalues β_{1_n} (or β_{2_n}).

The coefficients A_n are then given by

$$A_n = \frac{\int_o^{\xi_1} [-\theta_1^s] X_{1n}\, \xi\, d\xi + \left(\frac{K_1}{K_2}\frac{k_2}{k_1}\right) \int_{\xi_1}^{1} [-\theta_2^s] X_{2n}\, \xi\, d\xi}{\int_o^{\xi_1} X_{1n}^2\, \xi\, d\xi + \left(\frac{K_1}{K_2}\frac{k_2}{k_1}\right) \int_{\xi_1}^{1} X_{2n}^2\, \xi\, d\xi}$$

The various integrations may be performed giving:

$$\int_0^{\xi_1} [-\theta_1^s] X_{1n} \xi \, d\xi = \frac{1}{\alpha} \frac{\xi_1}{\lambda_{1n}} J_1(\lambda_{1n}\xi_1) - \frac{A_1 \xi_1}{\beta_{1n}^2} \left[\lambda_{1n} J_0(\beta\xi_1) J_1(\lambda_{1n}\xi_1) - \beta J_0(\lambda_{1n}\xi_1) J_1(\beta\xi_1) \right]$$

$$\int_{\xi_1}^1 [-\theta_2^s] X_{2n} \xi \, d\xi = \frac{A_2 B_n}{\gamma \beta_{2n}} \left[J_1(\beta_{2n}) - \xi_1 J_1(\beta_{2n}\xi_1) + C_n \{ Y_1(\beta_{2n}) - \xi_1 Y_1(\beta_{2n}\xi_1) \} \right]$$

$$- \frac{A_2 B_n}{\beta_{2n}} \left[-\xi_1 \ln \xi_1 J_1(\beta_{2n}\xi_1) + \frac{1}{\beta_{2n}} \{ J_0(\beta_{2n}) - J_0(\beta_{2n}\xi_1) \} \right]$$

$$- \frac{A_2 B_n C_n}{\beta_{2n}} \left[-\xi_1 \ln \xi_1 Y_1(\beta_{2n}\xi_1) + \frac{1}{\beta_{2n}} \{ Y_0(\beta_{2n}) - Y_0(\beta_{2n}\xi_1) \} \right]$$

$$\int_0^{\xi_1} X_{1n}^2 \xi \, d\xi = \frac{\xi_1^2}{2} \left[J_1^2(\lambda_{1n}\xi_1) + J_0^2(\lambda_{1n}\xi_1) \right]$$

$$\int_{\xi_1}^1 X_{2n}^2 \xi \, d\xi = B_n^2 \left[\frac{1}{2} \{ J_1(\beta_{2n}) + C_n Y_1(\beta_{2n}) \}^2 + \frac{1}{2} \{ J_0(\beta_{2n}) + C_n Y_0(\beta_{2n}) \}^2 \right.$$

$$\left. - \frac{\xi_1^2}{2} \{ J_1(\beta_{2n}\xi_1) + C_n Y_1(\beta_{2n}\xi_1) \}^2 - \frac{\xi_1^2}{2} \{ J_0(\beta_{2n}\xi_1) + C_n Y_0(\beta_{2n}\xi_1) \}^2 \right]$$

The problem is now ready for numerical computations.

TEMPERATURE DISTRIBUTION IN ISOTACHOPHORESIS COLUMNS OF RECTANGULAR CROSS-SECTION

1. Statement of the Problem

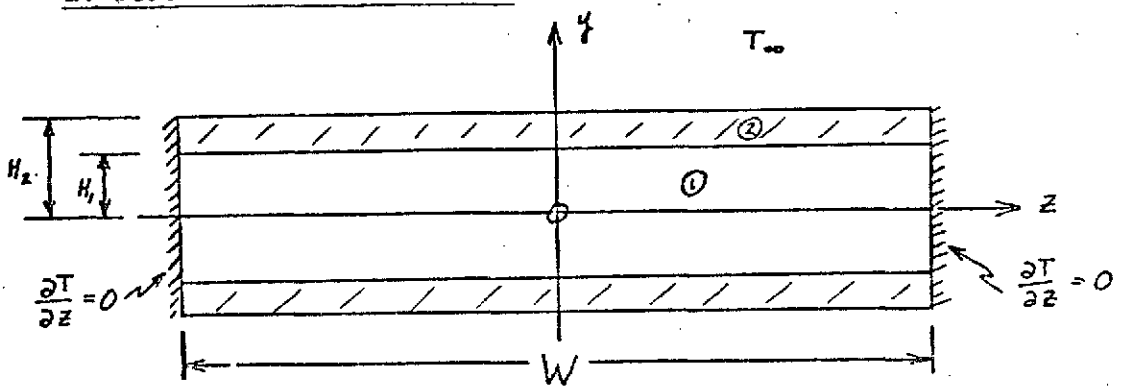

The assumptions are the same as those given for the problem treated in Appendix II with the addition that we now treat the side walls of the column as perfectly insulated.

In terms of the dimensionless variables

$$\theta = \frac{T-T_\infty}{T_\infty} \quad , \quad \eta = y/H_2 \quad \text{and} \quad \tau = \frac{K_1 t}{H_2^2} \quad \text{and writing} \quad S = \frac{Q_o H_2^2}{k_1 T_\infty}$$

the problem is:

$$\frac{\partial^2 \theta_1}{\partial \eta^2} = \frac{\partial \theta_1}{\partial \tau} - S(1+\alpha\theta_1) \quad , \quad 0 \le \eta \le \eta_1 \, , \; \tau > 0$$

$$\frac{\partial^2 \theta_2}{\partial \eta^2} = \frac{K_1}{K_2} \frac{\partial \theta_2}{\partial \tau} \quad , \quad \eta_1 \le \eta \le 1 \, , \; \tau > 0$$

where $\eta_1 = H_1/H_2$

θ_1 is finite at $\eta = 0$ with $\frac{\partial \theta_1}{\partial \eta} = 0$ (by symmetry).

$$\theta_1 = \theta_2 \text{ at } \eta = \eta_1 \ , \ \tau>0$$

$$k_1\frac{\partial\theta_1}{\partial\eta} = k_2\frac{\partial\theta_2}{\partial\eta} \text{ at } \eta = \eta_1 \ , \ \tau>0$$

$$\frac{\partial\theta_2}{\partial\eta} + \gamma\theta_2 = 0 \quad \text{at } \eta = 1 \quad \text{where } \gamma = \frac{hH_2}{k_2}$$

As before we resolve the problem into steady state and transient components by writing

$$\theta(\eta,\tau) = \theta^s(\eta) + \theta^t(\eta,\tau).$$

2. The Steady State Problem

$$\frac{d^2\theta_1^s}{d\eta^2} = -S(1 + \alpha\theta_1^s) \ , \ 0\leq\eta\leq\eta_1$$

$$\frac{d^2\theta_2^s}{d\eta^2} = 0 \ , \ \eta_1\leq\eta\leq1$$

$$\theta_1^s = \theta_2^s \quad \text{at } \eta = \eta_1$$

$$k_1\frac{d\theta_1^s}{d\eta} = k_2\frac{d\theta_2^s}{d\eta} \quad \text{at } \eta = \eta_1$$

$$\frac{d\theta_1^s}{d\eta} = 0 \text{ at } \eta = 0$$

$$\frac{d\theta_2^s}{d\eta} + \gamma\theta_2^s = 0 \quad \text{at } \eta = 1.$$

The solutions are:

$$\theta_1^s = A_1\cos(\beta\eta) - \frac{1}{\alpha} \ , \ 0\leq\eta\leq\eta_1$$

$$\theta_2^s = A_2\left[(\eta-1) - \frac{1}{\gamma}\right] \ , \ \eta_1\leq\eta\leq1$$

where

$$A_1 = \frac{1}{\alpha\left[\cos(\beta\eta_1) + \frac{k_1}{k_2}\beta\sin(\beta\eta_1)\left\{(\eta_1 - 1) - \frac{1}{\gamma}\right\}\right]}$$

$$A_2 = \frac{-\frac{k_1}{k_2}\beta\sin(\beta\eta_1)}{\alpha\left[\cos(\beta\eta_1) + \frac{k_1}{k_2}\beta\sin(\beta\eta_1)\left\{(\eta_1 - 1) - \frac{1}{\gamma}\right\}\right]}$$

3. The Transient Problem

$$\frac{\partial^2\theta_1^t}{\partial\eta^2} = \frac{\partial\theta_1^t}{\partial\tau} - \beta^2\theta_1^t \quad , \quad 0 \le \eta \le \eta_1$$

$$\frac{\partial^2\theta_2^t}{\partial\eta^2} = \frac{K_1}{K_2}\frac{\partial\theta_2^t}{\partial\tau} \quad , \quad \eta_1 \le \eta \le 1$$

$$\theta_1^t = \theta_2^t \quad \text{at } \eta = \eta_1$$

$$k_1\frac{\partial\theta_1^t}{\partial\eta} = k_2\frac{\partial\theta_2^t}{\partial\eta} \quad \text{at } \eta = \eta_1$$

$$\frac{\partial\theta_1}{\partial\eta} = 0 \quad \text{at } \eta = 0$$

$$\frac{\partial\theta_2^t}{\partial\eta} + \gamma\theta_2^t = 0 \quad \text{at } \eta = 1$$

$$\theta_1^t = -\theta_1^s \quad \text{in } 0 \le \eta \le \eta_1 \quad \text{at } \tau = 0$$

$$\theta_2^t = -\theta_2^s \quad \text{in } \eta_1 \le \eta \le 1 \quad \text{at } \tau = 0 \ .$$

Again we seek solutions of the form

$$\theta_j^t(\eta,\tau) = \sum_{n=1}^{\infty} A_n X_{jn}(\eta) e^{-\alpha_j\beta_n^2\tau} \quad \text{in region j; j = 1,2.}$$

In region 1 we easily show that $\alpha_1 = 1$ and that

$$X_{1_n}(\eta) = \cos(\lambda_{1_n}\eta) \qquad \text{where } \lambda_{1_n}^2 = \beta_{1_n}^2 + \beta^2$$

and the eigenvalues are the β_{1_n}.

Similarly in region 2 we find that $\alpha_2 = K_2/K_1$,

$$X_{2_n} = B_n[\cos(\beta_{2_n}\eta) + C_n \sin(\beta_{2_n}\eta)]$$

and the eigenvalues β_{2_n} are related to β_{1_n} by

$$\beta_{1_n}^2 = \alpha_2\beta_{2_n}^2 .$$

The boundary condition at $\eta = 1$ leads to

$$C_n = \frac{\beta_{2n}\sin(\beta_{2n}) - \gamma\cos(\beta_{2n})}{\beta_{2n}\cos(\beta_{2n}) + \gamma\sin(\beta_{2n})}$$

Equating θ_1^t and θ_2^t at $\eta = \eta_1$ gives

$$B_n = \frac{\cos(\lambda_{1n}\eta_1)}{[\cos(\beta_{2n}\eta_1) + C_n\sin(\beta_{2n}\eta_1)]}$$

and the remaining condition at $\eta = \eta_1$ yields the equation for the eigenvalues β_{1_n} (or β_{2_n}) as:

$$k_1\lambda_{1_n}\sin(\lambda_{1_n}\eta_1) = k_2\beta_{2_n}B_n[\sin(\beta_{2_n}\eta_1) - C_n\cos(\beta_{2_n}\eta_1)]$$

Then the coefficients A_n are given by:

$$A_n = \frac{\int_0^{\eta_1} [-\theta_1^s] X_{1n}(\eta)\, d\eta + \left(\frac{K_1}{K_2}\frac{k_2}{k_1}\right) \int_{\eta_1}^{1} [-\theta_2^s] X_{2n}(\eta)\, d\eta}{\int_0^{\eta_1} X_{1n}^2(\eta)\, d\eta + \left(\frac{K_1}{K_2}\frac{k_2}{k_1}\right) \int_{\eta_1}^{1} X_{2n}^2(\eta)\, d\eta}$$

Again the integrations are easily performed and the problem is ready for computation.

COMPARISON OF "EXACT" SOLUTION OF STEADY STATE TEMPERATURE DISTRIBUTION ASSUMING CONSTANT THERMAL PROPERTIES WITH A STEADY STATE PERTURBATION SOLUTION PERMITTING LINEAR TEMPERATURE DEPENDENCE OF THERMAL PROPERTIES

1. The Constant Properties Solution

The solution of the steady state problem assuming constant thermal properties (density, specific heat, and thermal conductivity) has been given in Appendix II. For the special case where $T_2 = T_\infty$ at $r = R_2$ we have:

$$\theta_1^s = \frac{J_0(\beta\xi)}{\alpha\left[J_0(\beta\xi_1) + \frac{k_1}{k_2}\beta\xi_1 J_1(\beta\xi_1)\ln\xi_1\right]} - \frac{1}{\alpha}$$

From which the maximum temperature, at $\xi = 0$, is

$$\theta_{1_{max}}^s = \frac{1}{\alpha}\left\{\frac{1}{\left[J_0(\beta\xi_1) + \frac{k_1}{k_2}\beta\xi_1 J_1(\beta\xi_1)\ln\xi_1\right]} - 1\right\}$$

For the purposes of obtaining a numerical comparison with the perturbation solution given below we have chosen the following values for the parameters involved.

$\xi_1 = 2/3$ $\qquad \alpha = 7.75$ $\qquad \theta_{1_{max}}^s = 0.1355$

$k_1 = 13.9 \times 10^{-4} \frac{cal}{cm\text{-}s\text{-}^\circ K}$ $\qquad k_2 = 26.7 \times 10^{-4} \frac{cal}{cm\text{-}s\text{-}^\circ K}$

The values of k_1 and k_2 are average values for the range of θ^s considered, i.e. $0 \leq \theta^s \leq \theta_{1\,max}^s$.

Solving for $\beta = \sqrt{\alpha S}$ then gives a value for the maximum permissible value of the dimensionless heat source strength S.

We find that $S_{max} = 0.480$.

2. Perturbation Solution for the Steady State Problem

The statement of the problem in terms of the dimensionless variables is

$$\frac{1}{\xi}\frac{d}{d\xi}\left[\xi\left(1+\beta_1\theta_1^s\right)\frac{d\theta_1^s}{d\xi}\right] = -S\left(1+\alpha\theta_1^s\right), \quad 0 \leq \xi \leq \xi_1$$

$$\frac{1}{\xi}\frac{d}{d\xi}\left[\xi\left(1+\beta_2\theta_2^s\right)\frac{d\theta_2^s}{d\xi}\right] = 0, \quad \xi_1 \leq \xi \leq 1$$

where now $k_1 = k_{10}(1 + \beta_1\theta_1^s)$

$$k_2 = k_{20}(1 + \beta_2\theta_2^s)$$

and k_{10}, k_{20} are the values of k_1, k_2 at $\theta_{1,2}^s = 0$.

Boundary conditions are taken to be

$$\theta_2^s = 0 \quad \text{at } \xi = 1$$

$$\theta_1^s = \theta_2^s \text{ at } \xi = \xi_1$$

$$k_1\frac{d\theta_1^s}{d\xi} = k_2\frac{d\theta_2^s}{d\xi} \quad \text{at } \xi = \xi_1$$

and the temperature at $\xi = 0$ must be finite.

We proceed by assuming that θ can be expanded in terms of a power series in the dimensionless source strength S.

$$\theta_1^S(\xi; S) \sim S f_0(\xi) + S^2 f_1(\xi) + S^3 f_2(\xi) + \ldots \quad , \quad 0 \le \xi \le \xi_1$$

$$\theta_2^S(\xi; S) \sim S \phi_0(\xi) + S^2 \phi_1(\xi) + S^3 \phi_2(\xi) + \ldots \quad , \quad \xi_1 \le \xi \le 1 .$$

The obvious procedural steps are not reproduced here, instead we shall quote the solution of θ_1^S which we require for comparative purposes.

We obtain the following:

$$\theta_1^S = S\left[B_1 - \frac{\xi^2}{4}\right] + S^2\left[(\beta_1 - \alpha)\left(\frac{B_1\xi^2}{4} - \frac{\xi^4}{64}\right) - \frac{\beta_1\xi^4}{64} + D_1\right] + \ldots$$

where, $0 \le \xi \le \xi_1$

$$B_1 = \frac{\xi_1^2}{4} - \frac{k_{10}}{k_{20}}\frac{\xi_1^2}{2}\ln\xi_1$$

$$D_1 = C\ln\xi_1 - \frac{\beta_2 A^2}{2}(\ln\xi_1)^2 - (\beta_1 - \alpha)\left(\frac{B_1\xi_1^2}{4} - \frac{\xi_1^4}{64}\right) + \frac{\beta_1\xi_1^4}{64}$$

$$C = \frac{k_{10}}{k_{20}}\left[(\beta_1 - \alpha)\left(\frac{B_1\xi_1^2}{2} - \frac{\xi_1^4}{16}\right) - \frac{\beta_1\xi_1^4}{16} - \beta_1\left(\frac{B_1\xi_1^2}{2} - \frac{\xi_1^4}{8}\right)\right]$$

$$A = -\frac{k_{10}}{k_{20}}\frac{\xi_1^2}{2}$$

For $\theta_{1\,\max}^S$ at $\xi = 0$ we then have simply

$$\theta_{1\,\max}^S = SB_1 + S^2D_1 + \ldots .$$

Numerical calculations assume the same values used in section 1 except that now we use

$$k_{20} = 26 \times 10^{-4} \frac{cal}{cm\text{-}s\text{-}^\circ K} \quad , \quad k_{10} = 13.19 \times 10^{-4} \frac{cal}{cm\text{-}s\text{-}^\circ K}$$

$$\beta_2 = 0.42 \quad , \quad \beta_1 = 0.808$$

We now find a value for S_{max}.

$$S_{max} = 0.576 \qquad \text{(variable properties)}$$

This value may be compared directly with that obtained from the perturbation scheme by setting $\beta_1 = \beta_2 = 0$ and replacing k_{10}, k_{20} by the average values for k_1, k_2 used in section 1, in which case we get

$$S_{max} = 0.561 \qquad \text{(constant properties)}.$$

Thus we see that within the perturbation steady state solution, taken to two terms, the effect of neglecting thermal property variations leads to a difference of some 2.5% in the calculation of S_{max}. Furthermore we note that the result obtained by assuming constant properties is conservative.

3. Comparison With the "Exact" Solution

It will be noted that the value of $S_{max} = 0.48$ given in section 1 is some 14 1/2 % below that obtained from the two-term perturbation

method also assuming constant properties. This however is a result of relatively slow convergence of the perturbation expansion. We have continued the expansion to three terms (assuming constant properties) and then obtain $S_{max} = 0.51$ which is only 6% higher than the "exact" solution. We conclude therefore that the error in neglecting the thermal properties dependence on temperature is justified and is probably less than 3% in view of the comparisons made within the perturbation solutions. Moreover the "exact" constant properties solution gives a conservative answer and is therefore safe for design calculations.

SECTION D

REPORT BY THE EXPERIMENTAL GROUP

by

M. Bier and A.J.K. Smolka

INTRODUCTION

Literature available at the beginning of this contract year indicated that Isotachophoresis shows particular promise on two levels: (a) as a fast analytical method for the quantitation of low molecular weight electrolytes. Several commercial instrument manufacturers, including LKB in Sweden, Philips in Holland, and Brandenburg in England, had, at one time or another, active programs in this direction. Mr. Hinckley came to Tucson, from directing the Brandenburg effort. (b) though published literature indicated that isotachophoresis has poorer resolution than the so-called high resolution techniques, i. e. isoelectric focusing, high density gels, or immunoelectrophoresis, it nevertheless had considerable appeal as a preparative electrophoretic technique for proteins. Its resolution is potentially better than that of conventional zone electrophoresis, but its main attraction is its ability to separate much larger quantities of proteins than any other method. This aspect of isotachophoresis, received, however, only minimal attention from both commercial companies and the individual researchers.

The possibility of applying isotachophoresis to cell separation was not raised anywhere in the literature, and was first proposed by the P.I. in various meetings of the USRA Committee on Electrophoresis. There were no obvious theoretical reasons why it could not be so applied, except for the practical difficulty of avoiding gravity-caused disturbances. As Nasa's program provided a unique approach to the gravity problem, the experimental program had for its primary objective the investigation of this attractive possibility.

The experimental approach was as follows:

(a) on the one hand, it was necessary to obtain a working knowledge of isotachophoresis as a preparative tool for the separation of proteins. While literature was full of promises in this direction, no serious effort had gone into it. Best resolution of proteins is obtained in gels,

thereby avoiding all gravity problems. A large part of our efforts went therefore into protein work with gels.

(b) On the other hand, separations of cells require working with free solutions. One of the methods which is partially successful in overcoming gravity effects is working in density gradients. This is most often used in isoelectric focusing. We had therefore a modest effort in this direction, mainly geared to gaining a working experience in density gradients, and applying them to isotachophoresis.

(c) Extensive laboratory work went into preparation for the Skylab experiment. Though, conceptually, this work should be included in the present experimental section, it was thought more appropriate to include it in the section dealing with all aspects of the space experiment.

(d) Finally, density gradients are not applicable to work in zero-gravity, and obscure some of the phenomena which arise in free solution, notably the effects of electroosmosis. We have therefore undertaken extensive studies of other palliative means to circumvent the effects of gravity. These include working in narrow horizontal capillaries, where viscosity effects minimize the gravity caused convection. Several modifications were tried: the use of very high electrical fields to accelerate the process; the addition of viscosity increasing colloids to the liquid system; and rotation around the axis of such tubes. None of these methods have succeeded in preventing the disastrous effects of gravity on isotachophoretic fronts. While it is easy to demonstrate in such systems some of the characteristic phenomena of isotachophoresis, such as boundary sharpening, restoration of disrupted boundaries, etc., these effects were always only transitory. Basically, while capillary work has been used extensively with small molecular weight ionic substances, where concentration differences between sample and buffer are lesser, they are unusable with high molecular weight substances, such as proteins and cells.

Organizationally, Mr. Hinckley was largely responsible for the last approach, described under point (d) , while Mr. Smolka has carried on the studies on the first two points. Both have collaborated on the Skylab experiment, Mr. Hinckley carrying out the preparative experiments on the red cells, Mr. Smolka those on the proteins. Obviously, these distinctions were only nominal, as there was continued interaction between these two collaborators and the P.I.

Mr. Hinckley came to this project with a substantial past experience in isotachophoresis. While much of his prior work was directed towards analytical purposes, it obviously had a substantial impact on our work, including that of the theoretical and engineering groups. He therefore felt compelled to write a major survey of the whole field of isotachophoresis, rather than restricting himself on covering only the work carried out under this contract. Unfortunately, this report is not yet available. Not to delay further the submission of this report, it has been decided to eliminate his section, and submit it at a later date, as an independent contribution.

ISOELECTRIC FOCUSING ON DENSITY GRADIENTS

A.J.K. Smolka

Research Associate

University of Arizona

INTRODUCTION

1. Purpose of the isoelectric focusing experiments

Our studies of isoelectric focusing were governed by the following objectives.

A. To gain a working knowledge of anticonvective stabilization by means of density gradient. Stabilization of boundaries using sucrose density gradients is widely used in isoelectric focusing, and we wanted to start with a well documented technique before venturing into the use of this stabilization mode in isotachophoresis. Instability of electrophoretic boundaries is caused by density gradients arising mainly from two sources; temperature gradients due to Joule heating and radial cooling of the vessels, and differences of density between pure buffer and protein solutions (or cell suspensions).

B. Isoelectric focusing is recognised as a standard of high resolution in protein electrophoresis. We used the technique to compare its resolution with that obtainable by isotachophoresis.

C. In isotachophoresis, separated compartments of proteins (or any other materials) are contiguous, without intervening zones of pure buffer. With hemoglobin and ferritin for example, the best separation by isotachophoresis would result in contiguous zones of brown and red proteins. To increase the visibility of such a separation, a colorless spacer is most desirable. The commercial product, Ampholine, marketed by LKB,* is frequently used for this purpose. It is available commercially in fractions of rather wide pH and mobility range. We used isoelectric focusing for

* LKB Instruments Inc., Rockville, Md.

finer subfractionation of Ampholine.

D. Electroosmosis has a disruptive effect on a number of electrophoretic techniques, including miscroscope electrophoresis (1) and the continuous method of Hannig (2) and Strickler (3). In the Apollo 16 experiment, electroosmosis was the main cause of boundary spreading due to the parabolic shape of the separated latex zones. However, electroosmosis is not apparent in other electrophoretic techniques, including Tiselius electrophoresis and isoelectric focusing. Part of our studies was directed towards elucidating the role of denisty gradients in eliminating or masking the electroosmotic effects.

2. Principle of Isoelectric Focusing

Isoelectric focusing, a method perfected by Svensson (4), occurs when a d.c. potential is imposed on an electrolyte system containing the ampholytic molecules to be separated in which the pH increases steadily from the anode to the cathode. The ampholytes, which may be proteins, migrate toward one or other of the electrodes, depending on their net charge, until they reach a region where the pH of the electrolyte is equal to their isoelectric point. Since proteins have no net charge at their isoelectric point, they cannot migrate any further, and if conditions are suitable, they will form a narrow stable zone, the sharpness of whose boundaries will be determined by the degree of diffusion of the protein into the electrolyte. Since the isoelectric point of a protein is a function of its aminoacid composition and sequence, and the degree to which functional groups are exposed on the surface of the molecule, every protein has a characteristic pI, so that focusing of a mixture of proteins results

in the formation of several discrete zones of protein material, each homogeneous as regards its protein content. Furthermore, because all proteins are characterised by steep titration curves, these zones are extremely thin and highly concentrated. The theory and practice of isoelectric focusing has recently been reviewed by Haglund (5).

3. Stabilization against Convection

A large number of methods exist to provide stabilization against convection in liquid systems (6). In the present experiments, sucrose density gradients were used to suppress convection. Density gradient solutes must meet certain specifications in order to be useful; they must have good solubility and low viscosity in water, they should have high density (the miminum density difference in a gradient should not be less than 0.12 g/cm^3), they must not interact with the sample, and finally they must not be ionic (5). Sucrose fulfills these conditions, and furthermore a wealth of evidence indicates that sucrose has a stabilizing effect on proteins (7,8). Such a gradient was found to be very stable, resisting pronounced tilting of the LKB 110 ml column used in this work. The use of tall columns, however, has certain disadvantages, in that the available density interval (using 50% w/v sucrose) is spread over a considerable distance, so that the density gradient becomes correspondingly weak. Thus electric potential has to be kept at low levels to minimize Joule heating. Philpot (9) has proposed using very short columns with strong density gradients, the principal advantages being extremely thin protein zones and short run times. This approach has not been investigated in this laboratory, but seems promising as a means of stabilization of isotachophoretic boundaries in small glass tubes.

4. The pH Gradient

For isoelectric focusing, the pH gradient should include in its range the predicted or known pIs of the components of the sample. The slope and the conductivity are other factors of importance. There are basically two forms of gradient, the natural pH gradient, and the artificial pH gradient (4). Since the latter form is not in stable equilibrium, the majority of isoelectric focusing methods utilize the former. Briefly, a natural pH gradient is formed when a d.c. potential is imposed on a mixture of low molecular weight ampholytes which exhibit large variety in their isoelectric pH, and which exert sufficient buffering action individually to dictate the pH of the background electrolyte. The most acidic ampholyte migrates to the anode and collects there at its isoelectric point. The next most acidic ampholyte will similarly migrate to the anode, but cannot pass the first because its own isoelectric point would be passed. Thus the ampholytes line up in sequence from the anode to the cathode, each at its isoelectric point, and each dictating the pH of the electrolyte in its immediate environment. Provided the system is stabilized against thermal convection, the pH gradient thus formed reaches a stable equilibrium. The profile of the gradient is determined by the number of ampholytes, their buffering capacity, relative concentrations and the range of their isoelectric points.

Artificial pH gradients are prepared by layering buffer solutions of different pH over one another, so that a gradient is formed by diffusion. During electrophoresis however, such a gradient is destroyed by the migration of buffer ions.

Vesterberg (10), who was responsible for the development of the Ampholine chemicals, has summarized the desireable properties of carrier ampholytes as the source of a natural pH gradient, LKB Ampholines fulfill there conditions and are available in several pH ranges.

a) They should have a buffering capacity at pH values close to their pI to dictate the pH of a 0.5% protein solution.

b) To permit a high degree of resolution the mixture of ampholytes should contain isomers which differ in pI by less than 0.1 pH unit.

c) Their solubility must be high in aqueous solution to guard against precipitation in highly focused zones.

d) They should have a low absorbance at 280 nm to allow detection of proteins.

e) Ampholytes should be separable from proteins by simple methods such as dialysis.

f) Since the field strength is a function of the conductivity distribution of ampholytes, the latter should be such as to allow good focusing of proteins in the major part of the pH gradient.

MATERIALS AND METHODS

1. Isoelectric Focusing Apparatus

A vertical glass column of annular cross-section and capacity 110 mls (LKB 8101), manufactured for this application by LKB Instruments Inc., was used in the present experiments (Fig 1). The column was cooled by circulating water at 4°C from a heat exchanger into the thermostatted jacket of the column. The platinum wire electrodes are situated so that gas evolution from the cathode does not disturb the focusing and that electrode decomposition products in general cannot enter the focusing compartment. The electrode solutions are formulated to protect the ampholytes in the region of the electrodes from anodic oxidation and cathodic reduction. Immersing the anode in 1% v/v sulphuric acid gives a net positive charge to the ampholytes so that they are repelled from the anode. Similarly, the cathode solution contained 10% w/v sodium hydroxide, giving adjacent ampholytes a negative charge.

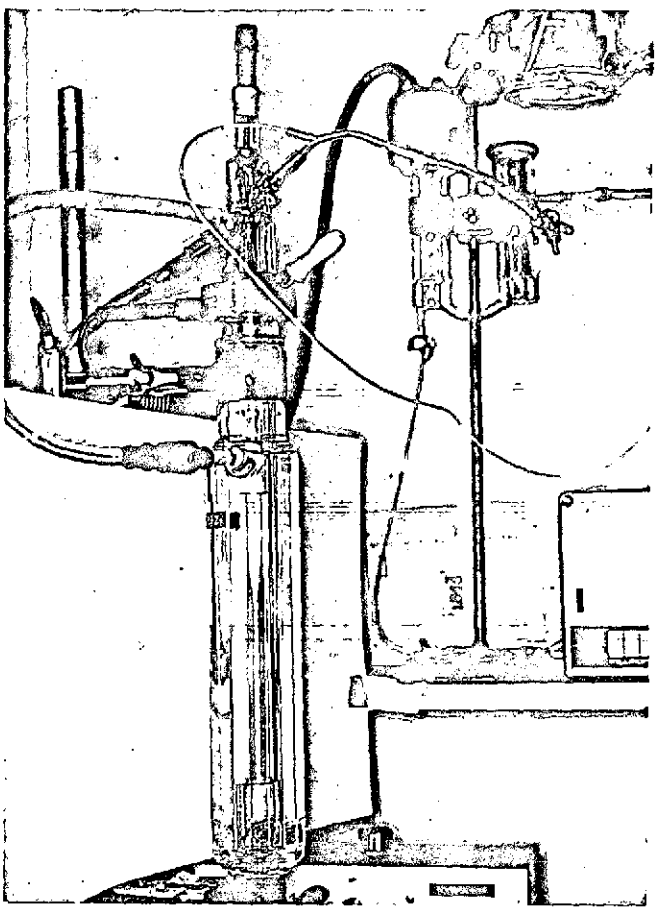

Fig. 1 Photograph of the LKB isoelectric focusing column used in the present experiments

2. Sucrose Gradient Formation

Sucrose density gradients were prepared using the 110 ml LKB mixing device. This consists of two 55 ml glass vessels, connected at their bases by a short length of teflon tubing. One vessel, which contains a dense sucrose solution, is stirred continually by an electric stirring arm; outflow of mixed dense and light solutions is from a nipple in the base of this vessel. Density gradients may also be prepared manually but this was not attempted.

3. Carrier Ampholytes

LKB Ampholine chemicals of pH range 5-8 were used in the protein fractionations,

at a concentration of 1% v/v. For the preparation of large numbers of ampholyte sub-fractions, Ampholines of pH range 3-10 were used at a concentration of 5% v/v. In all experiments, Ampholines were added to the light solution in the density gradient mixing device.

4. Samples

Human, dog and sheep hemoglobins were prepared by hemolysis of washed fresh red blood cells with distilled water, followed by centrifugation to remove ghosts and cell debris. The protein concentration was 7g%.

Human gamma-globulin prepared commercially for therapeutic use was diluted to a similar concentration.

A 1% w/v solution of Evans Blue dye in distilled water was used in our experiment to study electroosmotic and thermal convective effects.

All samples were stored in the deep freeze until required; before use, they were passed through a 0.22 micron filter to ensure clarity.

5. Power Requirements

A 1200 volts LKB power supply was utilized in all experiments. The starting voltage was 600 volts; initial currents were between 2 and 10 mA, and a focusing experiment was judged complete when no further drop in current occurred.

6. Recording of Results

Results were evaluated in two ways. An elution of the column contents at 2 mls/min through an LKB ultraviolet monitor (280 nm) coupled to a 10 mv sensitivity potentiometric recorder provided a graphical read-out of the focused protein zones. Alternatively, the results were assessed qualitatively by visual examination and photography of the focused zones; in several experiments it was unnecessary to elute the column contents since the emphasis of these experiments was on the structure and stability of focused zones.

RESULTS

The present experiments fall into five groups; only one or two experiments from each group are discussed here, since the objective and results were similar in each group.

1. Separation of Sheep Hemoglobin and Human Gamma-globulin

These experiments were performed to gain familiarity with the technique of isoelectric focusing using two rather dissimilar proteins, presumed to be easily separable.

A 50% w/v sucrose density gradient was prepared using the LKB mixing device. 2mls of the mixed protein solution, containing 1% v/v LKB Ampholines pH range 5-8, were added to the light solution, so that the sample was distributed throughout the gradient at the start of the experiment. The initial voltage and current were 500 volts and 2.3 mA respectively. After 25 hours, the voltage was 700 volts, the current had stabilized at 0.4 mA, and concentration of the hitherto diffuse reddish-brown sample into an 8 mm band had occurred. The lower electrode compartment was sealed, and the column contents were eluted through the monitor. Three major peaks were recorded (Fig 2), the first one being gamma-globulin, while the second, which is less regular and displays several shoulders, is the hemoglobin. The shoulders may represent hemoglobin allotypes or sub-fractions, and could possibly be resolved using a narrower pH gradient, eg. pH range 6.5 to 7.0. The third peak, which was eluted at pH 4.9, is albumin, a contaminant of the commercial gamma-globulin sample; this was confirmed by cellulose acetate electrophoresis of this fraction using standardised albumin as a control.

Another experiment in this group involved the fractionation of 1 ml of the same gamma-

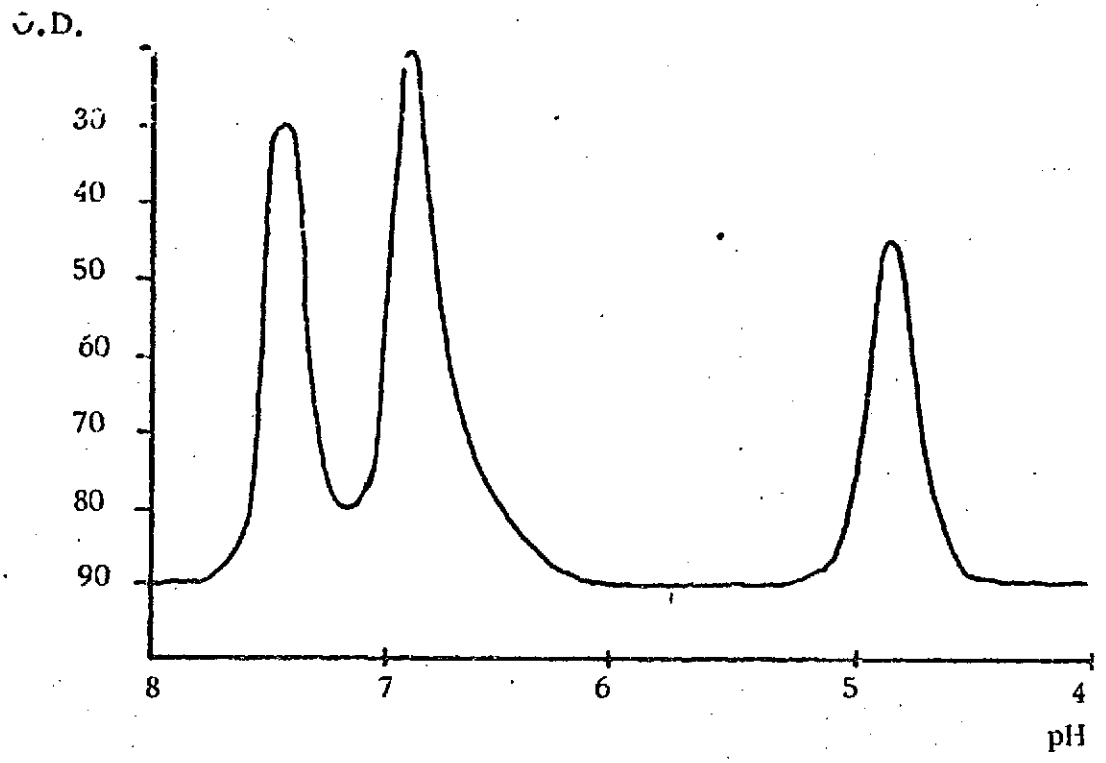

Fig. 2. Elution pattern at 280nm of fractions obtained in isoelectric focusing of hemoglobin and gamma-globulin.

globulin solution under the same conditions; a similar trace was obtained (fig 3) except that a second impurity was revealed, whose presence had been masked in the previous experiment by the hemoglobin peak.

2. Separation of Different Hemoglobins

The following experiment was concerned with the separation of basically similar proteins, a rather more demanding separation than that described above. Two mls of a mixture of human, sheep and dog hemoglobins were focused on a 40% sucrose gradient with 1% v/v Ampholines pH range 5-8. Initial voltage and current were 500 volts and 2.0 in A respectively. After 24 hours, the current had stabilized at 0.3 mA, and the

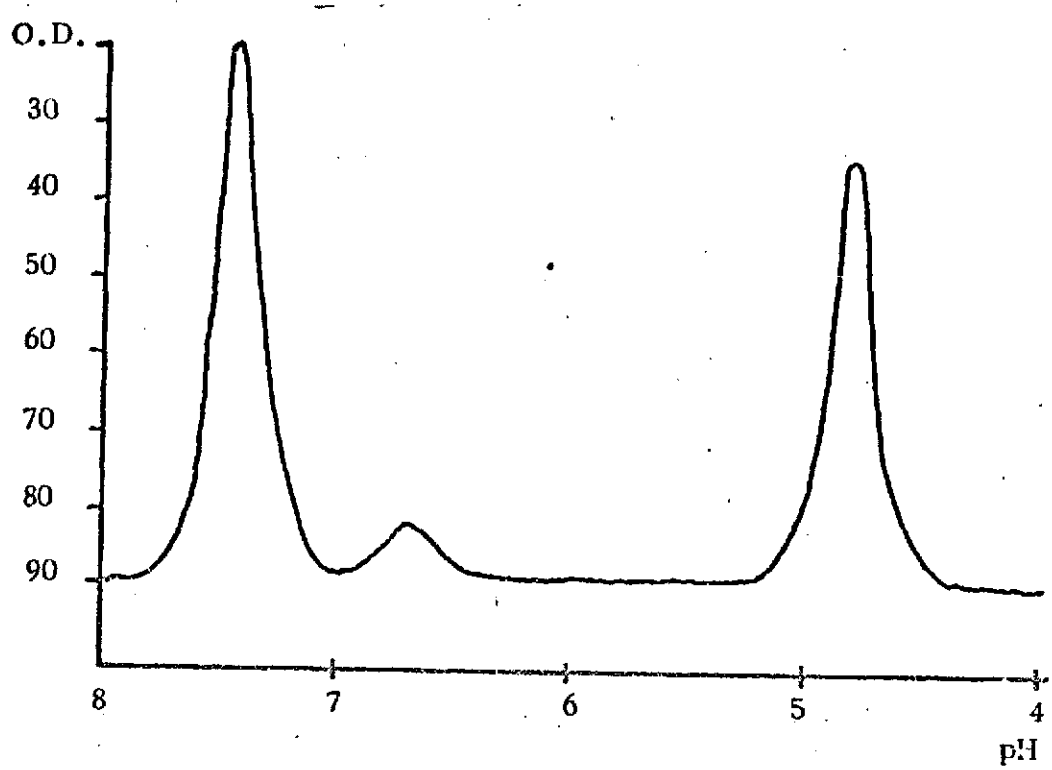

Fig. 3. Elution pattern at 280nm of fractions obtained in isoelectric focusing of human gamma-globulin.

proteins had focused into 5 sharp bands in the middle of the gradient, although the column contents still showed a faint reddish colour. In an effort to focus the zones more completely, the experiment was continued; after 48 hours, hemoglobin began to precipitate out of solution, destroying the separation which had been obtained.

A. Additional experiments not reported here, dealt with the analysis of each hemoglobin individually, or their binary mixtures. These experiments provided the basis for later comparison with isotachophoretic resolution.

3. Fractionation of Dyes and Pigments

This separation was used to investigate the stability conferred on focused boundaries by the density gradient. In addition, it presented an opportunity to compare the self-

sharpening properties of isoelectric focusing with those of isotachophoresis.* A 1% w/v solution of Evans blue dye was applied to a 50% w/v sucrose density gradient containing 1% v/v Ampholines pH range 5-8. After 24 hours of focusing, at 600 volts, a dark blue and a light blue band were observed in the region of the anode. With the current still flowing, the column was tilted 30° from vertical, then returned to its normal position. Throughout this procedure, the focused bands remained parallel to each other and to the bench top. Furthermore, an increase in the temperature of the circulating water in the thermostat jacket of the column, from 4°C to 20°C, did not result in any noticeable convective disruption of the zones.

4. Influence of Slope of Density Gradients

This group of experiments was concerned with the extent to which the slope of the density gradient influenced the stability of focused boundaries. These experiments were of particular importance in our study of effects of density gradients on electroosmosis. They consisted of five similar separations of three hemoglobins (sheep, human and dog), which differed only in the concentration of the sucrose density gradient. Thus the stability of the focused zones was assessed qualitatively in 0%-50%, 30%, 20%, 5% and 0% w/v sucrose gradients. Separation of the three hemoglobins occurred in all but the last experiment, in which no separation occurred, the sample remaining evenly distributed throughout the length of the column. Separated hemoglobins showed good resolution; their stability was not affected by tilting the column.

5. Ampholine Fractionation

Isoelectric focusing of 10 mls of LKB Ampholines pH range 3-10 was performed using

*cf. "Isotachophoresis on Density Gradients and Gels" A.J.K. Smolka, present report

a 50% sucrose density gradient and the usual electrode buffers. After 24 hours at 600 volts, the column contents were eluted into 3 ml fractions, the pH of which was measured. The indicated pH of each fraction located the general pH region encompassed by the fraction, while the pH of adjacent fractions set limits to the range. In this way, over 30 Ampholine fractions were collected; not only can these be used as spacer ions in isotachophoresis, but their individual pH values, when plotted against fraction volume and number, indicated that the natural pH gradient formed during isoelectric focusing is linear and stable for at least 24 hours.

DISCUSSION

The results reported in this paper showed that density gradients provide focused zones with excellent stabilization against thermal and concentration convection. Since both forms of convection are gravity-associated phenomena, neither are observed in space, and so to this extent, the use of density gradient stabilization of boundaries on earth is an approximation of conditions encountered in zero gravity. However, zero gravity does not eliminate the problem of electroosmosis. As electroosmosis is apparently suppressed by density gradients, which are inapplicable in space electrophoresis, alternative methods may have to be introduced to counteract these phenomena in a zero-gravity environment.

The apparent absence of electroosmotic effects in the present experiments was attributed to several contributing factors.

A. Electroosmosis is a surface phenomenon, in that charges present on the surface of the separation channel, will, in the presence of an electric field parallel to the wall, induce a flow of electrolyte in the direction opposite to the migration of the separands. Essentially,

electroosmosis is the converse of streaming potential, which results when an electrolyte flows across a surface. Electroosmotic flow of electrolyte may carry the sample with it, leading to parabolic boundary profiles. In the presence of a density gradient, however, this may be minimized since each element of liquid volume tends to return immediately to its original density "niche". It is possible that, as a result, there is an electroosmotic density correlated microcirculation of each fluid element in the region of the wall. Unfortunately, we have been as yet unable to prove the existence of this microcirculation and plan further experiments.

B. Adsorption of sucrose, the density gradient solute in the present experiments, onto the glass walls of the annular separation channel may decrease electroosmosis similarly to the known effect of more complex polysaccharides, such as agarose.

C. Isoelectrically focused zones are self-correcting since proteins will migrate electrophoretically to their isoelectric point. Thus any tendency for proteins to flow electroosmotically out of the isoelectric zone is countered by the migration of the now charged proteins back into the zone. Isotachophoretic boundaries are also self-correcting, for different reasons, and the Skylab experiment was basically designed to test the effect of electroosmosis in boundary shapes.

Other measures can be taken to minimise electroosmosis; these involve coating the walls of the separation channel with hydrophilic substances such as agarose, or by the inclusion of an non-ionic long chain polymer of high viscosity in the electrolyte. Hydroxyethylcellulose is such a substance, and has been shown by Hinckley to decrease electroosmotic disturbances in free solution capillary isotachophoresis of proteins, presumably by virtue of its viscosity and by coating the walls of the apparatus.

The preparation of large numbers of Ampholine sub-fractions by isoelectric focusing allows a study of the optimum pH range of carrier ampholytes used as spacer ions in isotachophoresis. The use of wide range Ampholines (pH 5-8) in isotachophoresis results in less sharp boundaries and takes longer. An ideal spacer ion is one which has a mobility intermediate to either of the separands (in a two component sample) and which reacts chemically with neither. It is possible that by careful quantitation of the separation achieved in a mixture of hemoglobin and ferritin using different Ampholine fractions of very limited pH and mobility range, a spacer molecule will be found that fulfills these conditions. This is an ongoing project at the present time.

REFERENCES

1. C. C. Brinton and M. A. Lauffer, in "Electrophoresis" M. Bier, ed. Vol. 1, p. 427, Academic Press, New York, (1959)
2. K. Hannig, in "Electrophoresis" M. Bier, ed. Vol. 11, p. 423, Academic Press, New York, (1967)
3. A. Strickler and T. Sacks. Ann. N.Y. Acad. Sci., Vol. 209, p. 497, (1973)
4. H. Svensson, Acta. Chem. Scand. 15 325, (1961)
5. H. Haglund, in "Methods of Biochemical Analysis" D. Glick, ed. Vol. 19, p. 1. Interscience, New York, N.Y. (1971)
6. E. Valmet, Science Tools 16 p. 1. (1969)
7. C. R. Hardt, I. F. Huddleson, and C. D. Ball. J. Biol. Chem. 163 p. 211 (1946)
8. R. E. Jones, W. A. Hemmings and W. P. Faulk. Immunochemistry 8 p. 299 (1971)
9. J. St. L. Philpot, Trans. Faraday Soc. 36 p. 38 (1940)
10. O. Vesterberg, Ann. N.Y. Acad. Sci., Vol. 209, p. 23 (1973)

ISOTACHOPHORESIS ON DENSITY GRADIENTS AND GELS

A.J.K. Smolka

Research Associate

University of Arizona

INTRODUCTION

The ultimate objective of our present research into isotachophoresis is the separation of living cells. However, certain isotachophoretic phenomena are still not fully understood, and a frontal assault on the problem of cell separation must await the acquisition of more complete theoretical and experimental data concerning separations of proteins and dyes. Four distinct though interrelated lines of inquiry were followed in this work.

A. Two forms of isotachophoresis were compared; free solution and gel, the latter using both agarose and polyacrylamide gels. The free solution work raised the problems of electroosmosis and slope of density gradient, while the gel work raised the possibility of quantitative isotachophoretic studies.

B. Quantitation of isotachophoretic phenomena was considered an important objective in that future cell separations will rest on definitive quantitation of the relationships between leader and sample concentrations. These studies were hampered somewhat by the difficulties we experienced in preparing polyacrylamide gels of different leader concentrations.

C. The whole question of optimum leader concentration was also investigated, and the dependence of sample concentration on the leader was verified.

D. Throughout the experimental series, a phenomenon known to us as "doming" was observed in gels; latterly, a possible analogue of doming has been observed in free solution isotachophoresis. Doming manifests itself as an retrograde upward bowing of the trailing sample boundaries. Since reproducible quantitation is impossible in

the presence of doming, some effort went into determining its cause. The present paper is restricted to free solution and gel isotachophoresis not directly related to the Skylab CPMD Experiment, as well as a report on preliminary red cell separations.

Owing to the large number of isotachophoretic experiments performed over the last year, only a few representative results can be reported in the present paper; Further isotachophoretic results are reported in "Skylab IV - Pre-Flight Protein Studies" (cf. present report).

MATERIALS AND METHODS

1. Commercial Apparatus

A 110 ml isoelectric focusing column* was used without modification in several free solution isotachophoretic studies. The relatively complex procedures involved in running this column were felt to be a hindrance, and so several simpler apparatus were constructed in the laboratory (Figs. 1-4).

A Canalco 12 tube Disc Electrophoresis** apparatus was used for gel isotachophoresis.

2. Other Apparatus

Since we wanted to investigate the effects on isotachophoresis of using long density gradients, glass or plexiglass tubes, and different leader and terminator volumes, several isotachophoresis unit were constructed in the laboratory. (The figures do not include the variants of the horizontal capillaries used by Hinckley, nor does this section discuss the design, construction, and operation of this equipment). The instruments shown

*LKB Instruments Inc., Rockville, Md.

** Canalco Inc., Rockville, Md.

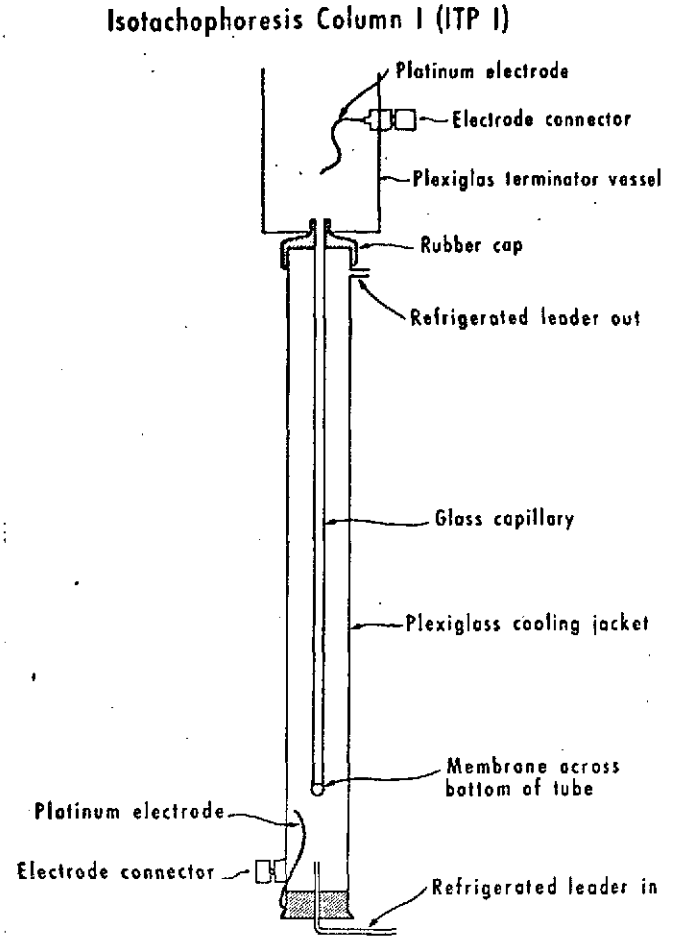

Fig. 1

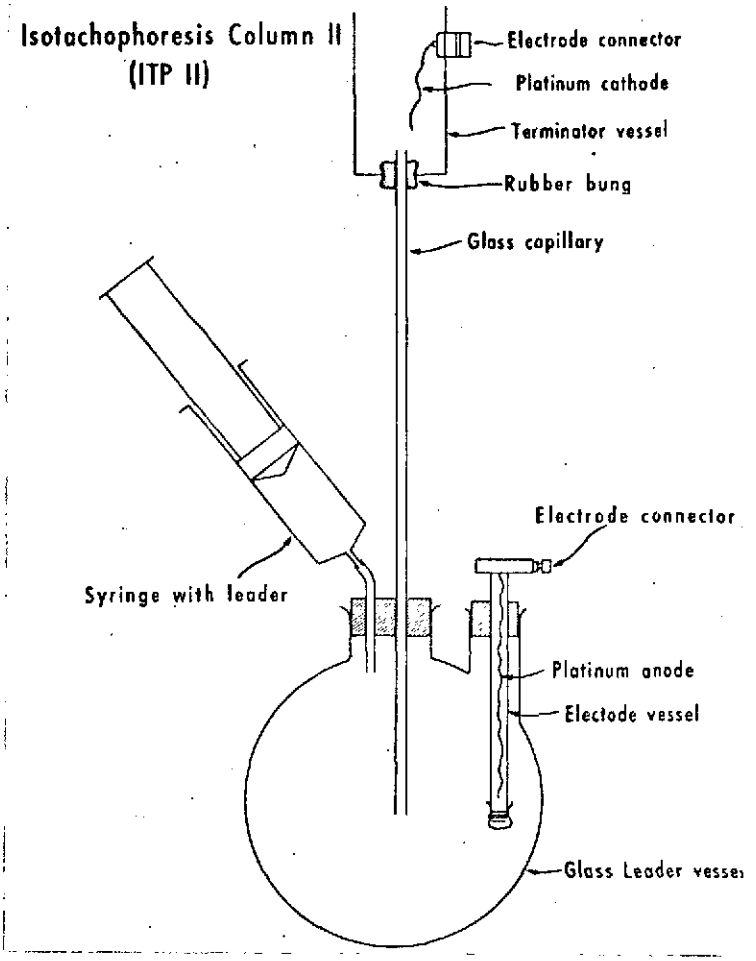

Fig. 2

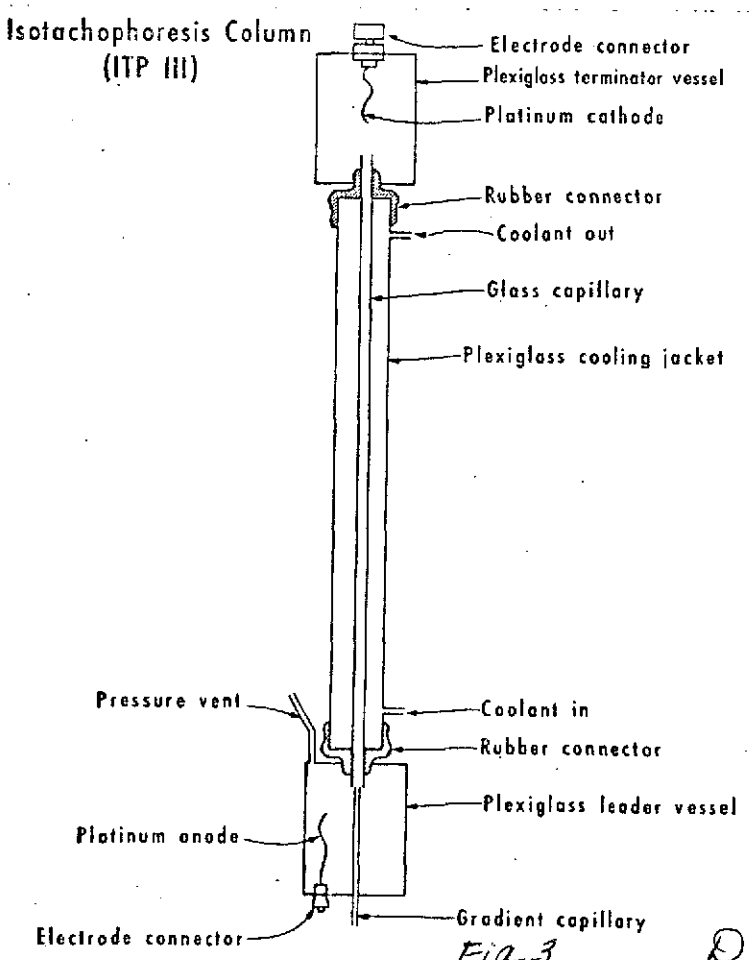

Fig. 3

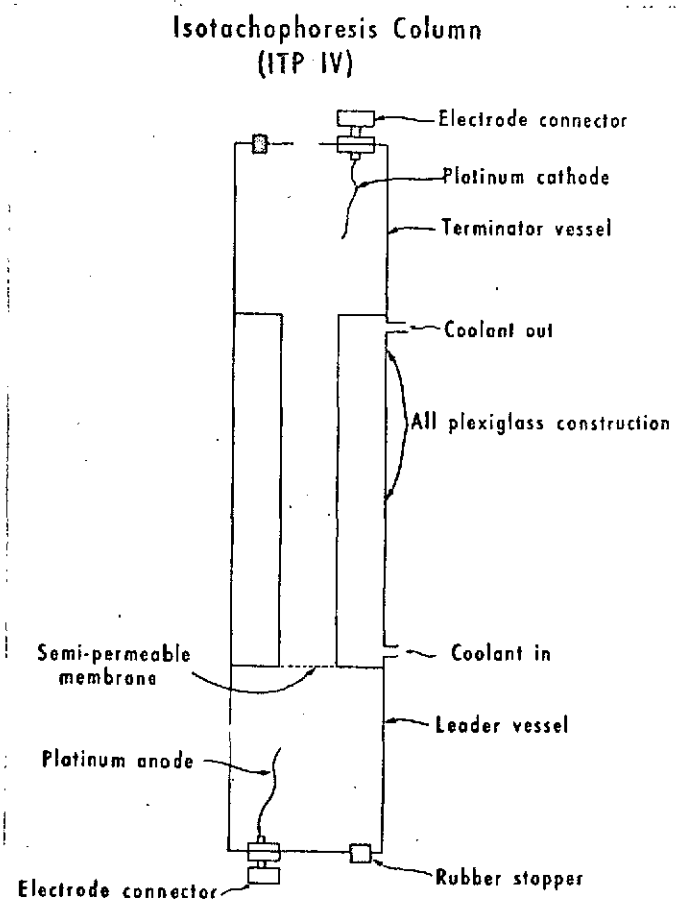

Fig. 4

D-24

possess several features in common, and these can be regarded as fundamental to any isotachophoretic technique.

a) A separation channel within which migration of resolved components of a sample mixture takes place. Our experiments have been conducted in tubes of various lengths and diameters, made of glass, plexiglass and quartz. Since potentially disruptive electro-osmostic effects are a function of the wall composition, all tubes have been used in both coated and uncoated configurations to determine the extent and to investigate the minimization of these effects. As far as free solution isotachophoresis in vertical tubes is concerned, the use of different tube materials and different wall coatings has not resulted in significantly improved separations, since the instability of boundaries and gross convective disturbances are usually of a magnitude sufficient to mask the insidious electroosmotic disruptions. Coatings were agarose; Hinckley has used hydroxyethyl-cellulose throughout the buffers as an anti-electroosmotic measure.

b) A leading buffer reservoir, of large volume compared to the separation channel, which communicates with the channel either directly or through a semi-permeable membrane, and which contains the anode. This reservoir may incorporate an electrode labyrinth designed to prevent diffusion of electrode decomposition products and gas bubbles into the separation channel, as well as a facility for introducing a density gradient into the channel. This feature is evident in Fig. 3 . .

c) A terminating buffer reservoir, again of large volume compared to the separation channel, which contains the cathode, as well as electrode labyrinths if considered necessary.

d) A pair of electrodes, preferably of platinum and silver, which present a large

surface area to the respective buffers, and which react minimally with the buffers. For the Skylab charged particle mobility demonstration, the anode was silver mesh, while the cathode was a palladium plate. This combination was demonstrated to be non-gassing with the buffers used, the silver being converted to silver chloride, and evolved hydrogen at the anode redissolving in the palladium.

e) A cooling jacket through which refrigerated coolant or leading buffer at 4°C can be circulated. This feature is evident in Figs. 3&4 and ensures that there is uniform radial cooling of the separation channel.

3. Gels

a) Agarose gels were prepared by dissolving agarose (Fisher Scientific Co.) in the leading buffer to give 0.5% w/v concentration. Gels were melted before use, and poured at 65°C.

b) Polyacrylamide. The large pore stacking gel of Ornstein and Davis ([1,2]) was used in all experiments, and was formulated as follows:

Solution A: 48 mls IN HCl

5.98 g Tris

0.46 mls N, N, N', N' Tetramethylethylenediamine (TEMED)

water to 100 mls

Solution B: 10.0 g Acrylamide

2.5 g N, N' Methylenebisacrylamide (BIS)

water to 100 mls

Solution C: 4 mg Riboflavin

water to 100 mls

Solution D: 40 g Sucrose

water to 100 mls

The working solution consisted of 1 part A, 2 parts B, 1 part C, and 4 parts D. The pH was adjusted to 7.2. Gels were prepared immediately before use, and polymerisation was induced by means of a daylight fluorescent tube placed 2 inches from the gels.

4. Density Gradients

These were sucrose gradients and were prepared as described previously.*

5. Carrier Ampholytes

LKB Ampholine chemicals pH range 5 to 8, 40% w/v, were used in the protein and dye fractionations. The large range of constituent mobilities in Ampholine chemicals allows their use as colorless spacer molecules in isotachophoresis. (3)

6. Samples

Three species of hemoglobin were prepared as described previously.*

2 x crystallised horse spleen ferritin was obtained commercially.**

1% w/v Amido Black and Ponceau S were chosen as indicator dyes.

9g% bovine albumin was coupled to amido black. All sample mixtures were clarified by passage through a 0.22 micron filter before use, and were applied either by direct layering of the sample onto the surface of the gel or density gradient, followed by careful layering of the terminator on top, or by injecting the sample into the terminator and

* Isoelectric Focusing on Density Gradients, A.J.K. Smolka, present report

** Miles Laboratories, Inc., Kankakee, Ill. 60901

allowing it to settle onto the leader terminator interface. In both cases, sample introduction was by means of a 5 ml syringe fitted with a fine teflon capillary tube.

7. Recording of Results

Results were evaluated qualitatively by visual examination of the separations, by photography, and by measurement of migration distances with a millimeter rule.

RESULTS

1. Free Solution Isotachophoresis

The following experiments are representative of a large number which were done to investigate the feasibility of separating two proteins, hemoglobin and albumin, by isotachophoresis. Albumin was stained blue by coupling with Amido Black, which rendered detection systems other than direct visual observation unnecessary. The initial isotachophoretic experiments in density gradients were characterised by high applied potentials in the 1 to 6 kilovolt range. Hinckley had achieved some success in rotating horizontal capillary tubes using high potentials. Experiments a, b, and c below were unsuccessful for a variety of reasons; experiment d was the first, and so far the only, reproducible isotachophoretic separation in a density gradient, and was possible only because a simple dye mixture with no Ampholines was used as the sample.

a) This experiment was to investigate the boundary stability conferred by a long shallow density gradient.

Apparatus: ITP II, (fig.2) 1 meter agarose coated glass capillary I.D. 2mm air-cooled.

Leader: 16 mM Tris-Veronal, pH 8.05

Terminator: 20 mM Tris-Glycine, pH 9.1

Density Gradient: 0-10% Sucrose

Sample: Human and sheep hemoglobins, 7g%, 0.2 mls, with 10 µl Ampholine

1.2 kilovolts, 170 micro-amps.

Results: Transient sharpening of rear boundary, followed after 2 minutes by severe convective disturbances. No separation, spearing of sample into leader observed. Repetition of this experiment with an untreated capillary gave similar results.

b) Apparatus ITP III, uncoated glass capillary, 2 mm I.D. Water-cooled, 4°C

Leader: 1mM Tris-HCl pH 8.9

Terminator: 1mM Tris-Glycine, pH 9.1

Density Gradient: 15% to 3% sucrose

Sample: 100 µl of a mixture of three hemoglobins and albumin coupled to amido black, with 10 µl Ampholines pH range 5-8. 1000 volts, 300_{m}A.

Results: Immediate rear boundary sharpening, and slow migration of the sample towards the anode. Very diffuse front, which after two minutes began to show myleloid droplet sedimentation caused by a local increase in density of the sample compartment as a result of isotachophoretic concentration. Since a shallow gradient was used in this experiment, density convection resulted. Separation was not observed.

c) This experiment was to investigate the boundary stability conferred by a steep density gradient in a short wide bore channel.

Apparatus: ITP IV (Fig 4) length of channel, 26 cms, I.D., 1.2 cms

Leader: 10 mM Tris HCl pH 7.2

Terminator: 6 mM Tris-Glycine, pH 8.3

Density Gradient: 40% to 10% Sucrose

Sample: 100_{μ}1 mixed sheep, dog and human hemoglobins, 100_{μ}1, 0.1% w/v Amido Black,

with 100 µl Ampholine, pH range 5-8. 50 volts, 4 mA

Results: Immediate boundary sharpening, front and rear, and differentiation of the sample into three contiguous bands, red, green and blue, (from the cathode). No migration until, at 2 minutes, the blue band began to migrate towards the anode; the red and green bands remained stationary, gradually becoming more diffuse, and after 5 minutes began to migrate very slowly, losing their sharp fronts and merging. No separation of the three hemoglobins observed.

d) Apparatus: 110 ml LKB isoelectric focusing column with no modifications.

Leader: 20 mM Tris-HCl, pH 7.2

Terminator: 190 mM Tris-Glycine pH 8.3

Density Gradient: 60% Sucrose

Sample: 1% w/v Amido Black and 1% w/v Ponceau S. No Ampholines

Power: 300 volts, 7 mA

Results: Very good separation of the red and blue dyes into two bands 4 mm apart, both with sharp front and rear boundaries. The formation of a colourless space between the two dyes, in the absence of Ampholines, was attributed to impurities in the Ponceau S, which were colourless and possessed mobilities intermediate to that of both dyes. The first band, red Ponceau S, showed equal distribution of material across the width of the annulus. The second band (blue Amido Black) showed a concentration of dye in the centre of the annulus, with less dye near the walls of the annulus. Repetition of the same experiment did not show this effect. Since one characteristic of doming in gels is its random occurence, the concentration effect mentioned above may be related to doming. Migration speed was 5 cm/hour. There was no evidence

of thermal or concentration convection. Both bands retained their spacing and stability for four hours, at reduced voltage and current; after 24 hours however, the amido black band had approached the Ponceau S so that there was no longer a space between the two zones, although they remained separated.

2. Gel Isotachophoresis

Isotachophoretic separations of proteins and dyes on gels constitute the bulk of experimental results obtained in our laboratory. In this section, only representative results directly illustrating the characteristics of isotachophoresis are reported. The objective of these experiments was threefold; 1) to verify the relationships between leader concentration and sample concentration predicted by the Kohlrausch Regulating Function, and, 2.) to compare the relative merits of agarose and polyacrylamide gels with respect to reproducibility of results, and suitability for quantitative work, and lll) to investigate the phenomenon of doming.

The Canalco Disc Electrophoresis unit, used in this series of experiments, consists of an upper buffer reservoir equipped with a centrally located cathode, and twelve grommetted holes which accomodate twelve glass tubes of 4 mm I.D.. These tubes hang downwards into a lower buffer reservoir similarly equipped with an anode. For the purposes of isotachophoresis, the upper reservoir contains the terminator, while the lower one contains the leader.

Experiment a) below was simply a demonstration of the superior resolution and sharpness of boundaries characteristic of isotachophoresis; experiments b) and c) investigated the roles of leader concentration and volume of ampholine present in the sample respectively.

a) Apparatus: Canalco disc electrophoresis unit (12 tubes)

Leader: 60 mM Tris-HCl, pH 7.2

Terminator: 38 mM Tris-Glycine, pH 8.3

Gel: 60 mM Tris-HCl polyacrylamide gel

Power: 230 volts, 4 mA per tube

Samples: Six 100µl samples were run in duplicate; their compositions were as follows:

1. 50µl mixed hemoglobins, 50µl Ampholine
2. 25µl mixed hemoglobins, 25µl albumin + bromophenol blue, 50µl Ampholine
3. 25µl mixed hemoglobins, 25µl albumin + amido black, 50µl Ampholine
4. 100µl mixed hemoglobin
5. 50µl mixed hemoglobin, 50µl albumin + amido black
6. 50 µl mixed hemoglobin, 50µl albumin + bromophenol blue

The results are shown in Fig. 5.

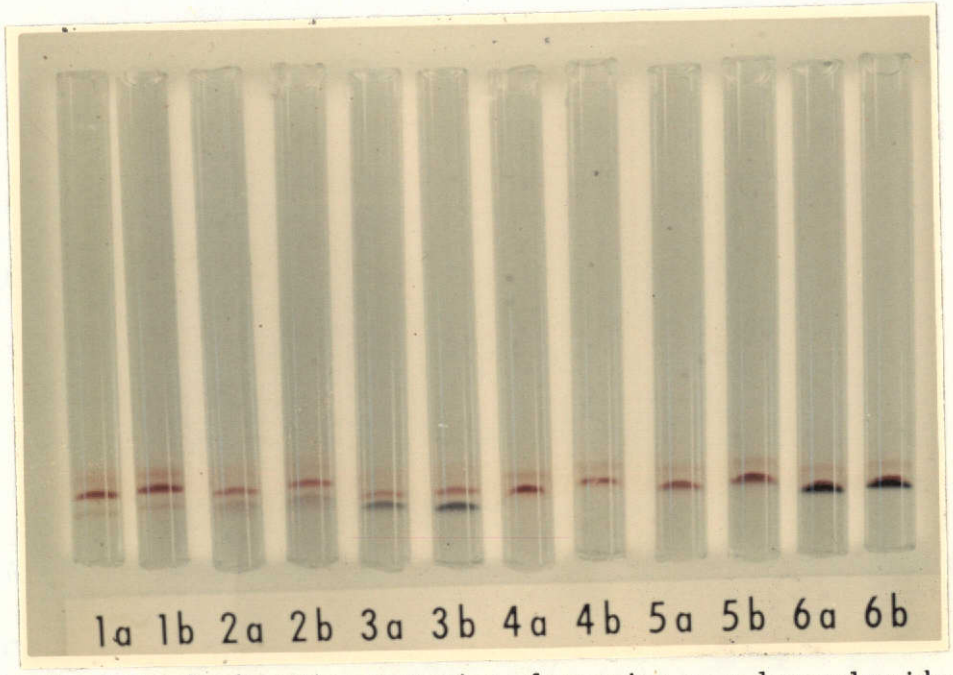

Fig. 5. Isotachophoretic separation of proteins on polyacrylamide gels.

This experiment was repeated using 60 mM Tris-HCl pH 7.2 in the terminator vessel in place of the Tris-glycine. Normal zone electrophoresis took place, although the separation achieved was poor in resolution and lacked the characteristic sharpness of isotachophoretic boundaries.

A similar experiment was carried out using 2% w/v agarose gels. Migration was somewhat slower than that observed in polyacrylamide, and the discs observed were not as sharply separated or well defined. When a 0.5% w/v agarose gel was used, the results were indistinguishable from the experiment reported in detail above.

b) Apparatus: 12 tube Canalco Disc electrophoresis unit

Leader: 30 mM Tris-HCl, pH 7.2

Terminator: 19 mM Tris-glycine, pH 8.3

Gel: 0.5% w/v agarose, 30 mM Tris-HCl

Power: 200 volts, 3 mA per tube

Samples: A range of six ferritin samples were run in duplicate, from 50μl to 300μl in 50μl increments. The results are shown in Fig. 6

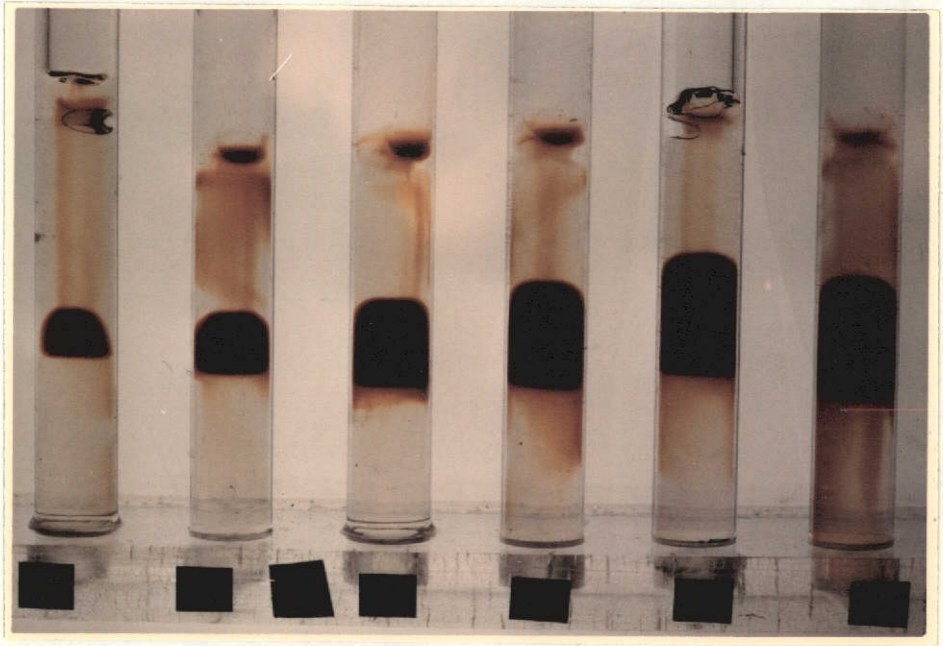

Fig. 6. Isotachophoresis of ferritin on agarose gels.

Two similar experiments were carried out using 60 mM and 10 mM Tris-HCl pH 7.2 as leader; these three experiments showed that step length is related to step concentration and to leader concentration.

c) Apparatus: 12 tube Canalco disc electrophoresis unit

Leader: 30 mM Tris-HCl, pH 7.2

Terminator: 19 mM Tris-glycine, pH 8.3

Gel: 0.5% w/v agarose, 30 mM Tris-HCl

Power: 200 volts, 4 mA per tube

Samples: Six samples of the following composition were run in duplicate.

1. 25μl human hemoglobin, 25μl ferritin, 10μl Ampholine
2. 25μl human hemoglobin, 25μl ferritin, 20μl Ampholine
3. 25μl human hemoglobin, 25μl ferritin, 30μl Ampholine
4. 50μl human hemoglobin, 50μl ferritin, 10μl Ampholine
5. 50μl human hemoglobin, 50μl ferritin, 20μl Ampholine
6. 50μl human hemoglobin, 50μl ferritin, 30μl Ampholine

Separation of the two proteins occurred in all tubes, and it was found that the length of the ampholine space was proportional to the volume of ampholine in the sample. The first three samples did not show the sharp front and rear boundaries characteristic of isotachophoresis. All the samples showed doming to a greater or lesser extent. (cf. Discussion). Further gel isotachophoresis results are reported in the Skylab pre-flight Protein Studies paper in this report.

3. Isotachophoresis of Red Cell Suspensions

The ITP IV column (Fig. 4) and the Canalco disc electrophoresis unit were used

in the red cell work. ITP IV consists of a water-cooled 11" long plexiglas column, 1/2" internal diameter, communicating with the leader vessel through a semipermeable membrane. For cell isotachophoresis, all 12 tubes of the Canalco apparatus were fitted with similar membranes at their lower end, to allow introduction of a density gradient. The separations were performed by layering a red cell mixture onto the leader, which in some cases incorporated a density gradient, layering terminator over the cells, and finally by applying current. The criterion for separation was merely the formation of two discs of cells separated by a clear zone of buffer. No attempt was made to identify the component cells of the discs. The sample in all experiments consisted of citrated sheep and human red blood cells, washed and suspended in normal saline with 5% dextrose for isotonicity. All buffers contained 5% dextrose, and gradients, if used, were either 25% Ficoll or 25% polyethylene glycol. The terminator was 38 mM Tris-glycine, pH 8.2; leaders used were 30 mM Tris-phosphate or 30 mM Tris-HCl, both pH 7.2. There was no difference in the separation when using one or other of the leaders, nor did presence or absence of density gradients produce significantly different results, presumably because the separations were destroyed in all cases after four or five minutes. Hemolysis, aggregation, precipitation and crenation of the cells were responsible for the disruption of boundaries. In all cases, however, separation did occur within the first four minutes at an applied potential of 200 volts, at 10 mA. Boundary sharpening occurred after 30 seconds. After 90 seconds, front and rear boundaries increased in concentration (deepening of colour in these regions) until a clear zone appeared between them. Maximum migration distance in the plexiglas instrument was 1.2 cms (See Fig. 7.)

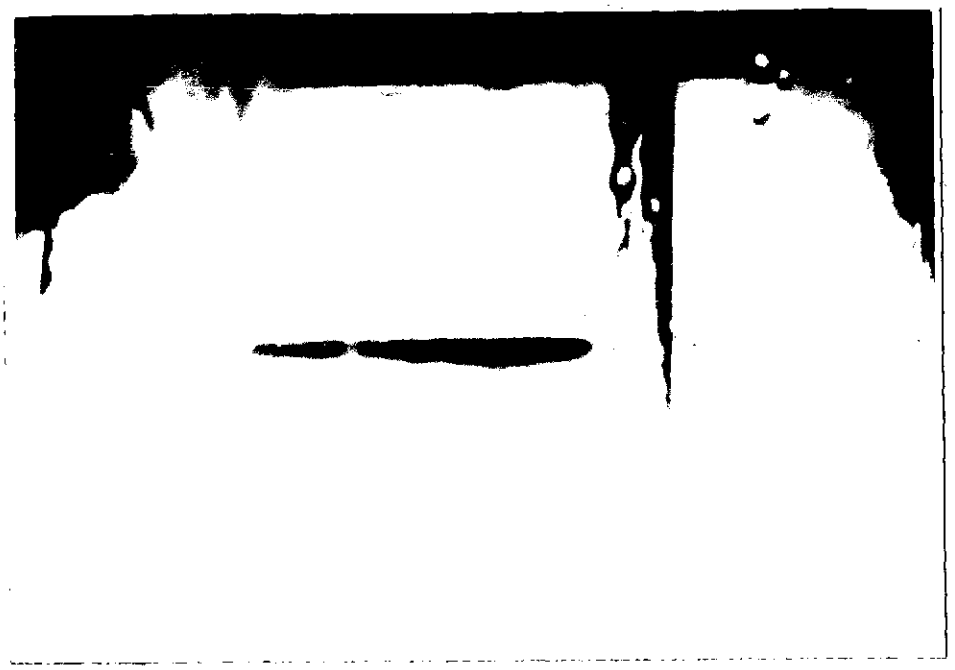

Fig. 7. Isotachophoresis of red cells.

DISCUSSION

A. Electrolyte Systems

The present experiments utilized Tris-HCl at pH 7.2 as the leading buffer, and Tris-glycine at pH 8.3 as terminating buffer. A preliminary study of electrolyte systems used in isotachophoresis showed that a wide and diverse range of electrolyte compositions and concentrations have been used in small anion isotachophoresis (4); by comparison, few well-documented systems of relative simplicity are available for protein isotachophoresis.[5,6] We have been concerned principally with quantitation and reproducibility of this technique; consequently, we have studied only the leader - terminator system of Ornstein and Davis (1, 2) which was shown to result in good separation of several coloured proteins and dyes.

B. Free Solution and Gel Isotachophoresis

Despite the stabilization conferred by density gradients, isotachophoresis of proteins in free solutions met with little success. Using Tris-HCl leader, and Tris-glycine terminator, both of varying concentrations, and respective pH values of 7.2 and 8.3, and using a sample mixture of three hemoglobins layered onto a sucrose

density gradient, it was possible to induce rear boundary formation, and occasionally front boundary formation, with an applied potential of 1 kilovolt. In no case was separation of the hemoglobins observed. The usual pattern of behaviour was transient formation of rear boundaries followed within two or three minutes by severe convective disturbances, which would degenerate, only to reform transiently, while the front boundary would either develop a spear-shaped configuration extending into the leader, or droplet sedimentation would occur.

One of the characteristics of isotachophoretic analysis is that the distribution of sample molecules in a resolved compartment is non-Gaussian, unlike zone electrophoresis and isoelectric focusing. This observation is of some importance in considering the stability conferred on isotachophoretic boundaries by density gradients. To be effective, density gradients must be positive, i.e., the density of a fluid element at any point in the gradient must be less than the density of fluid elements at any lower point in the gradient. In zone electrophoresis and isoelectric focusing, the density profile of the gradient with an applied sample is shown in Fig. 8 .*

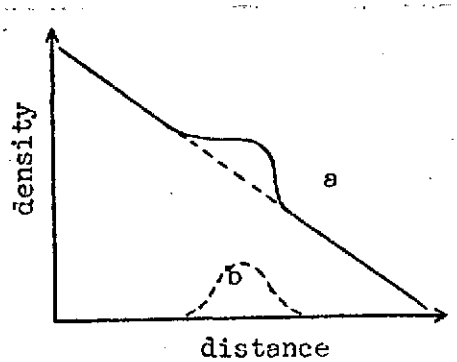

Fig. 8. Stable density gradients in isoelectric focusing. (a) sucrose gradient with sample; (b) sample in Gaussian distribution.

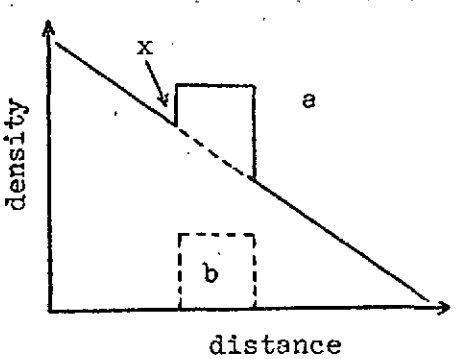

Fig. 9. Unstable density gradients in isotachophoresis. (a) sucrose gradient with sample; (b) sample in Kohlrausch distribution; (x) region of instability due to the negative density profile.

In isotachophoresis, however, the non-Gaussian distribution of sample gives the profile shown in Fig. 9 . In the region marked x , the resulting density profile is negative, and density convection will take place. In the case of a protein sample on a sucrose density gradient, the result will be the formation of myeloid droplets which sediment into the underlying buffer. Droplet sedimentation in such cases may be minimized by increasing the slope of the density profile, thus reducing the area x ' in Fig. 9 . Future experiments will include isotachophoretic resolutions in very steep gradients.

In the present experiments, it was observed that convective disturbances were less in a wide bore column, such as Fig. 4 , presumably because a dependable density gradient could be constructed in such a column. When isotachophoresis of two indicator dyes (see Results) was attempted in the LKB isoelectric focusing column, with an automatically constructed 50% sucrose gradient, perfect isotachophoretic separation of the dyes was observed which remained stable for 24 hours. Thus, lower voltages and well-constructed density gradients may be essential to any free solution isotachophoretic process in vertical columns.

The phenomenon of steady state stacking plays a fundamental role in the disc electrophoresis technique of Ornstein and Davis and is essentially an isotachophoretic phenomenon which takes place in a large pore "stacking" gel which imposes minimum restrictions on the migration of molecules, but which is thermostable, transparent, mechanically strong, relatively inert chemically and most important, is non-ionic. Gel isotachophoresis can be regarded as the stacking stage of disc electrophoresis, without the zonal separation which occurs once the proteins have migrated into the

small pore gel. The work of Griffiths and Catsimpoolas (3) showed that by the use of suitable "spacer" molecules, intermediate in mobility to the components of the sample mixture, an isotachophoretic separation of these components could be obtained in an extended "stacking" or large pore gel, a separation which equalled, if not surpassed, in resolution, boundary sharpness and boundary stability, the results obtainable by classical disc electrophoresis. The use of a large pore gel is intended primarily as an anti-convective medium, and so the problems of thermal convection which frustrated our attempts at free solution isotachophoresis are not encountered. Thus it seems that quantitation of isotachophoretic phenomena, such as the relations between leader concentration, sample concentration, spacer molecule concentration, length of steps, spacing between steps, and several related factors, for example, optimum pH and temperatures, is best performed in gels, which, in the case of polyacrylamide, and to a lesser extent, agarose gels, can be prepared reproducibly in a standardised formulation, which itself can be modified to introduce further separative parameters. The initial investigations of gel isotachophoresis in this laboratory were repetitions of the published work of Ornstein and Davis, and Griffiths and Catsimpoolas and were carried out in the 12-tube Canalco Disc Electrophoresis apparatus. From the start, the results were uniformly impressive. Using the buffer and gel formulations of Davis (2), we were able to show qualitatively the relations between leader concentration and step length, and between ampholine volume and the length of the ampholine space. These results showed the value of gel isotachophoresis in quantitating isotachophoretic phenomena, and a program is now under way to perform definitive quantitation in gels, using the apparatus in Fig. 10 .

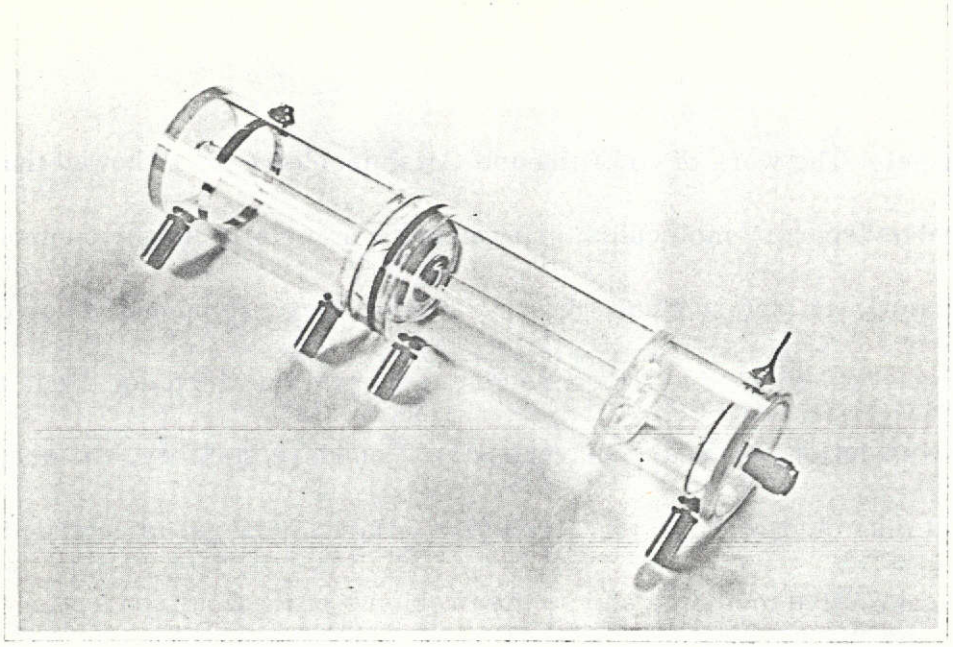

Fig. 10. Thermostatted plexiglas column for isotachophoretic quantitation studies.

C. A phenomenon which appears to be intricately involved in the mechanism of gel isotachophoresis is doming, which manifests itself as an upward bowing of the rearmost sample component, which is in contact with the terminating buffer. At the present time, there is no consensus as to the cause of doming. It may be of value to list the principal characteristics of doming, and the conditions under which it occurs. A summary of the hypotheses which have been proposed can be found in the paper by Hinckley.

1. Doming may occur at random. This observation, more than any other, has frustrated attempts to explain doming. In the Canalco disc electrophoresis apparatus, it was found, in the course of innumerable isotachophoresis runs, that a seemingly arbitrary percentage of the tubes displayed doming. Even in cases where all twelve tubes contained identical samples, and where all gels were identical, by the normal standards of laboratory accuracy, doming occurred absolutely at random.

2. Agarose gels more often display doming than polyacrylamide gels, although attempts

to correlate the relative frequency of doming in the two media have been inconclusive.

3. Dome formation is a gradual process, which occurs within the first four to five minutes of a gel isotachophoresis run; absence of doming after the first five minutes usually precludes later doming.

4. Domes may either go to completion, i.e., when they break away from the rearmost boundary and assume a spherical configuration which migrates at a constant rate, equal to the rate of migration of preceeding zones, or they may regress giving rise once again to the characteristically flat and sharp isotachophoretic boundary. (see Fig. 5)

5. When a dome arises in the rearmost boundary of a long single sample, it rarely goes to completion; when a dome originates in a narrow separated zone, the dome grows at the expense of that zone, although contact of the zone with the walls of the tube is maintained until just before the dome becomes spherical, thus domes have been observed which seem to rest on an extremely fine and tenuous interface which extends radially to the walls.

6. The formation of domes cannot be correlated with the temperature or concentration of pH of the buffers or gels used, nor is there any correlation between frequency of doming and the composition of the tube walls.

Hinckley has observed that passage of a sample train through an agarose gel induces an opalescence of the gel behind the terminator-sample interface, which can readily be observed through polarizing filters. However, this opalescence is present in cases where doming is absent.

A possible analogue of doming was observed in isotachophoretic separation of indicator dyes on a density gradient. The rearmost band was very narrow and displayed the sharp front and rear boundaries characteristic of isotachophoresis (see Results)

but there was a distinct concentration of dye in the middle of the zone, away from the glass walls of the apparatus. The depletion of stain in the wall region was not electro-osmotic in origin, since there was no coloration of the terminator buffer.

D. At the time of writing, there are no reports in the literature of red cell separations using isotachophoresis. The results reported in this paper are of a preliminary nature, but exceedingly encouraging. The problems mentioned previously which disrupted the separation after a few minutes can probably be overcome by a careful choice of isotonic density gradient compositions and concentrations. It seems that this can be done using different proportions of Ficoll and dextrose in the two compartments of the LKB density gradient mixing device. We are currently planning to perform isotachophoresis of red cells in the LKB isoelectric focusing column,, with a view to publication. Previous work has shown that this column can be used without modification for isotachophoretic applications.

REFERENCES

1. L.Ornstein, Ann. N.Y.Acad. Sci.121:321, 1964
2. B.J. Davis, Ann. N.Y. Acad. Sci.121 ; 404, 1964
3. A. Griffith and N. Catsimpoolas, Anal. Biochem. 45: 192, 1972
4. R.J. Routs, Thesis, Technological University, Eindhoven, The Netherlands, 1971.
5. P.J. Svendsen and C. Rose, Sci. Tools 17: 13, 1970
6. N. Catsimpoolas and J. Kenney, Biochim. Biophys. Acta. 285: 287, 1972

SECTION E

REPORT ON THE SKYLAB EXPERIMENT

by

M. Bier, J.O.N. Hinckley, A.J.K. Smolka, and G.T. Moore

SKYLAB EXPERIMENT

M. Bier, J. O. N. Hinckley and A. J. K. Smolka

INTRODUCTION:

Most significant development during the contract year was the opportunity to participate in the Skylab experiments through the inclusion of a Charged Particle Mobility Demonstration (CPMD) experiment in Skylab IV. This experiment was made possible only through the most intimate collaboration with our contracting officer, Dr. R. S. Snyder, and a number of his colleagues at the Marshall Space Flight Center, in particular, Messrs. B. O. Montgomery, A. C. Krupuick, S. B. Hall, and Dr. T. Bannister.

Unfortunately, the lead time available for the preparation of the CPMD was very short, and we had only a few weeks between the original concept and the delivery of the finished package. No comprehensive testing of the finished package under all conceivable environmental conditions was possible. Nevertheless, an apparatus was constructed, which appeared to satisfy the elementary requirements of the modest flight proposal. It was designed under the severest constraints of space and power available. The apparatus had to fit the inside of a cylinder 3.5"

in diameter, 3.5" long. The only power available was 28 volts.

The apparatus consisted of two plastic modules, described in greater details later on, and fitted between two metallic end-plates, with a suitable connector and switches. The plastic modules were made by the contractor, where special thanks are due to Mr. Anthony Clarkson, of Clarkson Research Corp., which machined them, under greatest pressure of available time. The metal plates and electrical wiring was provided for by Marshall Space Flight Center. The actual filling of the apparatus for flight was carried out in the decompression chamber at Marshall Space Flight Center by Mr. S. Hall and A. Smolka.

Unfortunately, the experimental package did not perform as well as expected. The protein module failed completely, as there was no migration of protein. The reasons for it remain a puzzle. Examination of the module, upon return from Skylab, showed all electrical parts to be operational, but the silver mesh anode showed no deposition of silver chloride, indicating that no passage of electric current occurred. The presence of protein in the cell contents was demonstrated by spectrophotometric analysis. The only possible explanation for the operational failure is that an air bubble completely obstructed the passage of electrical current, though this too appears highly unlikely. The debriefing of the astronauts did not clarify this point.

The blood module also showed extensive leakage, with numerous air bubbles in the observation channel. Nevertheless, the astronaut, Dr. E. Gibson, was able to perform two experiments with it. In the first experiment, the photographs of the observation channel are obscured by the presence of air bubbles, preventing the exact

determination of the shape of the advancing fronts. Unfortunately, the cautionary note in the instructions regarding the elimination of air bubbles was overlooked. This was corrected in the second experiment (unplanned, and carried out at the initiative of Dr. Gibson, who is highly to be complimented in this regard), and excellent photographs were obtained. Another unfortunate incident was the failure to refrigerate the module in the first weeks of the Skylab mission.

An important part of the overall Skylab experiment were the extensive earth-bound experiments which paralleled the development of the modules. The description of this work is also included in this section, though, obviously, it was an important part of the overall experimental program, and could have been included in the previous sections.

Though the Skylab experiment was only a partial success, it has been a most significant contribution to our overall effort. It has clearly demonstrated the possibility of isotachophoresis of living cells, and confirmed the sharpness of isotachophoretic boundaries, in clear distinction with the diffuse boundaries observed in zone electrophoresis of latex particles in previous Apollo 16 electrophoresis experiment. It is hoped that the state of art of zero gravity isotachophoresis will be further advanced in the presently planned experiments during the joint Apollo-Soyuz flight scheduled for 1975.

FLIGHT PROPOSAL: ISOTACHOPHORESIS IN SPACE

1. SUMMARY AND SIGNIFICANCE

a. Advantages of isotachophoresis

1. The electrochemical forces in isotachophoresis separate ionic substances, such as proteins or cells, into separate compartments, limited by boundaries of near infinite sharpness (best present estimate: boundary width of 10^{-3}cm).

2. These boundaries are self-sharpening, and there is no deterioration or degeneration with either time or distance of migration.

3. The boundaries are to a high degree self-recuperative, and reform if stirred, or disrupted by other factors, including convection.

4. The concentration of each substance within its compartment is uniform - no gaussian distribution of concentrations is present. This concentration remains constant throughout the run, once the separation has been achieved.

5. Higher concentrations of components can be handled by virtue of this uniformity, and the sharpness of interspecies boundaries. The concentration is independent of initial protein concentration - and depends only on molarity of leader buffer chosen.

6. It is the only high resolution technique at least potentially applicable to separation of living cells.

7. It has great potential for preparative purposes because of above factors, and because of reduced heat generation per unit of product, allowing for easier scale-up of apparatus.

b. Relevance of zero-gravity

The most successful earthbound separations of large molecules have been in gels (with all the disadvantages of gel methodology), which cannot be used for cells. In free solution,

gravity causes sagging of interfaces due to density differences of concentrated protein compartments, these concentrations being much higher than usually encountered in other forms of electrophoresis.

c. Experimental evidence for benefits of zero-gravity

Attempts to circumvent these difficulties, by rotation of horizontal columns and by use of density gradients in vertical columns, have not yet matched the resolution obtainable in gels. But these methods, which to some extent simulate the effects of zero-gravity, produce sufficient improvement to indicate that zero-gravity may be the unique solution to this problem.

d. Significance of the proposed experiments

Taking advantage of the possible inclusion of an electrophoretic experiment in the forthcoming Skylab flight in November 1973, we propose to test two basic hypotheses:

1. That separation of two colored proteins, hemoglobin and ferritin, will be as good in zero-gravity in free solution as in earthbound gels.

2. That living cells will behave in analogous manner once the effects of gravity are removed.

e. Proposed flight package, weight, dimensions, required facilities

To test these hypotheses one flight package is proposed consisting of two modules, one preloaded with protein, the other preloaded with red blood cells. The overall dimensions of the combined package will be 2" x 1" x 4" (two by one by four inches) , each module being 1" x 1" x 4". Total weight will be less than 240 grams. The power requirement is 28 volts at up to 10 milliamps, for one hour. We rely on the experimenter for visual observation and photographic recording, using the camera already on board. Photographs at one-minute intervals will suffice during the one hour of running.

Engineering Information

Weight (excluding photographic and power facility)		Size (excluding photographic and power facility)
At launch	Less than 240 grams in toto	8 cubic inches (1" x 2" x 4")
Return	Film only	Film only

Data Recording: Visual and photographic (60 exposures, 1 min. intervals, with existing camera and illumination)

Spacecraft interface:

Mechanical:	Two self-contained 1" x 1" x 4" composite plastic blocks
Electrical:	Standard spacecraft 28 V DC outlet
Data:	60 exposures at 1 min. intervals, standard photographic onboard equipment and illumination.
Thermal:	Stored whenever possible in refrigerator, otherwise ambient temperature. During experiment - ambient temperature.

f. Fabrication and delivery arrangements

The apparatus will be delivered by us, preloaded with sample, and brought to the flight center as close to departure date as possible (to minimize aging deterioration of sample). The module and package consist entirely of plastics, metal, and some rubber; there are no moving parts, no glass, no toxic, hazardous or infectious compounds.

g. Operation and instructions

Instructions to the experimenting astronaut will be:

1. Focus camera, with appropriate illumination, to include middle one-third of module (i.e., the central tube).
2. Establish electrical contact with power supply.
3. Pull one lever.

4. Take photographs, and observe.

5. Reverse current, continue photographs, and observe.

II. BACKGROUND

a. The significance of electrophoresis consists in its being the only method capable of good nondestructive separation of a large class of valuable biological materials (1) with high resolution and purity. Unfortunately, it has not yet been possible to scale-up electrophoresis to significant preparative dimensions.

b. The Apollo XVI flight elecrophoresis experiment showed the potential advantages of zero-gravity electrophoresis. It also demonstrated, however, that avoidance of gravity effects does not eliminate all problems: the boundaries were grossly parabolic because of electro-osmotic effects, and diffuse, because of poor sample insertion, diffusion, and possibly other forces, including random fluid movement of as yet undetermined origin. The boundaries were completely destroyed after a relatively short time. It is our opinion that this demonstrates the necessity of using a technique which provides self-sharpening boundaries, such as isotacho-phoresis.

c. Isotachophoresis (2) may overcome these difficulties, due to:

1. Self-sharpening boundaries between adjacent compartments of sample components.

2. Self-correction and recovery of boundaries against random fluid movements and other disturbing factors.

3. Nondegeneration of this stable geometry with time and distance of migration.

4. Reduction of heat-generation per unit of potential gradient, allowing relatively high restoring electrochemical forces to impose a gravity-independent geometry on the system, as outlined above.

III, SUPPORTING WORK ALREADY DONE

a. Separations by isotachophoresis in gels are excellent and prove the power of the technique at high resolution. We have separated albumin, hemoglobin, ferritin, spacer ampholytes and dyes in this way.

b. Similar but inferior transient separations of these proteins and of cells have been done here in density gradients in vertical columns, in free solution.

c. Similar but inferior separations of these proteins and of red blood cells have been done by us in rotating and in stirred horizontal columns, in free solution.

d. The density-gradient and rotating tube separations, while as yet inferior to gel separations, are sufficiently better than simple free solution isotachophoresis to indicate the improvement conferred by these gravity-alleviating measures.

e. The above experimental evidence, based on the same substances that we propose to separate in Skylab, is therefore firsthand evidence as to the possible unique benefits conferable by zero-gravity.

IV. DESCRIPTION OF PROPOSED INSTRUMENT FOR FLIGHT

a. Module A: This module is illustrated in the enclosed blueprint, drawn on 2x magnification. It consists of a rectangular block of plexiglas, 1" x 1" x 4", with a 0.25" diameter, 1.25" long observation channel. At either end are wider electrode compartments, provided with a silver electrode at the positive and a black platinum electrode at the negative pole. The block consists of two sections, a shorter section A and a longer section B, these being held together with spring-loaded bolts, exerting uniform pressure across the sliding gate. Both electrode vessels are provided with rubber expansion diaphragms to take into account possible volume variations due to thermal expansion. A plastic-covered metallic stirring ball is provided in the anode compartment to permit stirring of the cell suspension prior to the beginning of the experiment. A magnet will hold this ball in place at other times. Two filling ports

are provided for the fluid loading of the device. The sliding gate is made of 0.001" thick Mylar, and is provided with a central hole of the same diameter as the observation channel. On pulling of the gate by the flexible pull ring, as far as the restraining bar will permit, the hole in the gate will align with the observation channel, forming a continuous lumen. The electrodes have external terminals for connection to the power supply.

b. Module B: This is not illustrated in the drawing. It will be identical to Module A in all respects, except that the sliding gate will be made of 0.125" thick teflon strip, rather than the above-described 0.001" Mylar. The magnet and stirring ball will be omitted, being unnecessary.

V. PROPOSED EXPERIMENTS

a. Experiment A - Module A

The basic requirement of isotachophoresis is that the separation is achieved with a discontinuous buffer system, a leader and a terminator buffer, the sample being normally injected between the two. In this particular experiment we wish to demonstrate the behavior of red blood cells on isotachophoresis. Unfortunately, it will not be possible to inject a separate sample of blood cells between the leader and terminator buffers, as the cells are expected to settle out on standing, and there is no simple manner of bringing them into suspension in a narrow sample compartment. For this reason it was decided to include the sample into the terminator buffer, and use only a two-component system: leader and sample-terminator. As a result we will be able to observe only the frontal boundary of the migrating cells, and not the rear boundary (3) . This will in no way detract from the importance of the results, the lack of the visibility of the rear boundary being mainly an esthetic default and not of real significance. The leading buffer (contained in section B and the visual observation channel of the module) will be physiological glucose (5% w/v) , made 0.020 Molar with HCl, and

buffered with TRIS, pH 7.4. The terminator-sample mixture will be whole defibrinated human blood, diluted 1:10 in physiological glucose.

Prior to the experiment the astronaut will gently shake the apparatus to re-suspend the red cells in the section A of the module. The stirring ball will facilitate this process. Having suspended the red cells, he will immobilize the ball by bringing it in the proximity of the magnet. The module will then be installed in front of the camera, and electrical contact established. The pulling of the slide gate will establish the continuity of the electrophoresis channel, and migration will begin. We expect that the migration of the red cells will be visible as an advancing sharp front of red mass into the observation channel. This sharp front should remain essentially unperturbed during the whole course of migration for the length of the observation channel. The expected duration of the migration is about 15 minutes. Prior to the front having reached the end of the observation channel, the astronaut will be instructed to reverse the current polarity: this will cause the migration direction to reverse and the red front to recede towards its starting position. More important, this reversal abolishes the isotachophoretic mode of migration - from now on, the migrating red cells will be in a zone-electrophoretic mode. This should result in rapid deterioration of the sharpness of the migration boundary: diffusion, convection and other disturbances causing rapid degeneration of the previously sharp boundaries. The astronaut will be instructed to visually observe the nature of the boundaries: the isotachophoretic mode should result in straight or slightly bowed boundaries of near infinite sharpness. It is conceivable also that the astronaut will be able to observe a series of parallel boundaries near the front of the migrating cell suspension, as a result of separation of other components of whole blood, which may escape photographic observation.

b. Experiment B - Module B

In order to avoid the esthetic shortcoming of visual observation of frontal boundaries only - characteristic of the cell experiment A - we suggest this second experiment with two clearly visible darkly colored proteins: hemoglobin and ferritin. Hemoglobin is the red protein of the red cells, ferritin is a darker colored protein isolated from horse spleen. The ferritin has a higher mobility than the hemoglobin and migrates first. The leader in this case will be 0.020 M tris-hydrochloride buffer, pH 7.5. The terminator will be in the section A of the module behind the sliding gate, and will be 0.137 M glycine-HCl buffer, pH 8.9. The sample will also contain a small admixture of ampholines (synthetic polyamine compounds manufactured by LKB, Inc., Stockholm, Sweden) . The mobilities of the ampholines are intermediate between those of ferritin and hemoglobin: the purpose of its addition is to provide a colorless spacer between the two colored proteins - otherwise the two zones of hemoglobin and ferritin would be contiguous and their separation not clearly visible. This mixed sample will be enclosed within the thicker teflon gate of this module.

In this case, there is no need for the mixing operation prescribed to resuspend the red cells. After installation of the apparatus in front of the camera, the astronaut will establish the electrical contact and pull the sliding gate. This will insert the sample between the leader and terminator buffers. The migration should start proceeding instantaneously, with a flat colored disc advancing into the observation window. This disc should gradually resolve into a front darker disc of ferritin and a more reddish disc of hemoglobin, separated by the colorless spacer of ampholines. The astronaut will again be asked to observe the nature of the fronts: whether perfectly straight, slightly curved, etc. On approach to the end of the visual observation channel, he will again be requested to reverse current polarity. This will change the retrograde migration into a zone-mode, rather than isotachophoretic-mode. The change in nature of boundaries should be again most dramatic - proving the advantages of

the isotachophoretic mode of protein separation at zero gravity.

VI. INTERPRETATION OF RESULTS

We are firmly convinced that the most promising methods of space electrophoresis will be those which are characterized by self-sharpening and self-stabilizing boundaries. Only two methods have these characteristics: isoelectric-focusing and isotachophoresis. The first of these, the focusing technique, is more widely known - unfortunately, it is very slow, and is not applicable to living cells (for the simple reason that living cells have a very low isoelectric point - not compatible with their survival) . Isotachophoresis is relatively less known and has come into its own only in recent years (2) . All theoretical considerations and our preliminary data show that it is applicable to both proteins and living cells. Even for proteins, isotachophoresis may have significant advantages over isoelectric-focusing, being faster by several orders of magnitude, requiring therefore less energy, volume, weight, etc. As explained in the text, best results are obtained in gels, where effects of gravity are completely neutralized. We expect that the proposed experiments will:

1. Prove our basic premise that zero gravity isotachophoresis in free solutions will show equivalent resolution and boundary stability as obtainable only in gels in earthbound experiments.

2. Demonstrate the superiority of isotachophoretic mode over zone electrophoresis. The reversal of current polarity programmed for each experiment changes from the first to the second mode - while leaving all other conditions unchanged.

3. Establish that living cells will give equally good and stable boundaries as proteins if gravity effects are avoided.

To this effect we will reproduce the Skylab experiments in our own laboratory, using the same equipment, samples, buffers and other conditions, except for gravity. These experiments

will be conducted in free solutions, gels (for proteins only - not compatible with cells), and in free solution stabilized by density gradients or by rotation of horizontal tubes. These last two methods are often used to alleviate the effects of gravity. We expect that the results will serve to definitely establish the soundness of the zero-gravity electrophoresis concept.

VII. TIMETABLE

We are ready to deliver the complete instrumentation, loaded with samples and ready for use, by the November 1973 Skylab IV liftoff.

References:

(1) M. Bier: Electrophoresis, Theory, Methods and Applications, Academic Press, Inc., New York, N. Y., Vol I (1959) and Vol II (1967) .

(2) A.J.P. Martin and F.M. Everaerts: Displacement Electrophoresis, Proc. Roy. Soc. London, A 316, 493 (1970) .

H. Haglund: Isotachophoresis, Science Tools, 17, 2 (1970) .

D. Peel, J.O.N. Hinckley and A.J.P. Martin: Quantitative Analysis of Proteins by Displacement Electrophoresis, Biochem.J. 117, 69P (1970) .

(3) J.O.N. Hinckley: Transphoresis (Displacement Electrophoresis) , in Methodological Developments in Biochemistry (E. Reid, ed.) , Vol. 2, p. 201, 207 and 210, Longman, London (1973) .

DESIGN AND OPERATION OF THE SKYLAB APPARATUS

The size and shape of the experimental apparatus were largely governed by the constraints imposed by the limited space available in the Command Module. The apparatus had to fit excess space available in one of the student's demonstration packages, fitting into a cylinder roughly 3.5" in diameter, 3.5" long. The total voltage available was 28 volts. Fortunately, both of these constraints were consonant with the design of a meaningful instrument. Terrestrial experiments had shown that separation of colored proteins was achievable at this voltage within minutes, and in only a fraction of the first centimeter of a gel-filled column. A characteristic of isotachophoresis is that once resolution is obtained, there is no further degeneration (or improvement) of the pattern, no matter how long the migrating pathway. Therefore a visual observation channel of only 1.063" length appeared sufficient, not only to obtain complete resolution, but also to confirm subsequent stability of the resolved pattern. The anode compartment was made as large as possible, within the overall space available, as the constancy of leader buffer composition during the course of the separative process is of some importance in isotachophoresis. The anode was virgin silver mesh, is non-gassing, chloride depositing at the electrode. The cathode compartment was much smaller, as its changes in concentration during the separation are of lesser importance. The cathode was made of a sheet of pure palladium, o.oo3" thick. This is also a non-gassing electrode, palladium having a high solubility for evolving hydrogen.

The leader and terminator compartments were kept separated prior to the actual experiment by means of a sliding valve-gate, 0.105" thick, and gasketed by means of two sheets of silicone rubber. Four springs were supposed to keep the whole assembly water-tight, the sliding valve-gate being lubricated by silicone grease.

Silicone rubber diaphragms were also provided at the ends of both electrode compartments to provide for thermal expansion of fluid.

The body of the apparatus was made of plexiglas, and, when assembled, each module was a 3.5" long rectangular block, 1" sq. section. Its exploded view and complete set of blueprints are enclosed. Figure 1 shows a photograph of one of the modules.

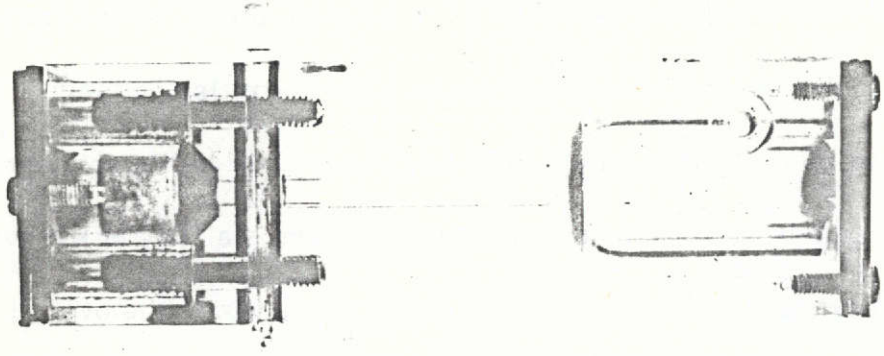

Fig. 1. Photograph of one isotachophoretic cell from the Skylab CPMD apparatus.

Two such modules were housed within metallic plates, as illustrated diagrammatically in Fig. 2. The first switch was an on-off and cell-selector switch. The second switch permitted reversal of current polarity. These switches and a connector adapted for the DAC power cable were fitted between the two plastic modules. Fig. 3 shows a complete photograph of the finished apparatus. The apparatus was housed within a metal cylinder lined with foam rubber. Three such units were made available.

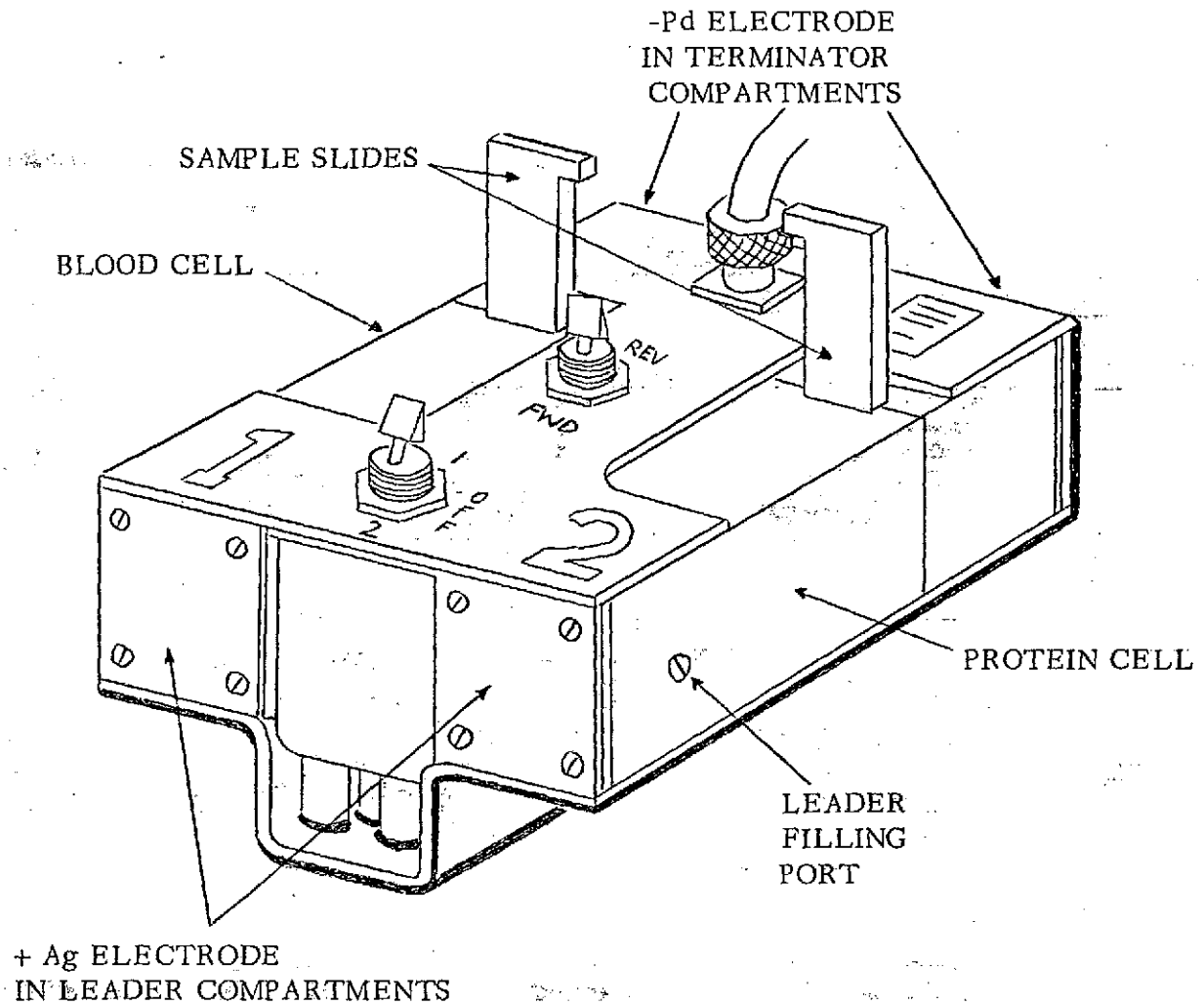

Fig. 2. Diagram of Skylab CPMD assembly, consisting of two plexiglas modules in metallic housing with associated switches.

The whole apparatus was gas sterilized utilizing ethylene oxide. All solutions were thoroughly degassed and sterile filtered before use, and the filling done in the high altitude chamber, using the procedures specified below. One will note that the protein sample was contained only within the lumen of the valve-gate, while the blood filled the whole cathode compartment. In this latter case, the valve-gate contained leader buffer. The reason for this was that it appeared to be necessary to provide a stirring mechanism

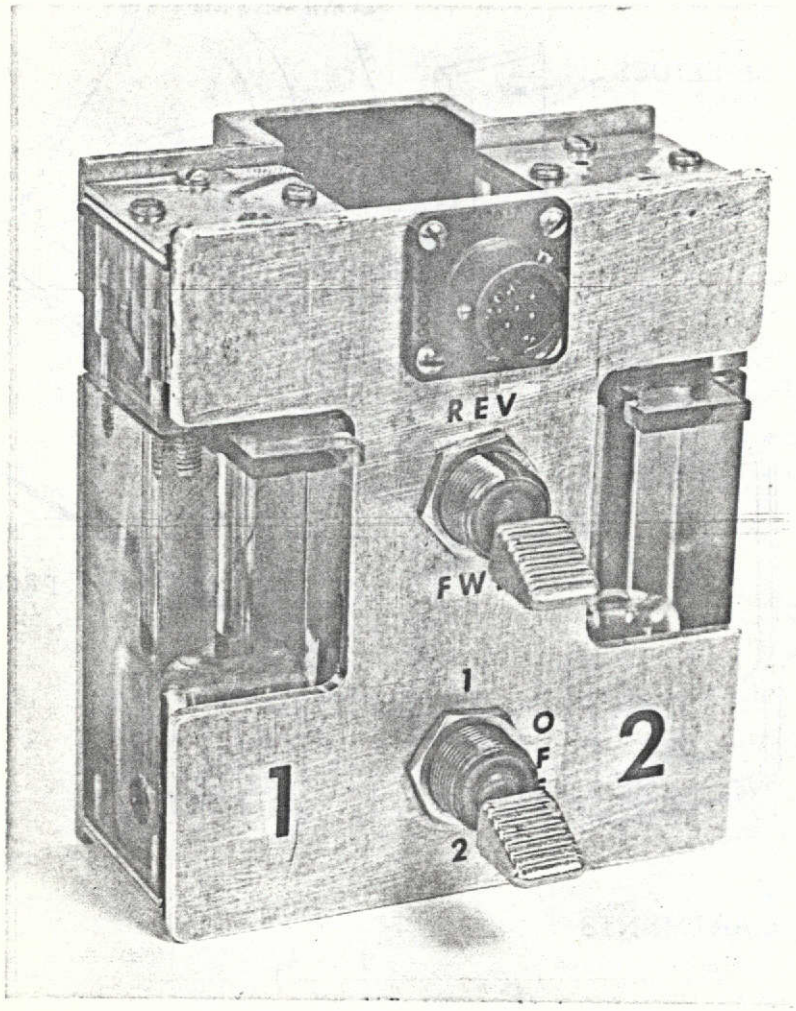

Fig. 3. Skylab apparatus

to suspend any sedimented cells, and this could not be inserted within the narrow confines of the gate.

BLOOD FILLING PROCEDURE

1. Identify the blood cell- stirring ring located in the terminator compartment.
2. Check that the gate is in the open position - down.
3. Put on sterile gloves, and spread sterile drape over working area.

4. Remove both filling screws.

5. Open Pack No. 1 (contents 10 ml syringe, long catheter, and 20 gauge needle). Fit long catheter to syringe and aspirate blood leader. Replace catheter with needle and expel air from syringe.

6. Inject blood leader through terminator filling port until cell is completely filled. When satisfied that there are not bubbles in gate area, close gate.

7. Check for air in leader vessel, and close leader filling port.

8. Open Pack No. 2 (contents 50 ml syringe, long catheter, and 20 gauge needle). Fit catheter to syringe, aspirate sterile saline washing solution, replace catheter with needle, and flush terminator with large volume of saline.

9. Inject air into terminator to remove excess saline.

10. Open Pack X (contents, 10 ml syringe and 20 gauge needle). Fit needle to syringe, stir blood vial, wipe rubber cap with alcohol, then aspirate 5 mls blood. Check syringe for air.

11. Fill terminator with blood, and inspect for air.

12. Replace terminator screws.

13. Inspect entire cells for air, and rectify if necessary.

PROTEIN FILLING PROCEDURE

1. Identify protein cell - no stirring ring.

2. Use sterile gloves and sterile drape.

3. Open Pack Y (contents 10 ml syringe and 20 gauge needle). Fit needle to syringe, wipe rubber stopper of protein vial with alcohol and aspirate 5 mls of protein.

Check for air, remove needle, and fit catheter to pre-inserted catheter in cell.

4. Fill cell as far as observation channel with protein.
5. Pull out cannula past gate, but leave in observation channel.
6. If satisfied there are no bubbles in gate area, close the gate. Tape the gate in the closed position.
7. Open Pack No. 3 (contents 50 ml syringe, long catheter). Fit catheter to syringe, aspirate 50 mls of protein leader, remove catheter and check syringe for air.
8. Fit syringe onto pre-inserted catheter and inject protein leader until leader compartment and observation channel are free of protein. (no colour)
9. Withdraw cannula and replace leader screws if satisfied that no bubbles or colour remain in leader vessel.
10. Open Pack No. 4 (contents 10 ml syringe, long catheter and 20 gauge needle). Fit catheter to syringe, aspirate protein terminator, and replace catheter with needle. Check for air.
11. Open terminator screw, rinse thoroughly with terminator, and fill with terminator.
12. Inspect for air, and replace terminator screw.
13. Inspect entire cell for air, and rectify if necessary.

In the Skylab, the apparatus was supposed to have been housed in the food chiller until use. Then the equipment was to be mounted with its velcro backing within the spider cage already in the Skylab, in the manner shown in the schematic drawing of Fig. 4. The instructions to the astronauts were as follows:

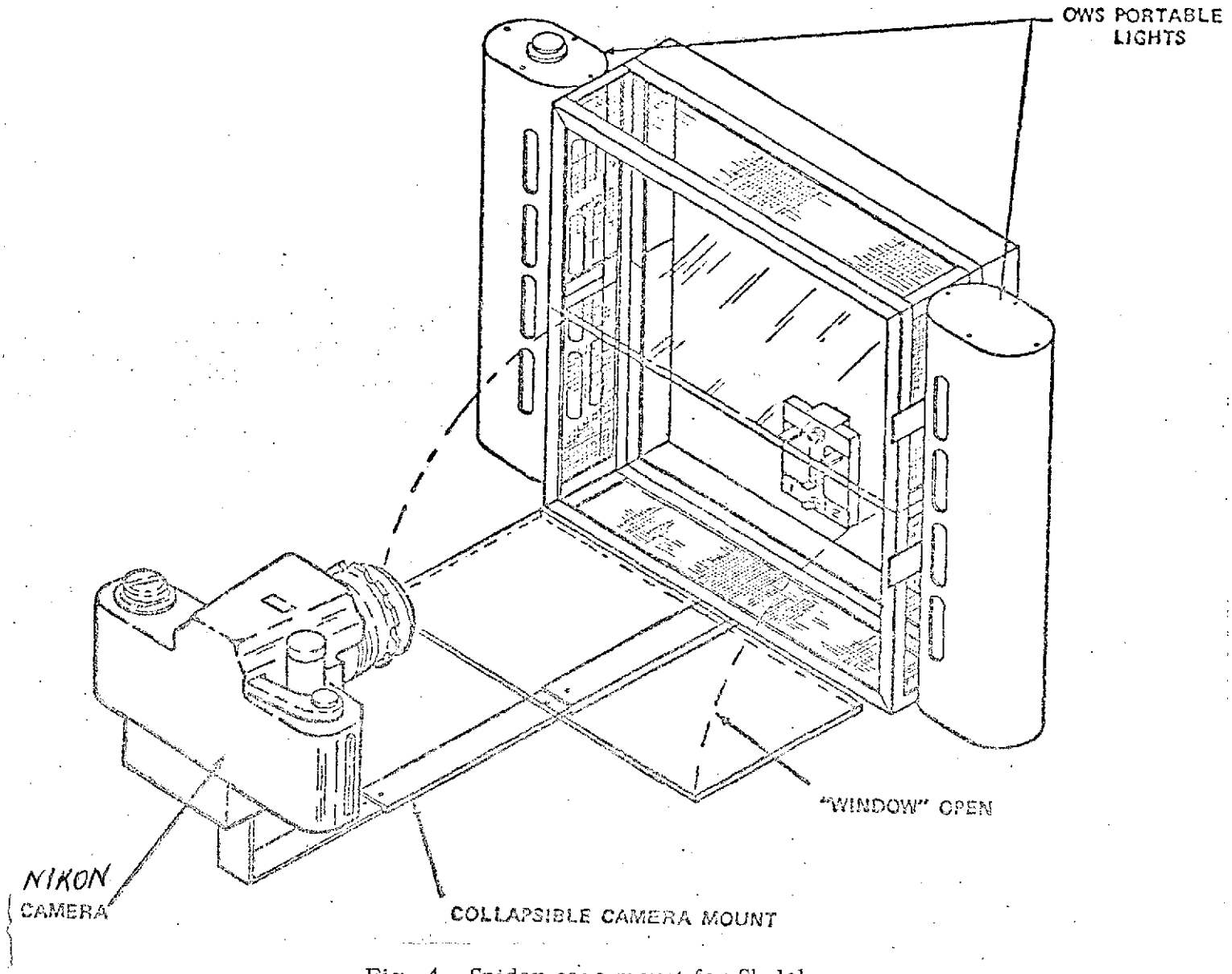

Fig. 4. Spider cage mount for Skylab CPMD with associated camera mount.

1. Remove charged particle mobility demo (CPMD) from food chiller, spider cage from W733, EDcamera mount with end assy (excluding extension) from F509, portable timer, two portable lights and two utility cables, one DAC power cable, utility strap, adhesive backed velcro.
2. Remove CPMD from launch container by handling metal parts only. Moderately

agitate CPMD along long axis for 5 minutes.

3. Allow 15 mins for CPMD to reach room temp.
4. Remove portable lights from housing and mount on spider cage side walls without door hinges.
5. Mount spider cage on MDA locker M157 with velcro, using utility strap, firmly secure assy to locker door.
6. Verify CPMD cell selector switch (bottom switch) is in off position.
7. Attach DAC power cable to CPMD.
8. Place CPMD in center of lower half of spider cage with velcro, tape lower door in open position. Place timer beside CPMD with velcro.
9. Attach ED mount to spider cage. Adjust end assy to ED 61/62 arrow.
10. Set up camera per photo pad.
11. Place particle migration switch in the forward position.
12. Place cell selector switch to position #1.
13. Slip index finger & middle finger of left hand behind cell #1 of CPMD. Place left thumb on red end of slide. Smoothly push slide completely in with thumb, balancing pressure with other fingers. Set timer to 45 minutes.
14. Take a photograph and repeat at approx 5 minute intervals for 20 minutes. Voice record observations.
15. Gently set particle migration switch to reverse position.
16. Wait 5 minutes; take a photograph and repeat at approx 5 minute intervals for 20 minutes. Voice record observations.

17. Set particle migration switch to forward position and cell selector switch to position #2. Repeat steps 13 thru 17 for cell #2.

Notes:

1. If bubble appears in observation channel prior to run, dislodge it and position it in the opposite end from slide by gentle tapping. Under no circumstances should the unit be disturbed once voltage is applied across one of the cells.
2. Return CPMD to its stowage container & replace in food chiller after demonstration is completed.

PRE-FLIGHT PROTEIN STUDIES

1. Materials and Methods.

(a) Samples. Human hemoglobin and horse spleen ferritin were chosen as the sample proteins because of their intense color and ease of separation. The red hemoglobin was prepared by repeated washing of human red blood cells in saline, followed by their lysis in distilled water, and centrifugation. The solution was then treated with carbon monoxide, the resulting carboxyhemoglobin being far more stable against denaturation than hemoglobin. It was stored at -10°C. until use, at a concentration of 7%. The brown horse spleen ferritin was obtained from Pentex Biochemicals and consisted of a 9% sterile solution.

Ampholine carrier ampholyes were supplied by LKB and covered the range pH 5 to 8; agamma calf serum and a selection of narrow pH range ampholines derived from isoelectric focusing of LKB ampholine pH range 3 to 10 were also used.

Sample mixtures were filtered through a 0.22 millipore filter before use to insure sterility and the exclusion of all particulate matter.

Sucrose, to 5% (weight volume) was added to the samples to insure even layering on the gel surface and to minimize sample turbulence into the terminator due to convective disturbances at the start of the run before sample migration into the gel.

(b) Gels. All isotachophoretic runs were carried out using either agarose or polyacrylamide support media to suppress convection. Agarose (Fisher Scientific Co.) was made up as a 0.5% w/v solution in leading buffer, while polyacrylamide gel was prepared according to Ornstein and Davis (1) with appropriate modifications of leading buffer concentration as necessary.

(c) Preservatives. All protein samples and buffers incorporated 0.01% merthiolate as preservative.

(d) Apparatus. Four isotachophoretic units were used in the present experiments (Figs. 5 and 6). These two figures show units constructed in the laboratory.

Isotachophoresis Column NASISO Mark I

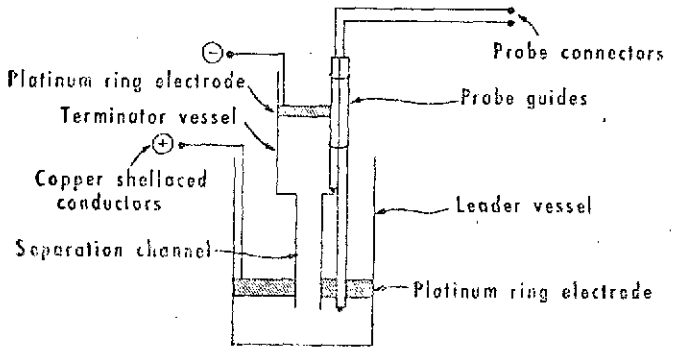

Fig. 5. Schematic drawing showing principal features of isotachophoretic unit used in Skylab experiments

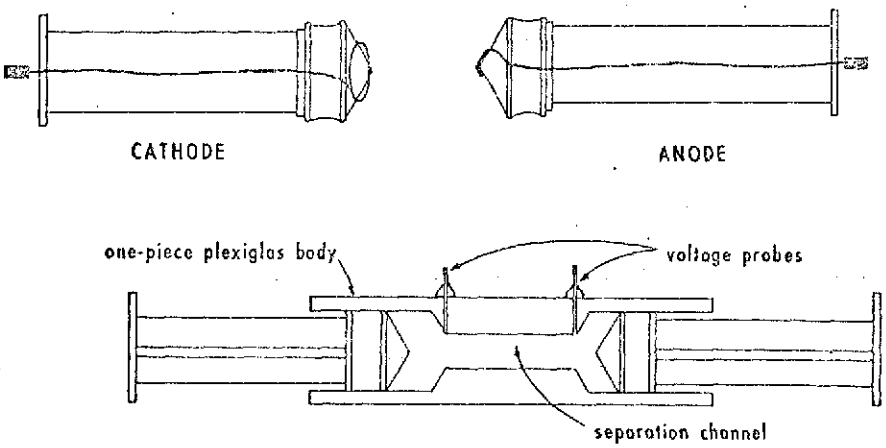

Isotachophoresis Apparatus NASISO Mark II

MATERIALS: ONE-PIECE MACHINED PLEXIGLAS BODY. REGULAR 20ml POLYTHENE AND RUBBER SYRINGE PLUNGERS. ELECTRODES OF SILVER WITH COPPER CONDUCTORS TO CONNECTORS. SEE ABOVE. VOLTAGE PROBES SILVER ANCHORED IN EPOXY.

Fig. 6. Schematic drawing of isotachophoretic unit with variable-volume electrode vessels

Two, NASISO Mk I and II, were specially constructed for the purpose, the third was a commercial Canalco disc electrophoresis apparatus, and the last was a prototype of the apparatus used on Skylab IV. Although differing substantially in design from the CPMD hardware, the first two units were designed to investigate the feasibility of the proposed experiment and to establish, if possible, its operational limits. Thus provisions were made in these units to vary the volumes of leading and terminating buffers, and to vary the position of the electrodes with respect to the separating channel. In addition, voltage probes were incorporated to monitor the voltage across the separation channel. The total voltage in all runs was 28 volts, this being the limit of the CPMD power source aboard Skylab IV. All experiments were run first in the isotachophoretic mode and then, following current reversal, zone electrophoresis of the samples was allowed to take place.

(e) Evaluation of Results. The progress of experiments was monitored by a stopwatch to measure migration times, and by reference to a fixed scale in close proximity to the separation channel in order to measure migration distances. Results obtained using these criteria were tabulated and expressed graphically; in addition, the quality of separation was assessed by visual examination, the principal criteria in this case being the distance between the separated hemoglobin and ferritin discs, and the degree of coloration of this space.

2. Results

A large series of experiments were carried out using the four units to investigate the optimum conditions for the isotachophoretic separation of hemoglobin and ferritin. A number of representative results are presented in this paper, and are grouped according to the parameters under investigation.

(a) Terminator Concentration. These experiments, performed in the NASISO Mk I apparatus (Fig. 5) were concerned principally with determination of the optimum terminating buffer

concentration for maximum migration of the ferritin front at 28 volts, and a preliminary investigation of the effect of buffer volumes. The results are tabulated in Table I. They indicate no gross effect of electrode volume, and confirmed the soundness of the design of modules.

Doming occurred in all experiments except No. 5, although it seemed to diminish somewhat after 8 minutes in experiments 3, 4 and 8. In all experiments sharp front and rear boundaries had formed within one minute, and separation was complete within five minutes. The separation was clearly visible but not sufficiently wide or colour-free.

TABLE I

Experiment Number	Terminator Concentration (mM)	Leader Volume (mls)	Terminator Volume (mls)	Migration in 15 minutes	Current (mA)
1	17	5	5	5	0.8
2	17	5	5	5	1.0
3	130	5	5	9	1.0
4	340	5	5	13	1.5
5	380	1	5	16	1.5
6	130	5	5	14	1.0
7	380	5	5	16	2.0
8	380	5	5	16	2.0
9	380	2	1.5	11	2.2
10	380	8	5	15	2.0
11	380	8	1.5	15	2.0
12	380	2	6	15	2.0

Anti-convective Medium: 0.5% w/v Agarose in 20mM Tris-Hcl, pH 7.2

Sample: 10μl of a mixture containing 100μl hemoglobin, 100μl ferritin and 10μl Ampholines pH range 5-8.

(b) Leader and Terminator Volume. The NASISO Mk II cell, (Fig. 6), was designed specifically to investigate the effect of buffer volume on isotachophoretic separation. Several experiments were performed using this cell, and the results were tabulated in Table II.

TABLE II

Experiment Number	Leader Volume (mls)	Terminator Volume (mls)	Migration in 15 minutes (mm)
1	8	5	16
2	7	2	16
3	1.5	1.5	18
4	1.5	7	18
5	7	7	20
6	7	7	19

Anti-convective Medium: 0.5% w/v Agarose in 20mM, Tris-Hcl, pH 7.2.

Leader: 20mM, Tris-Hcl, pH 7.2.

Terminator: 380 mM, Tris-glycine, pH 8.3.

Sample: 10_{μ} l of a mixture containing 100_{μ} l ferritin, 100_{μ} l hemoglobin, 50_{μ} l 5%. albumin, 50_{μ} l amido black and 10_{μ} l Ampholine pH 5-8. (In experiment 5, only 10_{μ} l ferritin were applied).

The results indicated that leader and terminator volumes had no significant influence on degree of separation of hemoglobin and ferritin, nor did they influence the distance migrated by the foremost boundary. Figs. 7 and 8 below are graphical representations of Experiment 1 in Table II, while Figs. 9 and 10 illustrate Experiment 5.

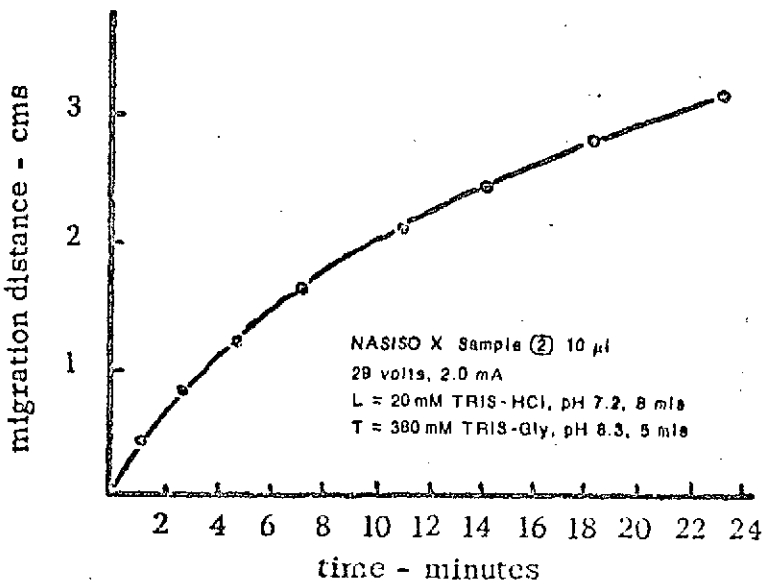

Fig. 7. Isotachophoresis of a hemoglobin-ferritin-ampholine mixture on agarose gel

The experiment was conducted at constant voltage, and the graph shows a curved line, indicating that the electrophoretic velocity of ferritin, in this experiment did not decrease at a constant rate. This is borne out in Fig. 8, where the electrophoretic velocity of the foremost band, ferritin, was plotted against distance of migration. The graph shows a tendency to approach a constant value.

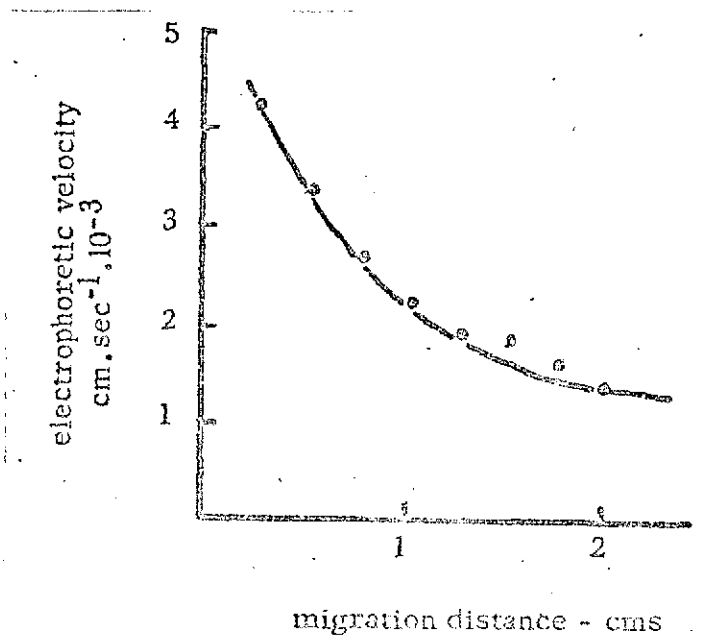

Fig. 8. Velocity of a separated ferritin part during isotachophoresis of a hemoglobin-ferritin-ampholine mixture on agarose gel

By contrast, Fig. 9, in which the migration distance of ferritin alone was plotted against time, shows a curve considerably straighter than the curve in Fig. 7, while Fig. 9, depicting the electrophoretic velocity of ferritin alone as a function of migration distance, is essentially a straight line. Thus these two graphs indicate that in the absence of other proteins and ampholines, the electrophoretic velocity of ferritin decreases at a constant rate during constant current isotachophoresis.

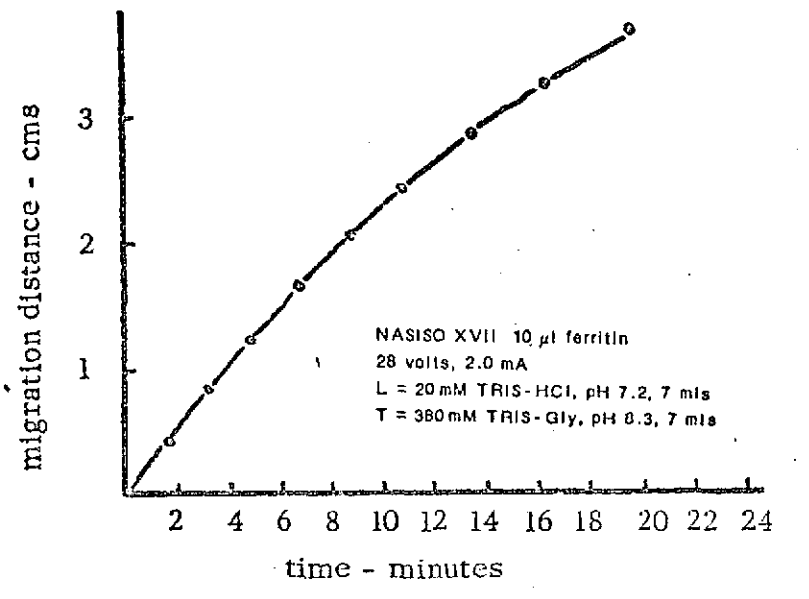

Fig. 9. Isotachophoresis of ferritin on agarose gel

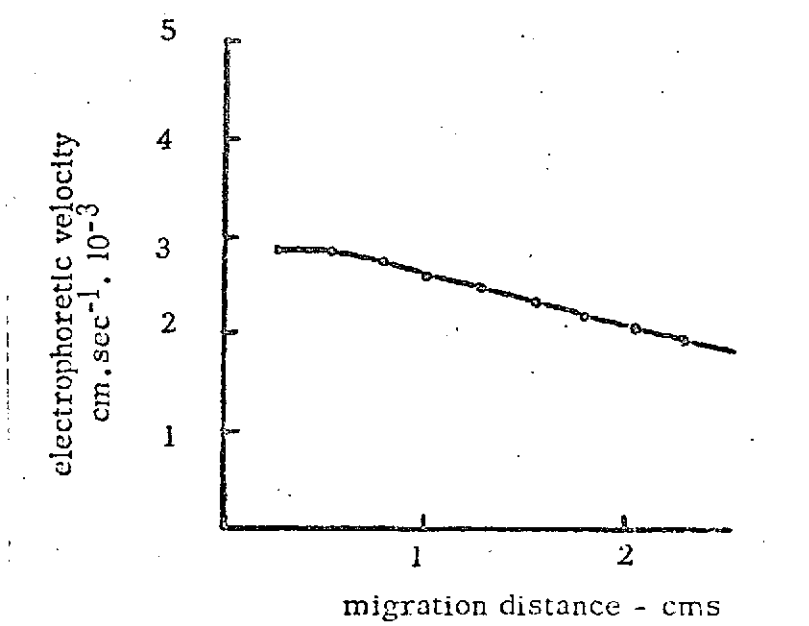

Fig. 10. Velocity of ferritin front during isotachophoresis of ferritin on agarose gel

(c) Ampholine Concentration. The Canalco Disc Electrophoresis apparatus was used to investigate the optimum choice and concentration of spacer molecules. Since 12 separations can be run simultaneously in this unit, a very large number of experiments, many in triplicate, were carried out. All experiments utilized 20 mM Tris-HCl pH 7.2 and 380 mM Tris-glycine pH 8.3 as leader and terminator respectively.

Samples included mixtures in varying proportions of a) hemoglobin, ferritin and spacer, b) hemoglobin, ferritin, albumin, and spacer and c) hemoglobin, ferritin, albumin, amido black and spacer.

The quality of separation was judged by three criteria, namely:

1. length of spacing between bands
2. color of the space
3. sharpness of front and rear boundaries.

We also tried utilizing agamma calf serum as spacer hoping that its colorless protein molecules may provide a better alternative to the known shortcomings of ampholine. Little or no separation was observed. The runs were characterized by gross discolorations and distortions of migrating zones, with no formation of discrete front and rear boundaries. On the basis of these results further investigation of agamma calf serum as a spacer for the Skylab experiment was abandoned.

Similarly, those runs utilizing ampholine fractions of limited pH range, derived from isoelectric focusing of pH range 3-10 Ampholine were unsatisfactory since reproducible separations of sample mixtures were not achieved. In addition, the uncertainty of the ampholyte and sucrose concentrations in these fractions was considered a disadvantage.

The results of using Ampholine pH range 5-7 were indistinguishable from those obtained using pH range 5-8 Ampholine, and it was felt that since earlier successful studies of isotachophoresis in gels in this laboratory had utilized the latter, there was little justification in changing to the narrower range Ampholines.

The results of one series of experiments in this group are tabulated in Table III. The proteins are easily recognizable, as the amido-black stained albumin gave a blue coloration, ferriting brown, and hemoglobin red, albumin being the fastest and hemoglobin slowest component. In the last column of the Table we list the observed spacings between the separated protein bands. It can be seen that this spacing is clearly a function of ampholine added. An excess of ampholine, however, delays separation, or, in still higher concentration, completely blurs it.

TABLE III

Tube No.	Sample	Ampholine	Inter-protein band spacing (mm)
1	(200$_\mu$ l	10$_\mu$ l	0.5
2	stained	20$_\mu$ l	0.9
3	albumin)	30$_\mu$ l	1.7
4	(100$_\mu$ l stained	10$_\mu$ l	0.4
5	alb.+ 100$_\mu$ l	20$_\mu$ l	0.9
6	ferritin)	30$_\mu$ l	1.5
7	(100$_\mu$ l stained	10$_\mu$ l	0.4
8	alb.+ 100$_\mu$ l	20$_\mu$ l	0.8
9	hemoglobin)	30$_\mu$ l	1.3
10	(100$_\mu$ l ferritin	10$_\mu$ l	0.5
11	+ 100$_\mu$ l	20$_\mu$ l	1.0
12	hemoglobin)	30$_\mu$ l	2.0

(d) Sample Dilution. The effects of premixing the sample with leader, terminator, or water were investigated; it was found that although dilution of the sample with either leader or

terminator led to faster separation initially, it led ultimately to coloration of the Ampholine space and the region of the gel behind the hemoglobin band. Premixing with water did not give this effect.

(e) Sample Composition. The final series of experiments consisted of 25 runs in the first prototype of the CPMD module. 20 mM Tris HCl pH 7.2 and 380 mM Tris-glycine pH 8.3 were used as leader and terminator respectively. Twelve runs were carried out on a 0.5% w/v agarose gel in leader; the last thirteen utilized the large pore polyacrylamide gel. The objective of these experiments was to formulate final sample composition for inclusion in the Skylab CPMD. Thus varying proportions of ferritin, hemoglobin and Ampholine, diluted with water, leader, or terminator, were run, in order to determine which system resulted in clear sharp boundary separation with good spacing.

Doming of the rear boundary (hemoglobin) occurred in all agarose runs, while none was observed in Polyacrylamide gels. Separation of the two colored proteins was achieved in all twenty-five runs, the length of the Ampholine space being roughly proportional to the volume of spacer in the sample. Addition of mertiolate, .01%, as preservative, did not alter the patterns.

The results indicated that ferritin and hemoglobin bands were equal in thickness after 15 minutes of isotachophoresis if the volume of hemoglobin originally in the sample was half that of the ferritin. Furthermore, an Ampholine space of 2 mm in length was obtained if the ratio of total protein volume to Ampholine volume was 10:1.

(f) Zone Electrophoresis of the Sample. Current reversal in all twenty-five experiments gave similar results; immediate loss of sharpness in all boundaries, followed by contraction of the Ampholine space. Within four minutes, hemoglobin and ferritin bands coalesced, and then travelled as one broad diffuse zone towards the terminator vessel.

Zone electrophoretic separation of the two proteins was not observed in any of these current reversal experiments.

3. Discussion

On the basis of these results, a sample solution containing the following volumes of constituents was prepared for the Skylab CPMD

1. 10 mls ferritin, 9%
2. 5 mls human hemoglobin, 7%
3. 24 mls distilled water
4. 1.5 mls Ampholine, pH range 5-8
5. 0.5 mls 1% merthiolate as bacteriostat

The solution was stored at 4°C until shipment to MSFC and there sterile filtered by passage through a 0.22 micron filter and degassed.

The initial selection of Tris-HCl and Tris-glycine as leader and terminator, respectively, was based on the published disc electrophoresis studies of Ornstein and Davis (1), which utilized an isotachophoretic stacking and concentration step prior to zonal separation in a sieving gel. Leader concentrations were not investigated, 20 mM Tris-HCl at pH 7.2 being used throughout the experimental series, for the following reasons.

The Kohlrausch Regulating Function predicts that sample concentration in an isotachophoretically migrating zone is directly proportional to leader concentration; for the purposes of the Skylab IV photographic analysis, it was desirable that the separated zones be relatively concentrated to provide a high contrast image. However, increased leader concentrations result in increased Joule heating of the cell contents on account of the lower resistance of the leader - this was considered undesirable. Preliminary experiments using leader concentrations ranging from 60 mM to 10 mM had indicated

that photographic definition and Joule heating were optimal at 20 mM Tris-HCl.

The results tabulated in Table I indicated that maximum migration of the ferritin front in 15 minutes was achieved using a 380 mM Tris-glycine terminating buffer of pH 8.3, although the Kohlrausch concentration of the terminator for this leader system is less than 20 mM. In the region immediately behind the migrating zones, the terminator concentration is indeed dictated by the Kohlrausch regulating function; the increased migration using terminator concentrations far in excess of this regulated concentration was attributed to the higher potential gradient across the cell resulting from the high conductivity of buffer in the terminator vessel.

With the exception of one anomalous result (Exp. No. 9) Table I also showed the lack of dependence of migration distance on leader and terminator volumes; this finding was corroborated by the results shown in Table II, and dispelled remaining doubts that the buffer compartment volumes of the proposed CPMD unit were too small.

The graphs showing migration distances of ferritin as a function of time, and its velocity as a function of migration distance cast an interesting light on the influence of ampholines on isotachophoretic processes. Since these experiments were conducted at constant voltage (the Skylab CPMD utilizes a constant 28 volts power supply) the electrophoretic velocity of ferritin decreased throughout the experiments as the current dropped; isotachophoresis at constant current would result in constant velocity throughout the duration of the run. We were able to show that the electrophoretic velocity of ferritin, in the absence of other proteins or ampholines, decreased at a constant rate, and that in the presence of hemoglobin and ampholine, the observed electrophoretic velocity of ferritin did not decrease at a constant rate, but tended to approach a constant value This modification of the electrophoretic velocity may underline the basic unsuitability

of ampholine chemicals as spacer ions in isotachophoresis. Ideally spacer molecules should possess a single known mobility; ampholines are known to consist of molecules exhibiting a large range of mobilities, and isotachophoretic resolution of such a mixture takes longer than the resolution of a single species of molecule.

The lack of sharp separation in those experiments utilizing agamma calf serum as a source of spacer molecules was similarly attributed to the number of molecular species of differing mobility in the serum, and the excessive time required for complete resolution of such a mixture. Furthermore, it is most probable that the mobility spectrum of agamma calf serum components includes the mobilities of both hemoglobin and ferritin, leading to the formation of mixed fronts, with a characteristic loss of definition.

No provisions were made in the design of the Skylab CPMD unit to minimize electroosmotic effects arising during electrophoresis, as an important objective of the space experiment was to assess the exact contribution of electroosmosis to boundary shapes in isotachophoresis. This information is impossible to obtain in earthbound experiments, where stabilization against gravity effects also modifies the electroosmotic behavior of the system.

PRE-FLIGHT RED CELL EXPERIMENTS

The choice of red blood cells for the Skylab experiment was motivated by the following consideration: a) their intense color; b) their longevity, blood being commonly preserved for 28 days for transfusion, c) their ready availability, and, d) their well known electrophoretic properties. Survival of the cells was of paramount importance, and our first task was to determine the conditions of their preparation consonant with maximum survival. Two opposite viewpoints had to be reconciled. On the one hand, from a purist point of view, one would want to have for isotachophoresis as simple a system as possible, i.e , a single ionic species, the red cells in this case, with a counterion common to that of the leader (in our case HCl-Tris). On the other hand, it is well established in blood-banking practice that optimum survival of red cells is obtained in acid sodium citrate. Choosing this preparation as our sample would have implied overloading the already large number of ionic species present in blood with additional amounts of added salts.

We also had to decide on the blood species, human and sheep red cells being the obvious alternatives. Both are known for their stability, and are readily available. We decided on human cells mainly because their collection could be delayed till the last minute, i.e., the filling of the Skylab module in the high altitude chamber in Huntsville, a few days before launch. Mr. Smolka was the volunteering donor of all human blood cells used in pre-flight experiments, and he also went to Huntsville to assume the responsibility for final loading of the apparatus, where his last blood sample was drawn.

Our first experiments were therefore designed to assess the survival of red cells in different preparations. Various alternatives were tried: (a) whole blood - defibrinated by means of shaking the blood with glass beads. This avoids the necessity of adding any

extraneous ionic species to blood. (b) citrated whole blood, using the usual blood banking procedures. (c) washed red cells suspended in 5% human serum albumin, in presence of sufficient glucose to render it isotonic, as determined by direct osmometry. We thought that the presence of albumin may render the medium more similar to whole blood, yet eliminate blood's multitude of ionic components. (d) washed red cells suspended in a variety of the usual tissue culture media, (e) washed red cells suspended in isotonic glucose.

In addition, we explored the effect of addition of various bacteriostatic agents on blood survival, though every effort was made to draw and handle all aspects of blood preparation in sterile manner. The following agents were tried: merthiolate, sodium azide, penicillin-streptomycin mixture and gentamycin. These were all added in their appropriate concentrations to samples of whole defibrinated blood.

To assess survival of blood, aliquots of it were taken in 2 ml syringes, and these were hermetically sealed, with absolute exclusion of any air. Because of shortage of time available, cell survival was assessed at room temperature, rather than refrigerated, though the Skylab samples were supposed to be kept cold. (As it happened, this did not materialize on the Skylab). The samples were examined at various time periods for the next two weeks for visual hemolysis, or liberation of gas bubbles.

The results were most conclusive. All blood specimens except citrated or declotted whole blood became soon heavily hemolyzed. This also happened to the whole blood stored with merthiolate or sodium azide. The presence of the latter agent also caused liberation of gas bubbles in the syringes, presumably because of the catalytic decomposition of the azide ion in presence of sulfhydryl groups of proteins, resulting in liberation of nitrogen gas. Whole blood appeared comparable to citrated blood, and

gentamycin was chosen over the penicillin-streptomycin combination because of its own greater stability and widespread use in tissue culture. The final decision was therefore to use whole blood, defibrinated by means of shaking with glass beads, and stabilized by addition of gentamycin.

This implied, of course, that the purist view of isotachophoresis had to be abandoned. Blood is a complex mixture with many ionic species, both proteins and small molecular weight components. Thus, the best that could have been expected is the formation of multiple ionic mixed steps between the red cells and the other ionic species.

1. Material and Methods

(a) Samples. Human and sheep red blood cells were used exclusively in this series of experiments. The human blood was defibrinated immediately after collection by shaking with glass beads, and thereafter stored at $4^{o}C$. Sheep blood was collected in acid-citrate-dextrose and stored similarly. The red blood cell working solutions were prepared just prior to usage, and consisted of whole defibrinated blood, aged whole blood, and washed red blood cells resuspended in 5% dextrose. All blood handling was carried out in aseptic manner, and the defibrinated blood was filtered through a fine screen stainless steel mesh, to eliminate micro-clots.

(b) Buffers. The leading electrolyte was 20 mM Tris-HCl, pH 7.5, with 5% dextrose for isotonicity. Since the experiments were by frontal analyses red blood cell suspensions were used as the terminator.

(c) Recording of Results. The speed of migration of fronts was measured using a millimeter scale attached to the exterior of the separation channels in conjunction with a stop-watch. Initial and isotachophoretically modified red cell concentrations were

estimated by hematocrit measurements of the sample before and after migration, i.e., after adjustment to its Kohlrausch regulated concentration. Qualitative assessment of the experiments was performed by visual examination of migrating fronts in the course of a run, and by photography. The results were expressed in graphical form, as functions of migration distance versus time, and current versus distance.

(d) Apparatus. Two cells were used in the present experiments.

(i) Prototype Skylab module, described in detail in an earlier section of this paper, (Flight Proposal). Blood was loaded in the terminator compartment with leader in the gate, observation channel and leader electrode compartment. Keeping the apparatus vertical, red cells down, the closing of the gate permitted the formation of sharp initial boundaries.

(ii) Autogenic density gradient apparatus, illustrated in Fig. 11. The mode of operation of this apparatus was as follows. The closed leader vessel was filled with leading buffer, and the open end of the plexiglass column submerged to a depth of 1 mm in the sample solution, contained in the open terminator vessel. The leading buffer was retained in the upper vessel by atmospheric pressure; in this way a sharp initial interface could be obtained between leader and sample.

2. Results. It is important to emphasize the objectives of the Skylab experiment, which was mainly the confirmation that red cells will move isotachophoretically, and the shape of the leader-red cells interface. The rate of migration in isotachophoresis is of little consequence, as it is the essence of the process that all ionic species in the sample move with the same rate as the leader ions. Thus, differences in mobility between different preparations of red cells do not reflect changes in electrophoretic properties of the red cells, but only changes in the overall distribution of electric field. As the

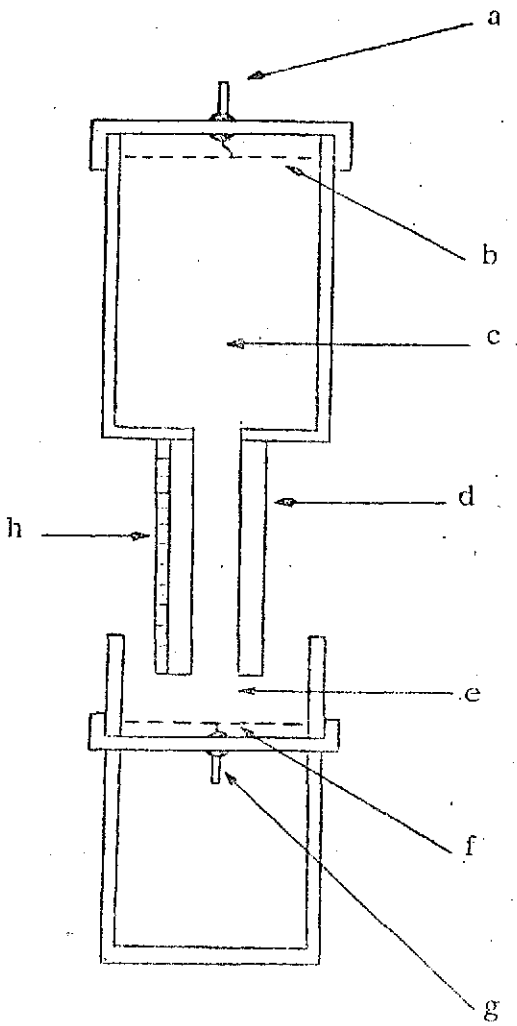

Fig. 11. Autogenic density gradient isotachophoresis apparatus

Key: (a) Anode connector
(b) Silver mesh anode
(c) Closed leader vessel
(d) 1/4" I.D. Plexiglas column
(e) Open terminator-sample vessel
(f) Silver/silver chloride mesh cathode
(g) Cathode connector
(h) Millimeter scale

leader was constant, and the cells were suspended in media of different overall conductivity, changes in migration rates only reflected the proportional change of voltage drop across the red cell zone.

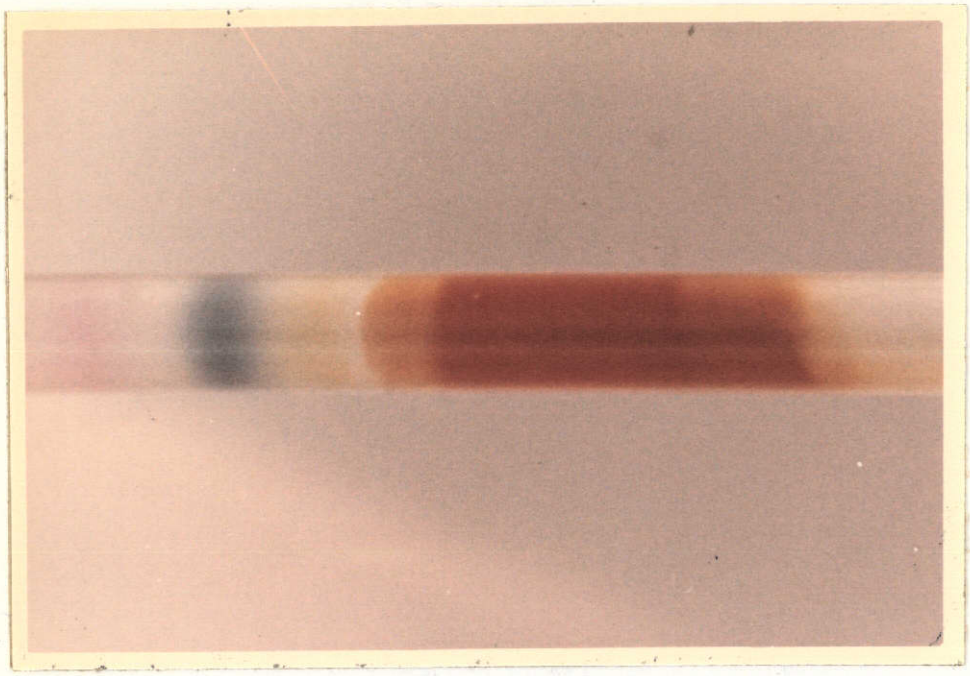

Fig. 12. Separation of red cells from amido black stain in rotating capillary isotachophoresis.

The fact that red cells migrate isotachophoretically and can be separated from other constituents was already established in our previous work. We may refer to the photograph of Fig. 7, of separated human-sheep red cells in ficoll gradients in the previous section. (D-3). Additional evidence was obtained by means of the rotating capillary tubes. In Fig. 12, we show the photograph of a red cell zone separated from a dye, amido black, in such a rotating capillary. Many additional such runs have been carried out. They bore little resemblance, however, to the planned Skylab experiment involving frontal analysis only. We wish to report at this time therefore, only the results obtained by frontal analysis, using the Skylab module, and its analogue, just described. While we have carried out a great many such runs, for sake of clarity, we shall report only a limited number of representative samples.

(a) Frontal Separations of Human Blood.

Three mls of defibrinated whole human blood were used as the terminator in the open vessel of the autogenic density gradient isotachophoresis apparatus. (Fig. 11). The leading electrolyte was 20 mM Tris-HCl, pH 7.5. The potential difference was 28 volts, and the run was terminated after 32 minutes.

Immediately upon the application of the electrical field, it was possible to detect changes in the appearance of the rising blood column. While there was no change in coloration of the cell mass below its original level, the advancing, migrating mass was a distinctly different shade of red. This was interpreted as evidence of readjustment of the red cell concentration according to the requirements of the Kohlrausch regulation (in mixed steps, of course). A photograph of such a separation is shown in Fig. 13.

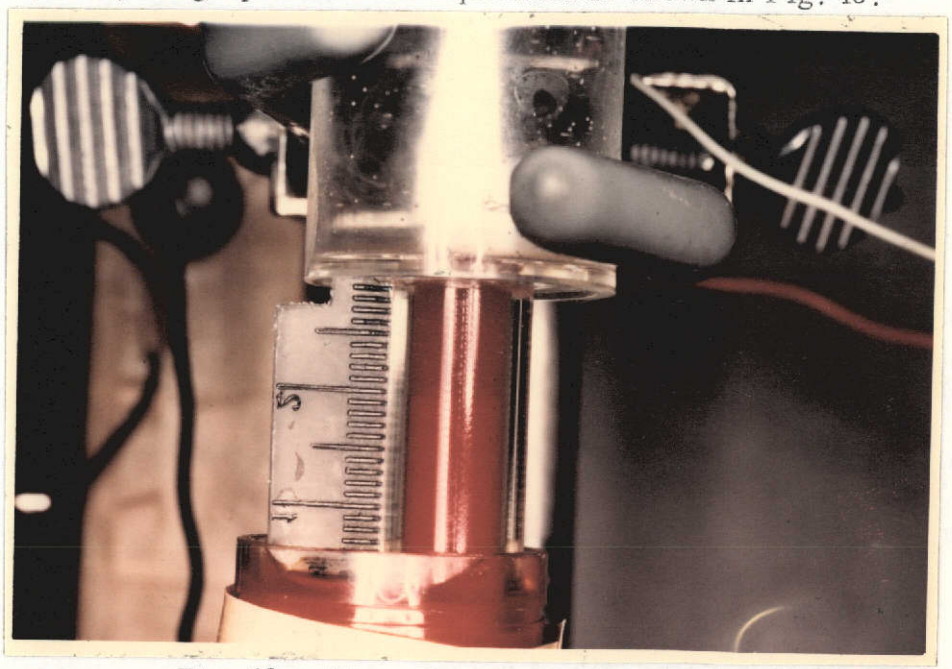

Fig. 13. Frontal analysis of human blood in the autogenic density gradient apparatus.

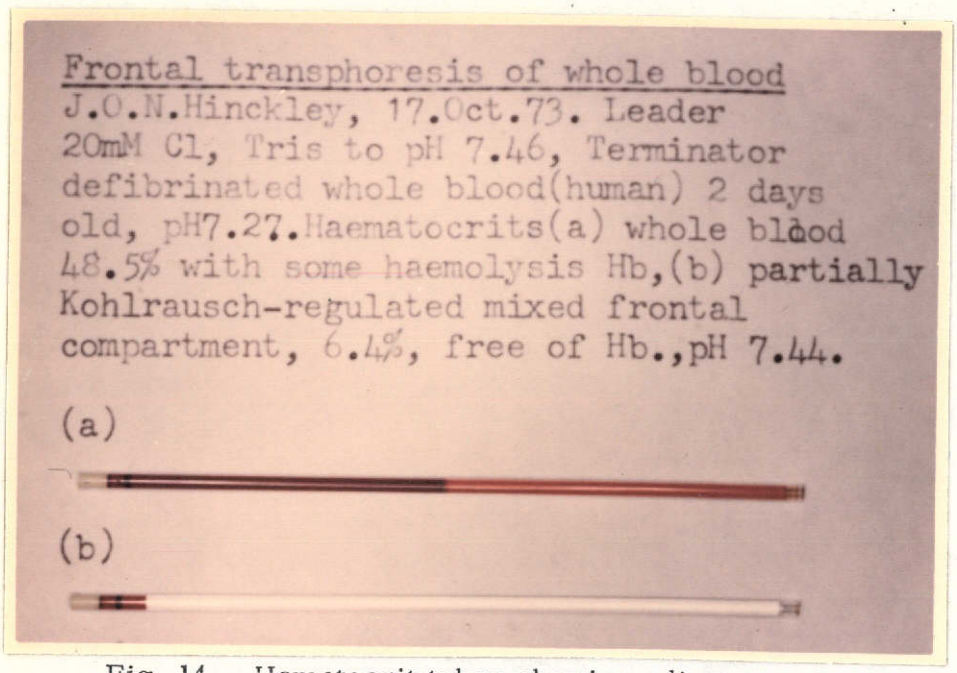

Fig. 14. Hematocrit tubes showing adjustment of red cell concentration following frontal analysis.

It should be emphasized that visually, the line of demarcation, was much clearer. The readjustment of concentration could be directly proven, by taking a capillary hematocrit of the original sample, and of the advancing column. The hematocrit values were 48.5% for original sample, and only 6.4% for the sample withdrawn. A photograph of the two hematocrit capillaries is shown in Fig. 14. One will also notice that there was separation of red cells from hemoglobin. The original sample was heavily hemolyzed, while the sample withdrawn from the advancing column was hemoglobin free. The sharpness visually observed of the color difference between sample and advancing column at the level of the initial blood-leader interface is taken as evidence that the difference in hematocrit values is due, indeed, to Kohlrausch regulation, rather than to sedimentation only. The values of 6.4% should not be taken as an exact value of Kohlrausch adjusted red cells. Frontal analysis results in a

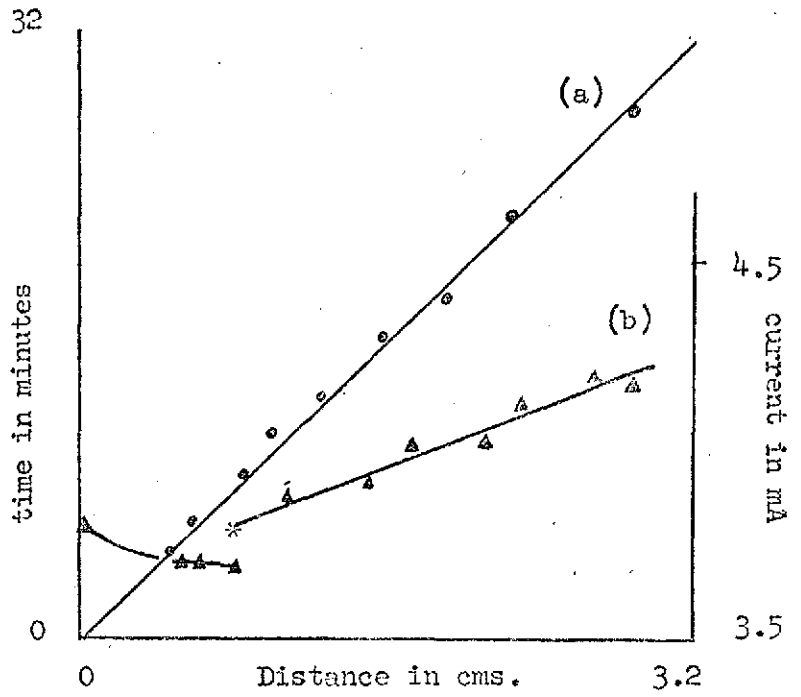

Fig.15 . Defibrinated human blood frontal analysis in cryptogenic density gradient. (a) Distance migrated vs time, (b) Distance migrated vs current, constant voltage (30 volts), * denotes voltage readjustment.

formation of a series of mixed steps, and therefore one could expect the formation of a series of different concentration steps along the vertical axis.

The data can be also plotted in terms of migration times versus distance, as shown in Fig. 15. The figure also shows corresponding variation in current.

(b) A similar run was carried out, using defibrinated whole human blood diluted 1:1 with 5% dextrose as terminator-sample. The run-time, and distance-time graph was similar to the previous experiment, as shown in Fig. 16.

The initial hematocrit was 18%, and the column hematocrit was 8.6%. Repetitions of these two experiments showed a consistent column hematocrit value in the region of 7%. The identity of column hematocrits for substantially different initial hematocrits, seem to be additional evidence of a Kohlrausch-type regulation. This confirms that cells not only

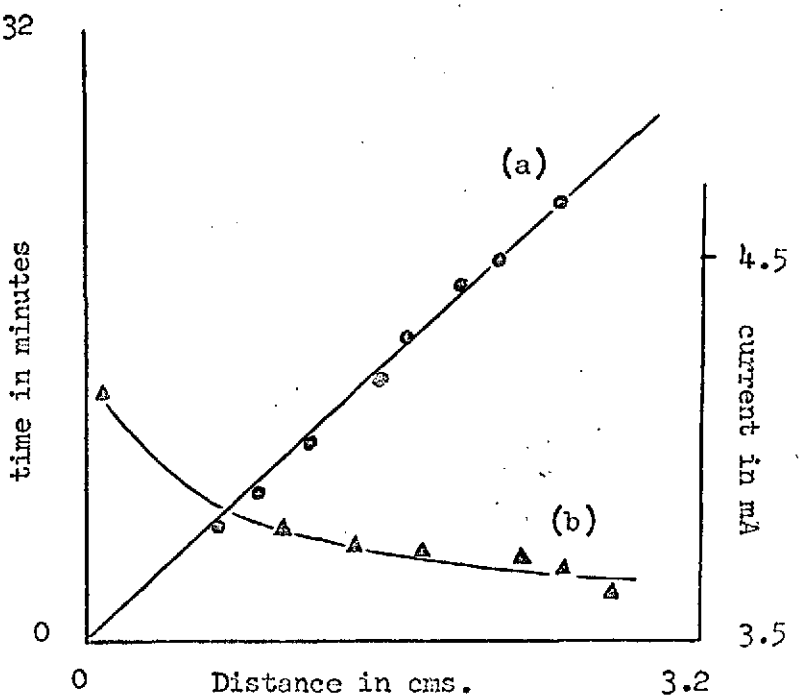

Fig.16. 1:1 dextrose diluted defibrinated human blood frontal analysis in autogenic density gradient. (a) Distance migrated vs time, (b) Distance migrated vs current, constant voltage (30volts).

exhibit the sharp interfaces characteristic of isotachophoresis, but also appear to obey its concentration laws.

(c) Frontal Analysis of Aged Human RBC

(i) In order to predict possible behavior of RBC in the preloaded Skylab experiment, two mls of defibrinated whole human blood (containing gentamycin as preservative), stored at room temperature for 2 weeks, was used as the terminator-sample in the autogenic density gradient apparatus. The leader was 20 mM Tris-HCl, pH 7.5, and the potential was 30 volts. The initial hematocrit and current were 40% and 4.2 mA respectively, and analysis was continued for 34 minutes. Three interfaces were observed. The first compartment, adjacent to the leader, was very dilute, and showed convective tendencies at the walls of the channel. The intermediate compartment was pale, and the lower one considerably darker.

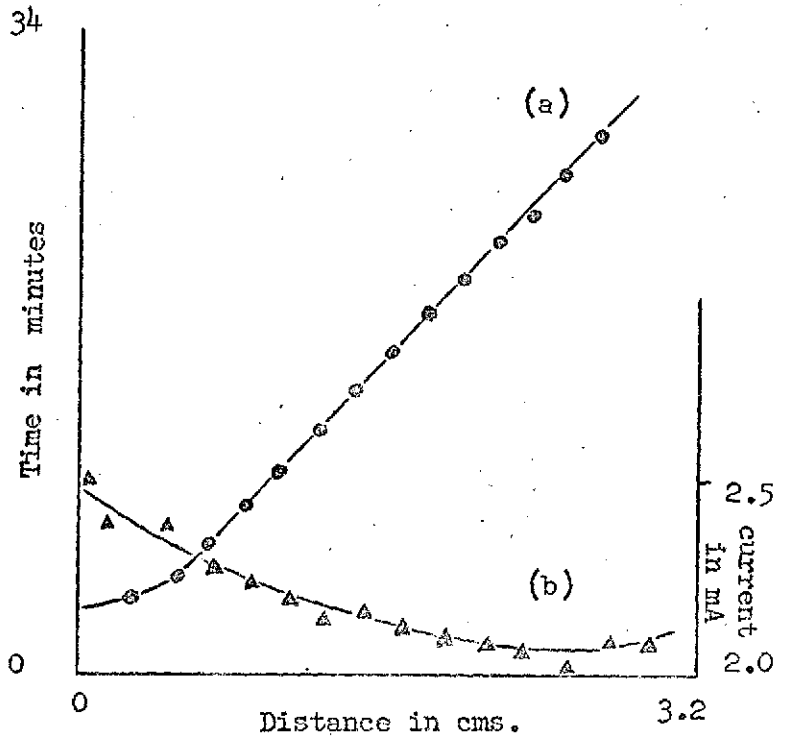

Fig. 17. Human blood aged with gentamycin, frontal analysis in autogenic density gradient. (a) Distance migrated vs time, (b) Distance migrated vs current, constant 28 volts, in Skylab prototype cell.

(ii) The Skylab prototype module was prefilled with a similar sample, and stored for two days at 4°C. Following resuspension of the cells by shaking, the sample was run at 30 volts, at 2.5 mA. The results are shown graphically in Fig. 17.

The interface was less sharp than those observed with fresh blood. The initial hematocrit was 38%, and showed considerable hemolysis, while the hematocrit of the first compartment was 2.4%, with no evidence of hemolytic hemoglobin. Clearly, after storage there are still surviving red cells, evidence of hemolysis, and separation of cells from hemoglobin.

(d) Numerous sheep red blood cell runs were carried out in a manner essentially similar with those reported here for human cells. No significant differences between sheep and human cells were observed. We therefore report only a summary table showing some of the hematocrit values obtained with both kind of cells. (Table IV).

TABLE IV

Hematocrit Values in Frontal Analysis

Blood Type	Suspension	Hematocrits of Initial Sample	Column cpt 1
Human male	1:1 dextrose	18	8.6
Human male	undiluted	5	6.3
Human male	undiluted	49	6.4
Human male	more than 1:1 diluted	27	6.4
Sheep	ACD-citrated, dilute	9.8	2.9
Sheep	dextrose diluted	2.9	2.9
Human male	aged with gentomycin, undiluted	38	2.4

(e) Temperature cycle testing for leaks. The prototype Skylab module was filled with leader, and a sample of sheep red blood cells in acid-citrate-dextrose was injected into the terminator compartment containing the teflon coated brass stirring ring. The module was stored at 4°C for three days. Subsequent examination showed no evidence of external leaking, although several bubbles were observed in the terminator vessel, and the expansion diaphragm was distended. The stirrer operated satisfactorily.

3. General Conclusions

1) Autogenic density gradient methods are applicable to a very restricted range of separations of cells from other substances, as compartments must be in proper density order.

2) Rotation in wide tubes, and at low mobility differences, with high density differences gives rise to disruptive behaviour, under the conditions tested.

3) The autogenic density gradient method was satisfactory in most cases for a single blood cell-leader interface, in the presence of gravity stabilisation, which exceeded thermal convection.

4) The interfaces thus formed were sharp, except for the aged blood run.

5) Results of storage tests and the anticipated ageing of the blood meant that the blood-gentomycin run was the only choice.

6) Leak tests were satisfactory, as far as they went, in spite of many doubts raised by Hinckley on the engineering of seals, which could not be accommodated in the available lead-time.

7) Theory of frontal isotachophoresis disfavours use of whole blood with its multiplicity of mixed compartments, and weakly restrained interfaces, due to the presence of many anions more and less mobile than cells.

8) The last reservation gains strength in view of the behaviour of aged blood in the presence of gravitational stabilisation, and the low (28 volts) potential gradient available.

9) Runs were nonetheless sufficiently encouraging to show that there was a good possibility of learning something of the behaviour of isotachophoresis of cells in Skylab. The main information sought was the shape of the blood-leader interface, when free from gravity constraints.

SECTION F

CONCLUSIONS

Theoretical and experimental analysis of various modes of electrophoresis have indicated that isotachophoresis is an attractive prospect for space electrophoresis. It has numerous apparent advantages over zonal modes, and these have been elaborated upon in the preceeding reports. Theoretical and engineering analysis has focused on the special properties of isotachophoretic boundaries, and has resulted in signficant advancement of our understanding of this intriguing technique. Most important work which remains to be carried out is a tri-dimensional analysis of the structure of ionic interfaces, which is now in progress. When completed, it should result in a major contribution to the field. The engineering calculations of temperature gradients in isotachophoresis are essential for any careful planning of large scale electrophoresis. They apply equally well to zone electrophoretic methods, and fill a real need in electrophoresis.

The main contribution of the experimental program was the demonstration that living cells can be separated by isotachophoresis. Earthbound experiments on cell separation face overwhelming problems due to gravity, and this is why the Skylab experiment was particularly important. Unfortunately, it was less than completely successful. It confirmed the sharpness of isotachophoretic boundaries of cells, but the exact shape of the boundary remains equivocal. It is hoped that some of the difficulties which have plagued this experiment will be overcome in the presently planned experiment for the Apollo-Soyuz experimental program.

Future work towards the design of a space facility for electrophoresis has to center on the solution of the technical problems of handling fluids in zero gravity, including the introduction of the sample, and withdrawal of the separated fractions. Novel approaches have been taken in this direction since the completion of last year's work, and will be included in the next report. Equally important for cell separation is the exploration of optimal buffer systems for isotachophoresis. This problem is complicated by the failure to achieve good enough palliative measures to overcome the effects of gravity here on earth. This failure, while disheartening for earth-bound work, only points out the importance of Nasa's efforts towards the development of the space facility.

APPENDIX 1

OFFPRINT FROM AN INTRODUCTION TO SEPARATION SCIENCE
EDITED BY B L KARGER
ELECTROPHORESIS

AIAA PAPER NO. 74-210 APPENDIX 2
ELECTROPHORESIS IN SPACE AT ZERO GRAVITY
M BIER VETERANS ADMINISTRATION HOSPITAL
TUSCON, ARIZONA AND R S SNYDER NASA MARSHALL SPACE FLIGHT CENTER
HUNTSVILLE, ALABAMA

APPENDIX 3
SEPARATION AND PURIFICATION METHODS, 2(2), 259-282 1973
FREE FLUID PARTICLE ELECTROPHORESIS ON APOLLO 16
BY ROBERT S SNYDER MILAN BIER RICHARD N GRIFFIN ALAN J JOHNSON

APPENDIX IV

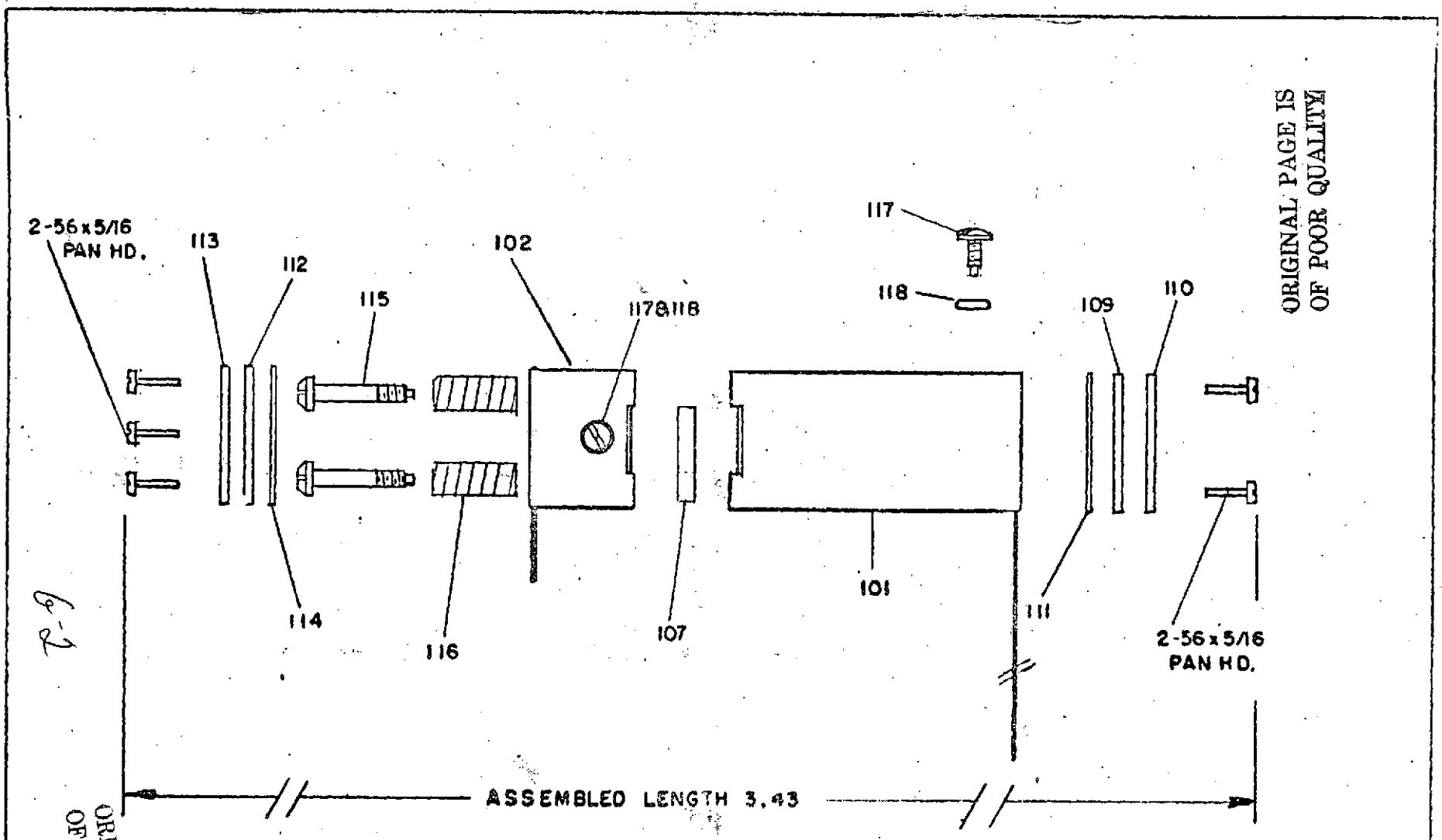

ORIGINAL PAGE IS
OF POOR QUALITY

ORIGINAL PAGE IS
OF POOR QUALITY

ISOTACHOPHORESIS CELL - EXPLODED ASSY.

FULL
10/25/73 M. BIER

A.T.C.

VETERANS ADMIN. RESEARCH
TUCSON ARIZONA

CLARKSON COMPANY
TUCSON, AZ.

ITP-100

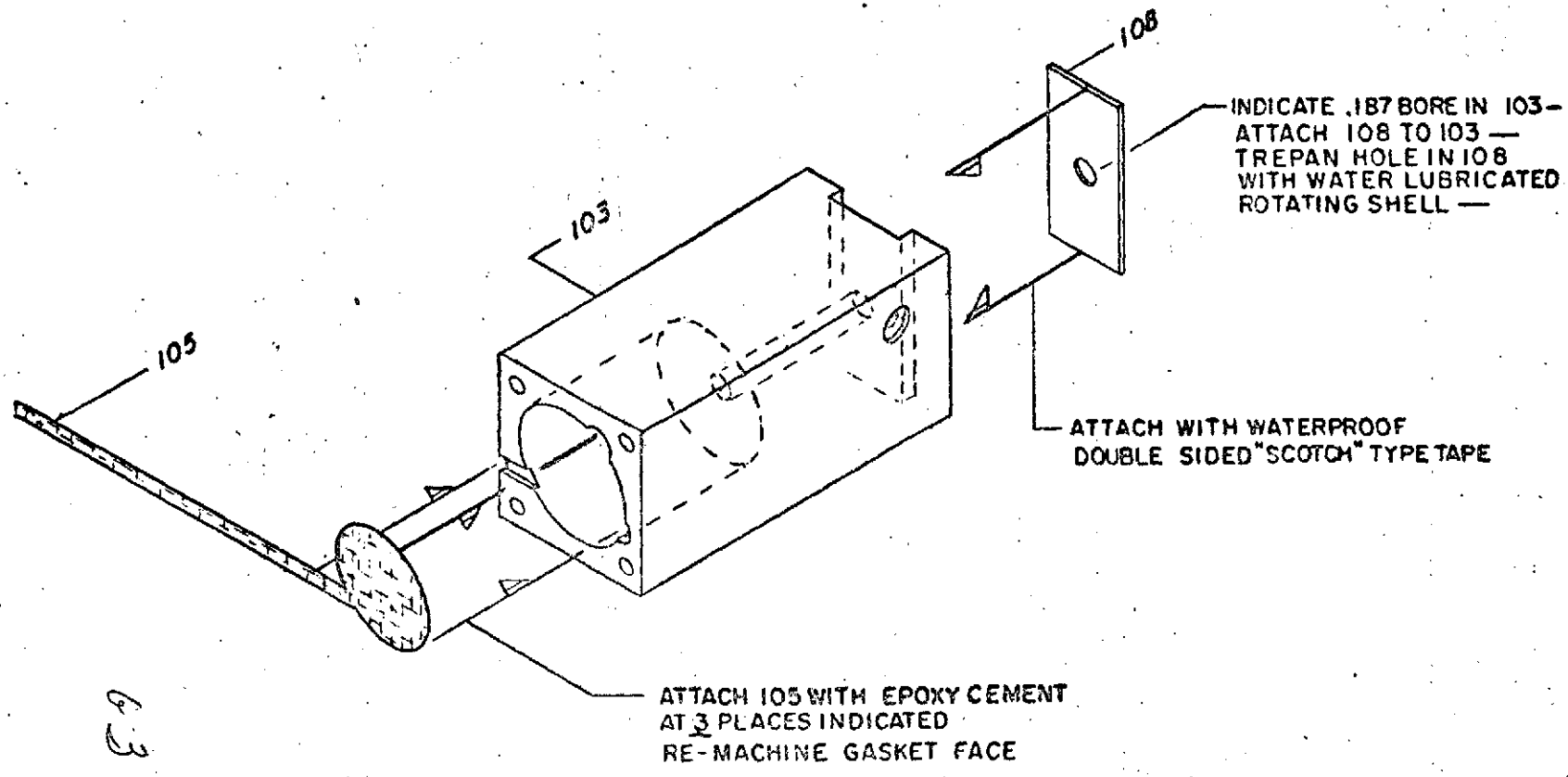

E3

ANODE CHAMBER - ASSY.

FULL		A.T.C.
10/25/73	M. BIER	

VETERANS ADMIN. — RESEARCH
TUCSON ARIZONA

CLARKSON COMPANY
TUCSON, AZ.

ITP — 101

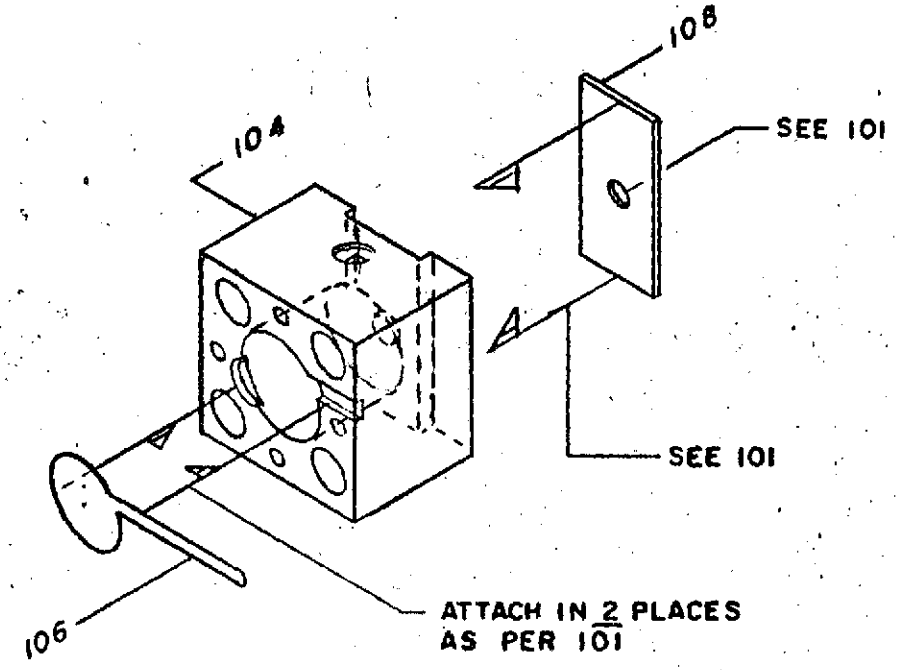

H-9

CATHODE CHAMBER - ASSY.

FULL		A.T.C.
10/25/73	M. BIER	

VETERANS ADMIN. RESEARCH
TUCSON ARIZONA

CLARKSON COMPANY
TUCSON, AZ.

ITP-102

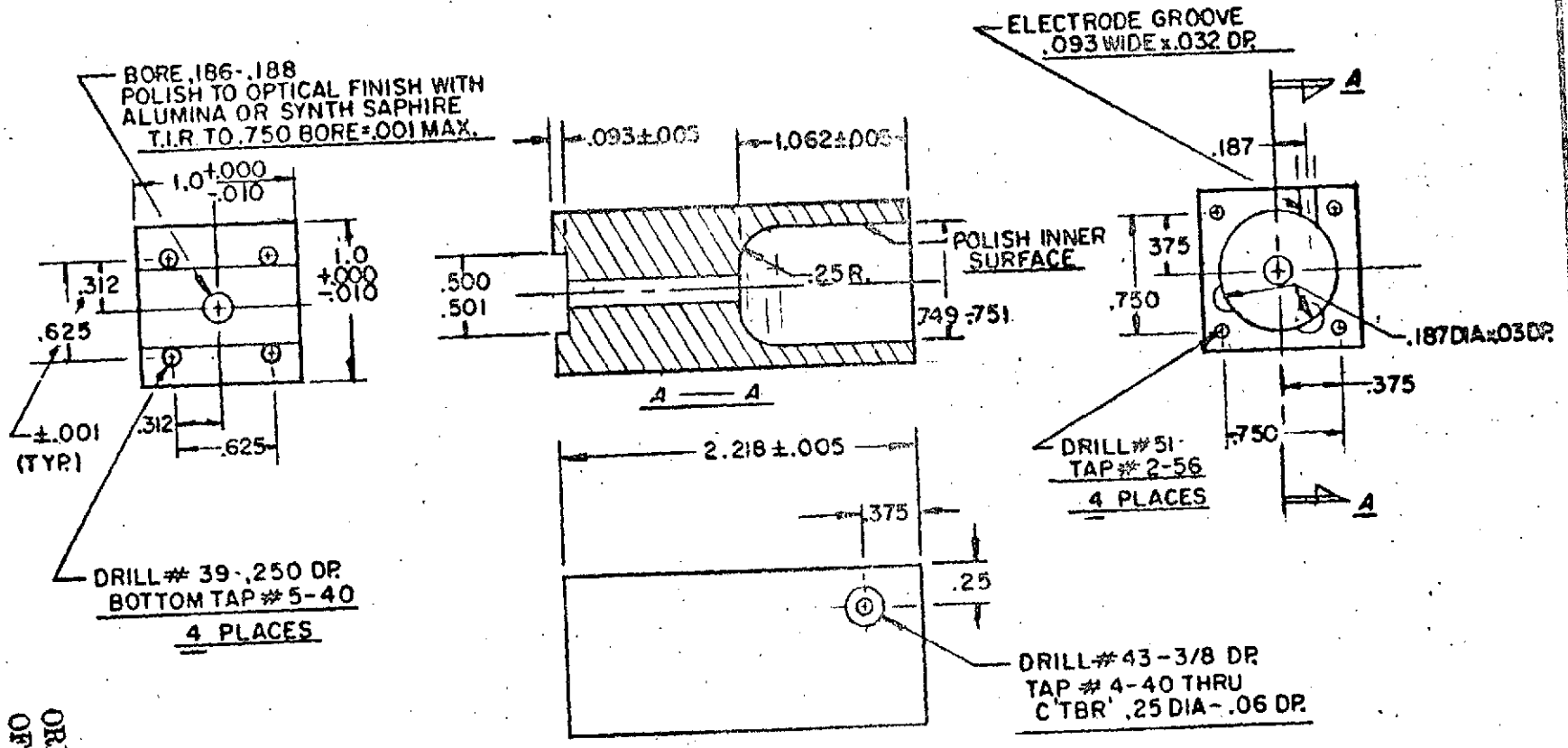

MATL: "PLEXIGLAS" OR EQUIV.

ANODE CHAMBER

SCALE FULL	APPROVED BY	DWN. BY A.T.C.
DATE 10/25/73	M. BIER	

VETERANS ADMIN.—RESEARCH
TUCSON ARIZONA

CLARKSON COMPANY
TUCSON, AZ

ITP-103

6-5

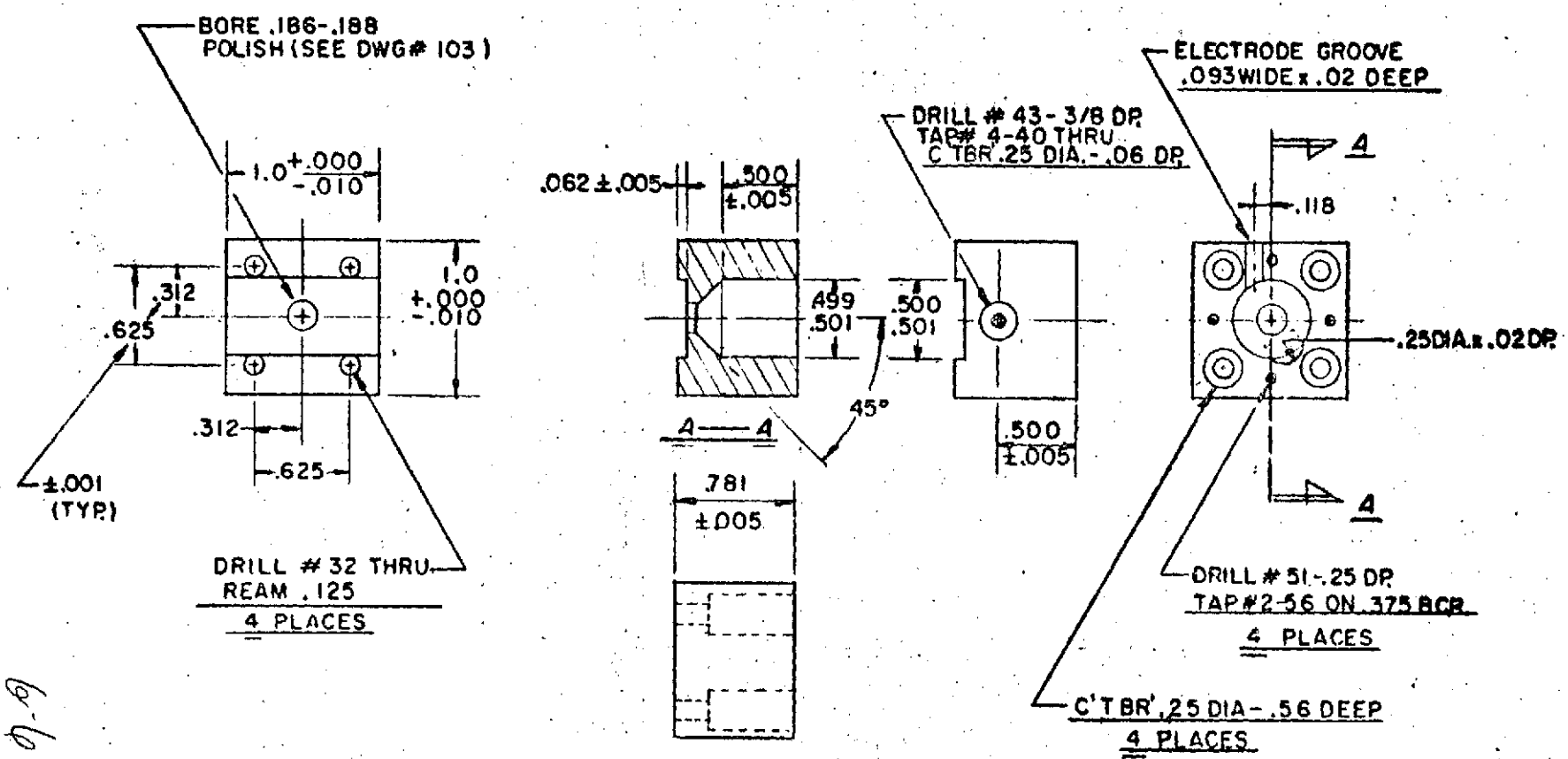

ORIGINAL PAGE IS
OF POOR QUALITY

CATHODE CHAMBER

FULL		A.T.C.
10/25/73	M. BIER	

VETERANS ADMIN. RESEARCH
TUCSON ARIZONA

CLARKSON COMPANY
TUCSON, AZ.

ITP - 104

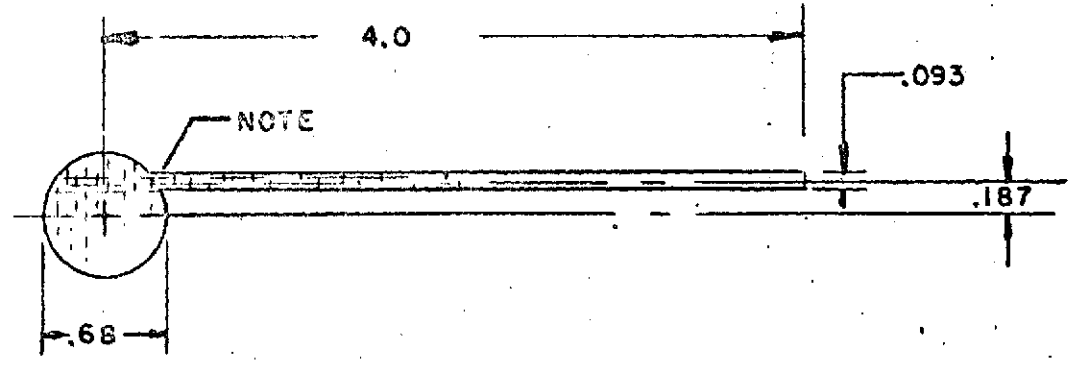

NOTE: WIRE GRAIN MUST BE PARALLEL TO LEAD PORTION

MATL: PURE SILVER WIRE MESH - 60/in - .0065 WIRE DIA.

ANODE

FULL
10/25/73 M. BIER

A.T.C.

VETERANS ADMIN. RESEARCH
TUCSON ARIZONA

CLARKSON COMPANY
TUCSON, AZ.

ITP-105

6-7

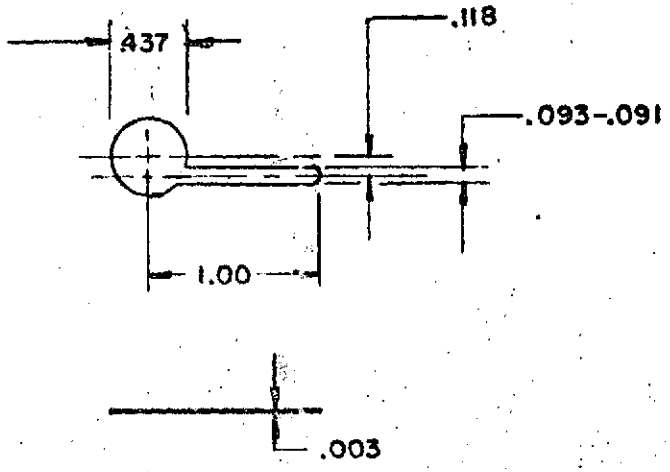

6-8

ORIGINAL PAGE IS
OF POOR QUALITY

MATL: PURE PALLADIUM SHEET .003 THK.

CATHODE

FULL
10/25/73 M. BIER

A.T.C.

VETERANS ADMIN. RESEARCH
TUCSON ARIZONA

CLARKSON COMPANY
TUCSON, AZ

ITP- 106

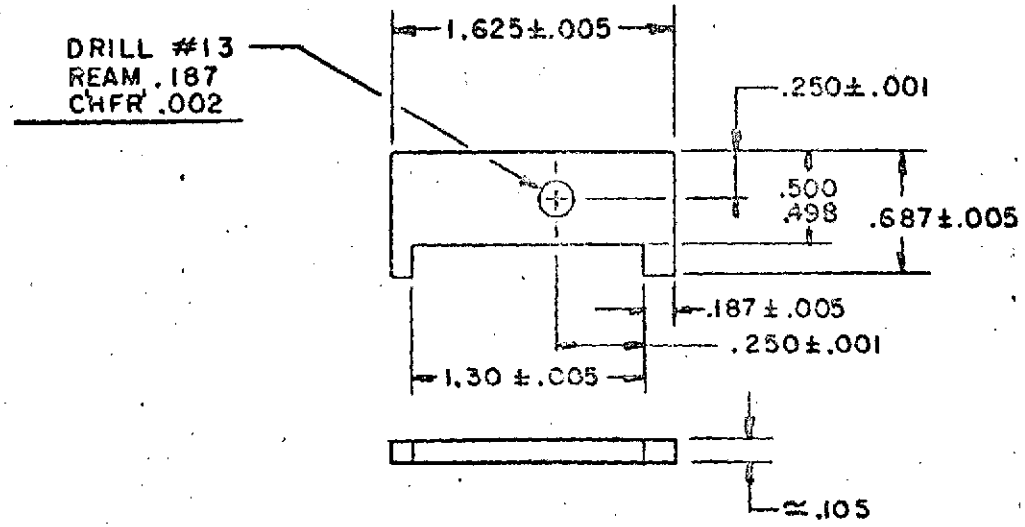

MATL: "1/8" "PLEXIGLAS 70"

VALVE

FULL

10/25/73 M. BIER

A.T.C.

VETERANS ADMIN. RESEARCH
TUCSON ARIZONA

CLARKSON COMPANY
TUCSON, AZ.

ITP-107

6-9

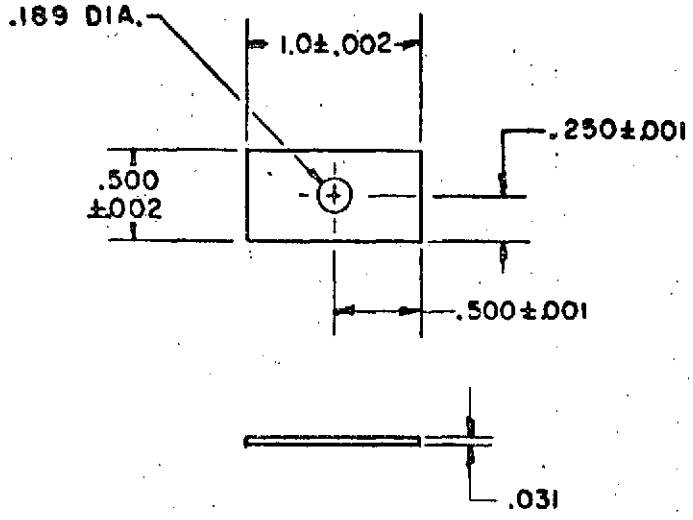

G-10

2 REQ.

MATL: RED SILICONE RUBBER SHEET .031 THK. 90 DURO.

VALVE GASKET		
FULL 10/25/73	M. BIER	A.T.C.
VETERANS ADMIN. RESEARCH TUCSON		ARIZONA
CLARKSON COMPANY TUCSON, AZ.		ITP-108

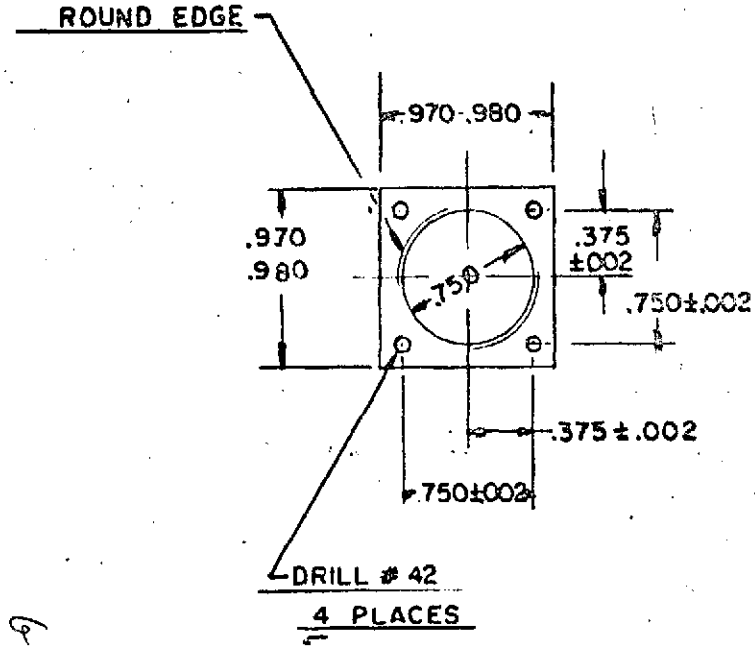

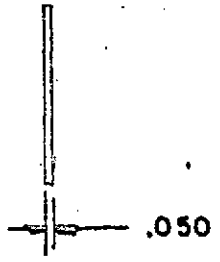

6 11

ORIGINAL PAGE IS
OF POOR QUALITY

MATL 18GA. 304 STAINLESS STEEL

ANODE CHAMBER COVER - INNER		
FULL		A.T.C.
10/25/73	M. BIER	
VETERANS ADMIN. RESEARCH TUCSON ARIZONA		
CLARKSON COMPANY TUCSON, AZ.		ITP-109

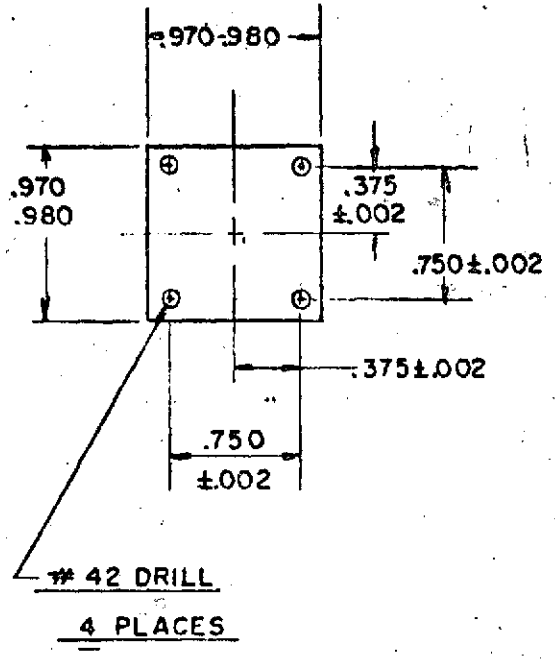

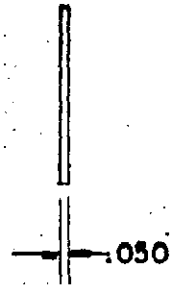

MATL: 18GA. 304 STAINLESS STEEL

ANODE CHAMBER COVER - OUTER

FULL 10/25/73	M. BIER	A.T.C.

VETERANS ADMIN. RESEARCH
TUCSON ARIZONA

CLARKSON COMPANY
TUCSON, AZ

ITP-110

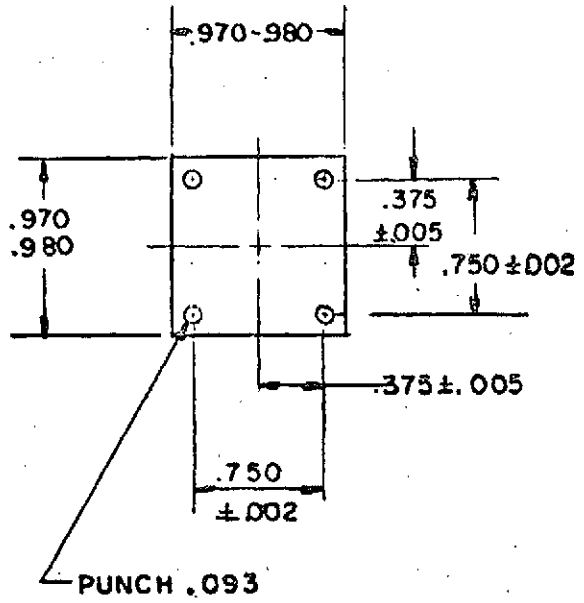

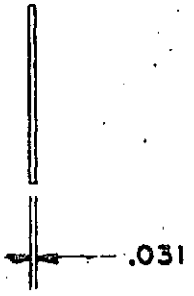

6-13

MATL: RED SILICONE RUBBER SHEET .031 THK. 90 DURO.

ANODE CHAMBER COVER GASKET		
FULL 10/25/73	M. BIER	A.T.C.
VETERANS ADMIN. RESEARCH TUCSON ARIZONA		
CLARKSON COMPANY TUCSON, AZ.		ITP-111

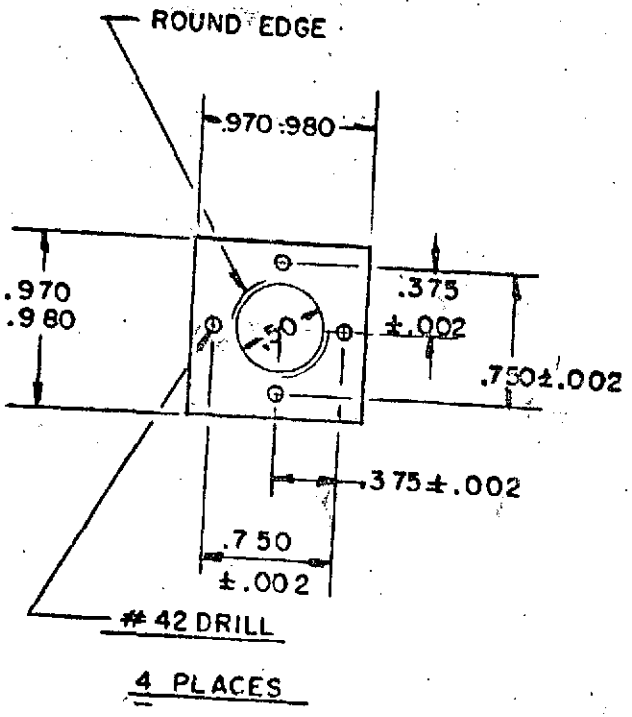

6-14

MATL: 18 GA. 304 STAINLESS STEEL

CATHODE CHAMBER COVER — INNER

FULL		
10/25/73	M. BIER	A.T.C.

VETERANS ADMIN. RESEARCH
TUCSON ARIZONA

CLARKSON COMPANY
TUCSON, AZ.

ITP-112

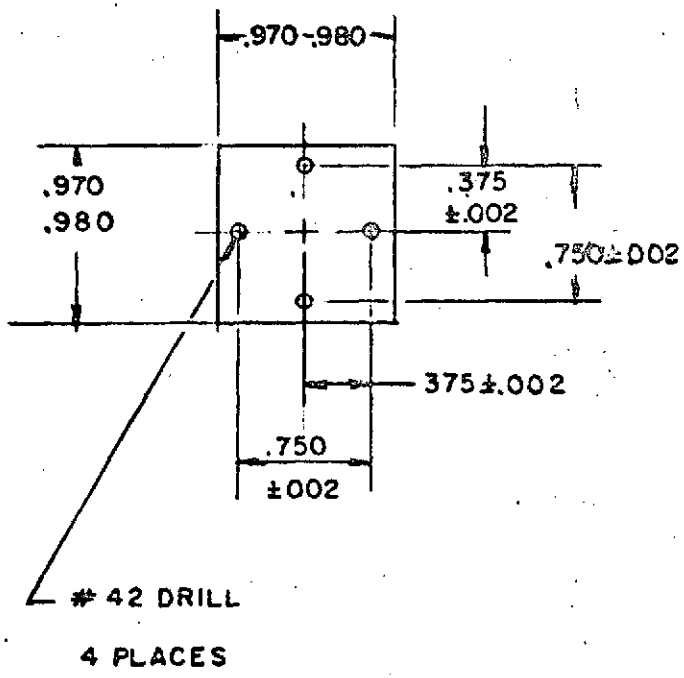

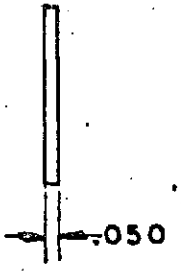

6+9

MATL: 18 GA. 304 STAINLES STEEL

CATHODE CHAMBER COVER - OUTER

FULL 10/25/73	M. BIER	A.T.C.

VETERANS ADMIN. RESERCH
TUCSON ARIZONA

CLARKSON COMPANY
TUCSON, AZ.

ITP — 113

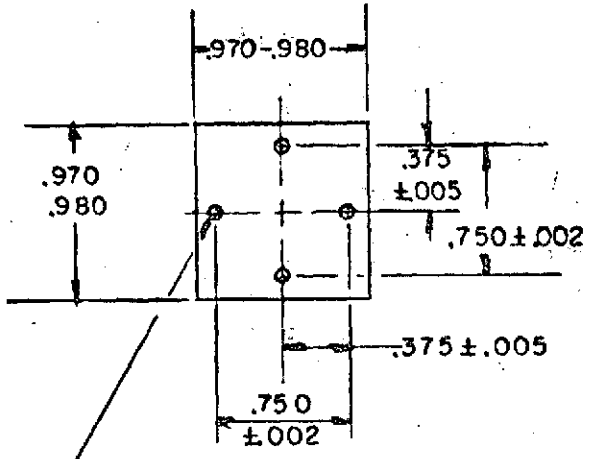

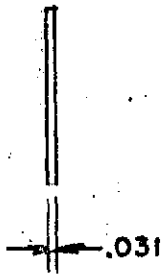

PUNCH .093

4 PLACES

6/6

MATL: RED SILICONE RUBBER SHEET .031 THK. 90 DURO

CATHODE CHAMBER COVER GASKET

FULL 10/25/73	M. BIER	A.T.C.

VETERANS ADMIN. RESEARCH
TUCSON ARIZONA

CLARKSON COMPANY
TUCSON, AZ.

MP-114

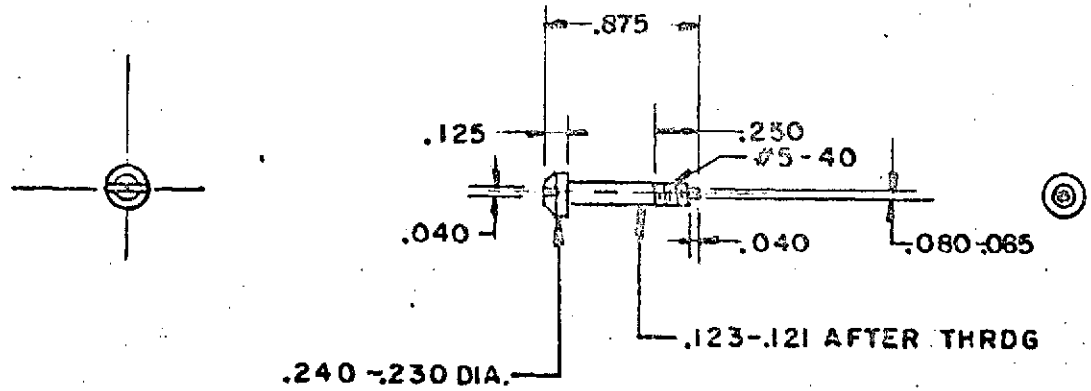

6-14

MATL: 304 STAINLESS STEEL

PILLAR SCREW		
FULL 10/25/73	M. BIER	A.T.C.
VETERANS ADMIN. RESEARCH TUCSON ARIZONA		
CLARKSON COMPANY TUCSON, AZ.		ITP-115

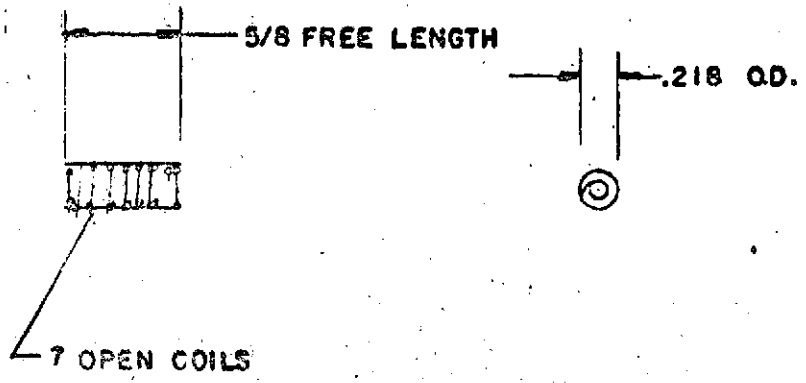

8-9

4 REQ.

PRESSURE SPRING

FULL 10/25/73		A.T.C.

VETERANS ADMIN. RESEARCH
TUCSON ARIZONA

CLARKSON COMPANY
TUCSON, AZ.

ITP-116

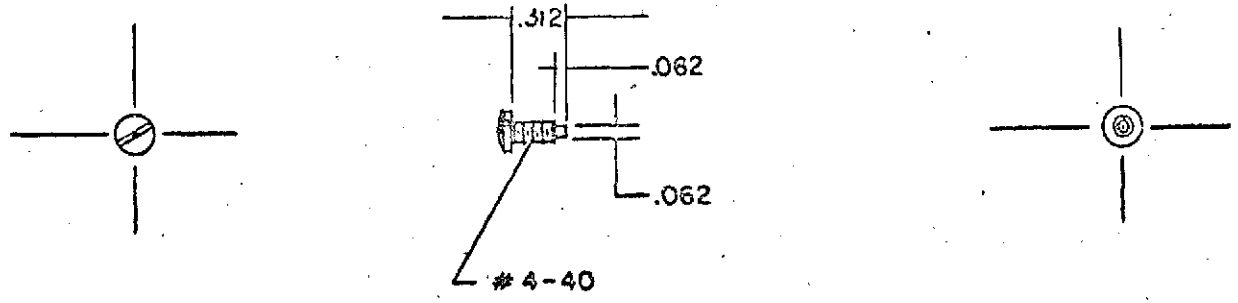

2 REQ.

MATL: 4-40 "NYLON" MACH. SCREW- BINDING HD.

FILLING PORT SCREW

FULL		A.T.C.
10/25/73	M. BIER	

VETERANS ADMIN.— RESEARCH
TUCSON ARIZONA

CLARKSON COMPANY
TUCSON, AZ.

ITP—117

6-19

2 REQ.

G-10

FILLING PORT CLOSURE SEAL

FULL		A.T.C.
10/25/73	M. BIER	

VETERANS ADMIN. RESEARCH
TUCSON ARIZONA

CLARKSON COMPANY
TUCSON, AZ.

ITP-118

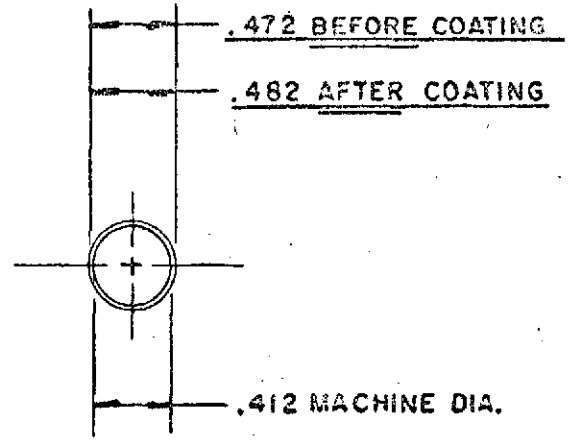

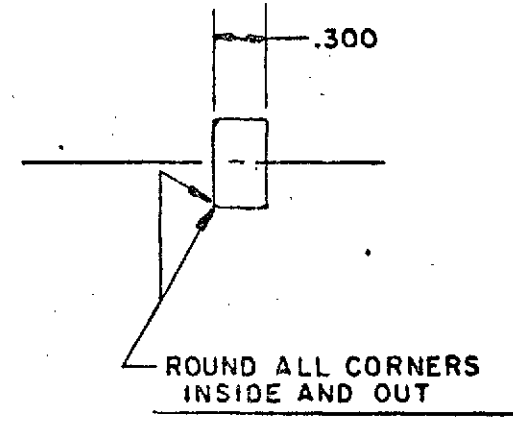

COAT WITH "TEFLON"

6-21

MAT: HALF HARD BRASS

STIRRING SHUTTLE		
FULL		A.T.C.
10/25/73	M. BIER	
VETERANS ADMIN. - RESEARCH TUCSON ARIZONA		
CLARKSON COMPANY TUCSON, AZ.		ITP – 119